ESA CCI Soil Moisture for improved Earth system understanding: state-of-the art and future directions

Wouter Dorigo[1], Wolfgang Wagner[1], Clement Albergel[2], Franziska Albrecht[3], Gianpaolo Balsamo[4], Luca Brocca[5], Daniel Chung[1], Martin Ertl[6], Matthias Forkel[1], Alexander Gruber[1], Eva Haas[3], Paul D. Hamer[7], Martin Hirschi[8], Jaakko Ikonen[9], Richard de Jeu[10], Richard Kidd[11], William Lahoz[7], Yi Y. Liu[12], Diego Miralles[13,14], Thomas Mistelbauer[11], Nadine Nicolai-Shaw[8], Robert Parinussa[10], Chiara Pratola[15,16], Christoph Reimer[1,11], Robin van der Schalie[10], Sonia I. Seneviratne[8], Tuomo Smolander[9], Pascal Lecomte[17]

[1]Department of Geodesy and Geo-Information, Vienna University of Technology, Gusshausstrasse 27-29, A-1040 Vienna, Austria (wouter.dorigo@geo.tuwien.ac.at; wolfgang.wagner@geo.tuwien.ac.at; daniel.chung@geo.tuwien.ac.at; matthias.forkel@geo.tuwien.ac.at; alexander.gruber@geo.tuwien.ac.at;)

[2]CNRM, UMR 3589 (Météo-France, CNRS) Toulouse, France (clement.albergel@meteo.fr)

[3]GeoVille Information Systems GmbH, Innsbruck, Austria (albrecht@geoville.com; haas@geoville.com)

[4]European Centre for Medium-range Weather Forecasts, Reading, United Kingdom (gianpaolo.balsamo@ecmwf.int)

[5]Research Institute for Geo-Hydrological Protection, National Research Council, Perugia, Italy (luca.brocca@irpi.cnr.it)

[6]Angewandte Wissenschaft Software und Technologie GmbH, Vienna, Austria (ertl@awst.at)

[7]NILU, Kjeller, Norway (wal@nilu.no; pdh@nilu.no)

[8]Institute for Atmospheric and Climate Science, ETH Zurich, Switzerland (martin.hirschi@env.ethz.ch; nadine.nicolai@env.ethz.ch; sonia.seneviratne@ethz.ch)

[9]Finnish Meteorological Institute, Arctic Research, Helsinki, Finland (jaakko.ikonen@fmi.fi; tuomo.smolander@fmi.fi)

[10]VanderSat B.V. / Transmissivity B.V., Noordwijk, the Netherlands (rdejeu/rparinussa/rvanderschalie@vandersat.com)

[11]Earth Observation Data Centre for Water Resource Monitoring GmbH, c/o Vienna University of Technology, Department of Geodesy and Geoinformation, Gusshausstrasse 27-29/CA 02 06, A-1040 Wien, Austria (richard.kidd@eodc.eu; thomas.mistelbauer@eodc.eu; christoph.reimer@eodc.eu)

[12]School of Geography and Remote Sensing, Nanjing University of Information Science and Technology, Nanjing, China, 210044 (yiliu001@gmail.com)

[13]Department of Earth Sciences, VU University Amsterdam, Amsterdam 1081 HV, The Netherlands.

[14]Laboratory of Hydrology and Water Management, Department of Forest and Water Management, Ghent University, B-9000 Ghent, Belgium (diego.miralles@UGent.be)

[15]MaREI Centre- Environmental Research Institute (ERI), University College Cork, Co. Cork, Ireland

[16]Starlab, Barcelona, Spain (chiara.pratola@starlab.es)

[17]ESA Climate Office, ECSAT, Fermi Avenue, Harwell Oxford, Didcot, OX11 0FD, United Kingdom (Pascal.Lecomte@esa.int)

Correspondence to: Wouter Dorigo (wouter.dorigo@geo.tuwien.ac.at): Tel: +43-(0)1-58801-12243; Fax: +43-(0)1-58801-12299)

Keywords: soil moisture; microwave remote sensing, Earth observation, Climate Data Record; Essential Climate Variable; climate change; Earth system modelling, biogeochemistry

Abstract

Climate Data Records of soil moisture are fundamental for improving our understanding of long-term dynamics in the coupled water, energy, and carbon cycles over land. To respond to this need, in 2012 the European Space Agency (ESA) released the first multi-decadal, global satellite-observed soil moisture (SM) dataset as part of its Climate Change Initiative (CCI) program. This product, named ESA CCI SM, combines various single-sensor active and passive microwave soil moisture products into three harmonised products: a merged ACTIVE, a merged PASSIVE, and a COMBINED active+passive microwave product. Compared to the first product release, the latest version of ESA CCI SM includes a large number of enhancements, incorporates various new satellite sensors, and extends its temporal coverage to the period 1978-2015. In this study, we first provide a comprehensive overview of the characteristics, evolution, and performance of the ESA CCI SM products. Based on original research and a review of existing literature we show that the product quality has steadily increased with each successive release and that the merged products generally outperform the single-sensor input products. Although ESA CCI SM generally agrees well with the spatial and temporal patterns estimated by land surface models and observed in-situ, we identify surface conditions (e.g., dense vegetation, organic soils) for which it still has large uncertainties. Second, capitalising on the results of more than 100 research studies that made use of the ESA CCI SM data we provide a synopsis of how it has contributed to improved process understanding in the following Earth system domains: climate variability and change, land-atmosphere interactions, global biogeochemical cycles and ecology, hydrological and land surface modelling, drought applications, and meteorology. While in some disciplines the use of ESA CCI SM is already widespread (e.g. in the evaluation of model soil moisture states) in others (e.g. in numerical weather prediction or flood forecasting) it is still in its infancy. The latter is partly related to current shortcomings of the product, e.g., the lack of near-real-time availability and data gaps in time and space. This study discloses the discrepancies between current ESA CCI SM product characteristics and the preferred characteristics of long-term satellite soil moisture products as outlined by the Global Climate Observing System (GCOS), and provides important directions for future ESA CCI SM product improvements to bridge these gaps.

1 Introduction

1.1 The role of soil moisture in the Earth system

Soil moisture is at the heart of the Earth system. Through its impact on the partitioning of the incoming water and energy over land, soil moisture affects the variability of the coupled water (evapotranspiration and runoff) and energy fluxes (latent and sensible heat fluxes)(Seneviratne et al. 2010). As such, a surplus or lack of soil moisture can favour the occurrence of floods (Brocca et al. 2012; Koster et al. 2010) or droughts (Wang et al. 2011), respectively. The feedback of soil moisture on evapotranspiration is important for temperature variability and the occurrence and persistence of heatwaves (Fischer et al. 2007; Hirschi et al. 2011; Miralles et al. 2014a; Mueller and Seneviratne 2012), as well as for the generation and location of precipitation (Findell et al. 2011; Guillod et al. 2015; Taylor et al. 2012). In addition, regional gradients in soil moisture can induce mesoscale atmospheric circulation patterns (Taylor et al. 2012). Moreover, the role of soil moisture in driving photosynthesis, ecosystem dynamics, and soil respiration, and hence the terrestrial carbon balance, is undisputable (Ciais et al. 2005; van der Molen et al. 2012). However, the impacts of soil moisture on ecosystems may be indirect and non-linear, e.g. by controlling the likelihood of fires and pest outbreaks (Forkel et al. 2012; Papagiannopoulou et al. 2016; Reichstein et al. 2013).

1.2 Global monitoring of soil moisture

Tracking soil moisture variability and change over time is fundamental for estimating bounds on water availability and for quantifying its sensitivity to global warming and human pressures. This requires high-quality soil moisture datasets that are long enough, contiguous, and consistent in time and space (Findell et al. 2015; Loew 2013). While detailed soil moisture information is provided by in-situ soil moisture databases such as the International Soil Moisture Network (ISMN; Dorigo et al. 2011b; Dorigo et al. 2013; Ochsner et al. 2013), ground-based observations lack sufficient global coverage and consistency for comprehensive Earth system assessments. Seamless spatial and temporal coverage is offered by reanalysis land surface model products, which are driven by various types of - mostly atmospheric – observations (e.g., Balsamo et al. 2015; Reichle et al. 2011; Rodell et al. 2004). Though seemingly gap free, the skill of reanalysis products during a specific period hinges on the number, quality, and spatial availability of the forcing datasets used as input during that period, and the model physics used to infer soil moisture fields from them Microwave remote sensing of soil moisture has long been recognised as a valuable means to overcome the spatial limitations of in-situ observations and to provide a global independent reference for land surface model and reanalysis evaluations (Albergel et al. 2013a; Schmugge 1983; Szczypta et al. 2014). It may help detecting relevant trends (Dorigo et al. 2012) but it is mainly restricted to the surface soil layer. Although gravity missions such as the Gravity Recovery and Climate Experiment (GRACE; Rodell et al. 2009) are sensitive to moisture in the total soil column (Abelen and Seitz 2013), their use is not straightforward, since besides soil moisture they are also sensitive to changes in snow, surface water, and groundwater, and require estimates of atmospheric total column water vapour, while operating at very coarse spatial and temporal resolutions. Moreover, the limited length of any observational or modelled soil moisture dataset may hamper the detection of long-term trends, particularly in areas with reduced data quality or experiencing large inter-annual variability (Findell et al. 2015; Loew 2013; Miralles et al. 2014b). For the future, model projections suggest that in specific regions soil moisture may decrease, even though there exists considerable spread in these projections (Greve and Seneviratne 2015). These trends, their inherent uncertainties and the large amount of human activities connected to soil water highlight the crucial importance of on-going monitoring of soil moisture at the ground and from space.

1.3 Climate research requirements on satellite soil moisture

Surface soil moisture information has been inferred from a wide range of space-borne instruments using various retrieval approaches (e.g., De Jeu and Dorigo 2016; Jackson 1993; Kerr et al. 2012; Naeimi et al. 2009; Njoku et al. 2003; O'Neill et al. 2016; Owe et al. 2008; Wagner et al. 2013b). In 2010, the Global Climate Observing System (GCOS) panel considered soil moisture remote sensing mature enough for systematic, global observation of the climate and endorsed it as one of the 50 Essential Climate Variables (ECVs) supporting the work of the United Nations Framework Convention on Climate Change (UNFCCC) and the International Panel on Climate Change (IPCC; GCOS-138 2010). Scientific consensus on the minimum requirements of satellite soil moisture datasets for climate monitoring, so-called Climate Data Records (CDRs), has been outlined in the latest GCOS Implementation Plan (GCOS-200 2016). Within the Climate Change Initiative (CCI) of the European Space Agency (ESA), these requirements have been further refined, supported in particular by the CCI Climate Modelling User Group (CMUG), which represents leading climate modelling organisations in Europe. Within the CCI, these requirements are updated yearly based on continuous feedback from GCOS, CMUG, and the CCI soil moisture user community at large.

Table 1 lists the combined GCOS, CMUG, and wider ESA CCI soil moisture user community's requirements on satellite soil moisture. Although surface soil moisture (SSM) is the target variable specified by GCOS, there is also a large interest in satellite-based root-zone soil moisture (RZSM). The latter seemingly contradicts the user requirement of model-independency of the satellite products, as land surface models (LSMs) are typically required to propagate surface soil moisture observations to the root-zone (Albergel et al. 2012). No agreement exists yet on the soil column that a potential RZSM product should represent, as the vegetation rooting depth is species-specific. Similarly, neither the depth of the surface layer is precisely defined, since differences in microwave frequencies and soil moisture conditions lead to different soil penetration depths, and thus reflect different depths. The preferred unit for soil moisture products is m^3m^{-3}, although different communities may adopt different physical units, e.g. kg m^{-2} or percentage/degree of saturation. However, with appropriate metadata on soil porosity at the scale of the satellite footprint the observations can be transferred from one physical unit to the other (Dorigo et al. 2011b). It has been suggested that for some applications, e.g., model evaluation, soil moisture anomalies may be more useful than absolute values (Nicolai-Shaw et al. 2015). With increasing spatial resolutions of both regional and global climate models the need for higher resolution observational soil moisture datasets also increases. While the minimum requirement was previously 50 km, now a spatial resolution ranging between 1 and 25 km is advocated. The preferred observing cycle is one day, even though a sub-daily temporal resolution is desired for specific process studies (Guillod et al. 2014). Soil moisture CDRs should be reliable, without jumps or data gaps, and stable over time. The provision of error information, preferably per pixel and per observation, shall be an integrated part of any soil moisture CDR. In addition, GCOS advises the concurrent provision of related variables such as freeze/thaw state, surface inundation, and vegetation optical depth (VOD) to complement and better characterise the quality of the SSM products.

Data quality requirements depend strongly on the application, in particular with regard to precision (i.e., the random error) and accuracy (the combined effect of precision and systematic error). This is reflected by the large spread of accuracy requirements for different applications as reported in the Observing Systems Capability Analysis and Review Tool (OSCAR; https://www.wmo-sat.info/oscar/) database, maintained by the World Meteorological Organization (WMO). The current GCOS accuracy requirement of 0.04 m^3m^{-3} volumetric soil moisture unbiased root-mean-square-error (ubRMSE) is in line with the accuracy goals set for the exploratory satellite missions Soil Moisture Ocean Salinity (SMOS; Kerr et al. 2016) and Soil Moisture Active Passive (SMAP; Entekhabi et al. 2010a). The requirement for the stability was set to 0.01 $m^3m^{-3}y^{-1}$ random year-to-year variability. For both requirements, there is no fundamental research supporting these thresholds. The assessment of these qualities hinges on the availability of stable, long-term reference datasets, something which is currently still lacking (GCOS-200 2016). In addition, it is important to point out that the process of comparing satellite-derived products to independent reference data requires standardisation, which is why GCOS collaborates closely with the Land Product Validation sub-group (LPV) of the Committee of Earth Observation Satellites (CEOS) to establish good practice validation protocols. For soil moisture such a protocol does not yet exist. Nonetheless, CEOS LPV judges the maturity of soil moisture validation activities to be relatively high thanks to the dedicated validation efforts of the SMAP and SMOS satellite teams (Colliander et al. 2016; Kerr et al. 2016), the availability of a relatively large number of in-situ soil moisture networks worldwide (Dorigo et al. 2011a), and the recent emergence of advanced statistical methods for estimating accuracy metrics in the presence of scaling errors (Chen et al. 2016a; Gruber et al. 2013; Gruber et al. 2016b).

Table 1 Current specifications for satellite-based soil moisture CDRs, based on requirements of GCOS, CEOS, CMUG, and the ESA CCI soil moisture user community at large

Variable	Surface[1] soil moisture content, root-zone soil moisture content
Measuring units	m^3m^{-3}
Horizontal resolution	25 km, with increasing need to advance towards 1 km
Accuracy	0.04 m^3m^{-3} (unbiased root-mean-square-error)
Stability	0.01 $m^3m^{-3}y^{-1}$ (year-to-year variability of systematic differences)
Observing cycle	Daily, growing preference for sub-daily observations
Timeliness	1 month
Record length	>30 years
Additional requirements	Products should be satellite only, i.e. no land surface model should be involved
	Error estimate should be provided for each observation
	Additional information on freeze/thaw status, surface inundation, and vegetation optical depth is requested for better quality characterisation

[1]There is no common definition of the surface layer but it is generally assumed to range between 0.02-0.05 m (Ulaby et al. 1982).

1.4 ESA CCI Soil Moisture to meet climate observation demands

The ESA CCI Soil Moisture (SM) project (http://www.esa-soilmoisture-cci.org) has been established to fulfil the soil moisture monitoring needs in support of climate research. Although most of the basic requirements can potentially be met by a single sensor product (Table 1), individual satellite missions are clearly too short to provide a CDR of more than 30 years (Dorigo et al. 2010). To bridge this gap, ESA's Water Cycle Multi-mission Observation Strategy (WACMOS) project (Su et al. 2010) provided the financial incentives to develop a long-term soil moisture product from multiple active and passive microwave sensors. The multi-satellite approach merged various Level 2 (i.e. in swath geometry) single-sensor soil moisture products into a harmonised record by synergistically combining the strengths of the individual products (Liu et al. 2012; Liu et al. 2011; Wagner et al. 2012). The success of this demonstration activity was a critical argument in favour of including soil moisture in ESA's CCI program, which supports the development and pre-operational production of ECVs. The first ESA CCI SM product (v0.1) was publicly released in 2012. Since then, the dataset has been continuously upgraded by expanding its spatial-temporal coverage, by including new sensors, through algorithmic updates and sensor inter-calibration efforts, and by improving the assessment and description of product errors. This is an ongoing effort that will continue into the future.

1.5 Scope and overview of this study

The objective of this paper is to provide the state-of-the-art of the ESA CCI SM products and to review its impact on various climate-related research sectors. Section 2 provides a detailed overview of the current specifications of the ESA CCI SM product and the major updates to the retrieval algorithm, first released in 2012 (Liu et al. 2012; Liu et al. 2011; Wagner et al. 2012). A thorough understanding of the errors and limitations of ESA CCI SM is crucial for a correct use and interpretation of the data. Therefore, we dedicate Section 3 to quality characterisation of the products and synthesise the results of the numerous error assessments that were made in the past. In Section 4, we provide an extensive overview and synthesis of more than 100 studies that used the ESA CCI SM products to gain improved insights into Earth system processes. In Section 5, we confront the ESA CCI SM product quality characteristics identified in this study with the requirements of the climate community to identify potential deficiencies in the current product and make prioritised recommendations for future developments.

2 The ESA CCI soil moisture product

2.1 Soil moisture retrievals from microwave remote sensing

The microwave domain is particularly useful for the observation of moisture conditions in the upper few centimetres of the soil (Ulaby et al. 1982). This capability is the result of the large contrast between the dielectric properties of dry soil and water, which makes the microwave radiance emitted or reflected by the surface soil volume almost linearly dependent on the soil-water mixing ratio (Ulaby et al. 1982). Both active microwave systems (radars, measuring variations in reflected backscatter) and passive systems (radiometers, measuring natural emissions) can make observations under nearly any weather conditions, independent of daylight. Satellite microwave observations have footprints with typical resolutions on the order of 25×25 km^2 to 50×50 km^2. The coarse spatial resolution is however compensated by the global coverage and high revisit times, generally daily or sub-daily, depending on sensor characteristics such as swath width. Such short revisit times are very valuable since soil moisture is generally highly variable in time as a function of rainfall, irrigation, and evaporation.

Despite their general usefulness for soil moisture retrievals, microwave observations have several limitations. Retrievals are impossible under snow and ice or when the soil is frozen (Ulaby et al. 1982), while complex topography, surface water, and urban structures have an adverse effect on the retrieval quality (Wagner et al. 1999a). In particular, passive microwave observations can be affected by human-induced radio frequency interference (RFI), which may obstruct feasible observations over large areas (Oliva et al. 2012b). However, much progress has been made to mitigate RFI by enforcement of legislation, by new on-board hardware-driven detection and mitigation capabilities (e.g. for AMSR2 and SMAP), or by filtering or replacing affected observations using alternative microwave frequencies (Nijs et al. 2015). In addition, vegetation water attenuates the microwave emission and backscatter from the soil surface and may eventually completely obscure the soil moisture signal above wavelength-dependent vegetation water content density thresholds (Parinussa et al. 2011). The L-band frequency (1.4 GHz), as used by SMOS and SMAP, has a better capacity to penetrate vegetation than the higher microwave frequencies of C-band (i.e. AMSR-E, AMSR2, WindSat, ERS, ASCAT) and X-band (i.e. AMSR-E, AMSR2, TMI, Fengyun-3B) (Ulaby et al. 1982). Observations at the lower L-band microwave frequency (longer wavelength) generally also sense the soil profile to a greater depth than C- and X-band sensors, typically up to 5 cm depth (Ulaby et al. 1982). At the same time however, it is more difficult to achieve a suitable spatial resolution with high radiometric accuracy for L-band than for C- and X-band.

Most soil moisture retrieval algorithms for passive microwave observations (e.g., Jackson 1993; Kerr et al. 2012; Mladenova et al. 2014; Owe et al. 2008; Wigneron et al. 2007) are based on solving the radiative transfer model by Mo et al. (1982). The algorithms differ in their treatment of the observations, e.g. by using different frequencies, polarizations, or multiple overpasses or incidence angles, and in the parameterisation of the different geophysical variables, e.g., surface roughness, vegetation impact, and the conversion of the soil dielectric constant to soil moisture. Alternatively, statistical retrieval approaches train the passive microwave observations towards a reference dataset through machine learning (e.g., Rodríguez-Fernández et al. 2015) or linear regressions (e.g., Al-Yaari et al. 2016). In summary, all these differences in microwave frequencies, sensor specifications, and retrieval algorithms result in soil moisture dataset qualities that vary both in space and time. Characterizing the accuracy of these various satellite-based soil moisture estimates has been the subject of numerous studies (e.g. Naeimi et al. 2009; Dorigo et al. 2010; Parinussa et al. 2011; Wanders et al. 2012).

Table 2 shows an overview of all openly accessible coarse-resolution microwave soil moisture products. Since none of the single sensor missions complies with the minimum CDR length requirement of 30 years, a multi-satellite approach is needed to bridge this gap. Retrievals based on synthetic aperture radars (SARs) yield higher spatial resolutions but at the expense of reduced revisit times and are therefore currently not considered appropriate for global CDR production.

Table 2. Available global coarse resolution surface soil moisture products from passive and active satellite microwave instruments. Products are grouped according to platform sensor in order of platform launch date.

Platform Sensor	Frequency used for SM retrieval (GHz)	Product name/producer	Dataset availability	Reference
Radiometers				
Nimbus7 SMMR	6.6	VU University Amsterdam (VUA)/ National Aeronautics and Space Administration (NASA) (Land Parameter Retrieval Model (LPRM))	1978/10 – 1987/08	Owe et al. (2008)
DMSP SSM/I	19.4	VUA/NASA (LPRM)	1987/06 – Onwards	Owe et al. (2008)
TRMM TMI	10.7	VUA/NASA (LPRM)	1997/11 – 2015/04	Owe et al. (2008)
		Princeton University (LSMEM)	1998/01 – 2004/12	Gao et al. (2006)
AQUA AMSR-E	6.9, 10.7	VUA/NASA (LPRM)	2002/06 – 2011/10	Owe et al. (2008)
		University of Montana / Numerical Terradynamic Simulation Group	2002/06 – 2011/10	Jones et al. (2010)
		US National Snow and Ice Data Center (NSIDC)	2002/06 – 2011/10	Njoku et al. (2003)
		Japanese Aerospace Exploration Agency (JAXA)	2002/06 – 2011/10	Koike et al. (2004)
		Princeton University (LSMEM)	2002/06 – 2011/09	Pan et al. (2014)
Coriolis WindSat	6.8, 10.7	VUA/NASA (LPRM)	2003/01 – 2012/08	Parinussa et al. (2012)
		U.S. Naval Research Laboratory	2003/01 – Onwards	Li et al. (2010)
SMOS MIRAS	1.4	ESA/ Centre Aval de Traitement des Données SMOS (CATDS)	2009/11 – Onwards	Kerr et al. (2010)
		ESA/EUMETCAST (for L2-SM-NRT-NN product)	2009/11 – Onwards	Rodríguez-Fernández et al. (2015)
		VUA/VanderSat (LPRM)	2009/11 – Onwards	van der Schalie et al. (2016)
Aquarius	1.4	NSIDC	2011/08 – 2015/06	
FengYun-3B MWRI	10.7	VUA/NASA (LPRM)	2011/07 – Onwards	Parinussa et al. (2014)
GCOM W1 AMSR2	6.9, 7.3, 10.7	VUA/NASA (LPRM)	2012/07 – Onwards	Parinussa et al. (2015)
		JAXA	2012/07 – Onwards	Koike et al. (2004)
SMAP	1.4	NASA	2015/02 – Onwards	O'Neill et al. (2016)
		VUA/NASA (LPRM)	2015/02 – Onwards	van der Schalie et al. (2016)
Scatterometers				
ERS-1/2 AMI WS	5.3	Vienna University of Technology (TU Wien/WARP), ESA	1991/08 – 2011/07	Scipal et al. (2002); Wagner et al. (2007)
MetOp-A/B ASCAT	5.3	EUMETSAT H-SAF, (TU Wien/WARP)	2007/01 – Onwards	Wagner et al. (2013b)

2.2 The ESA CCI SM multi-sensor merging approach

Combining single sensor data into a multi-satellite soil moisture data record can either start from Level 1 data (brightness temperatures for passive microwave sensors, backscatter coefficients for active microwave sensors) or from Level 2 soil moisture retrievals (Wagner et al. 2012). Starting from Level 1 would allow using the brightness temperature and backscatter measurements complimentarily in the soil moisture retrieval itself. For example, Kolassa et al. (2016) produced superior soil moisture products by merging Level 1 products of AMSR-E and ASCAT. However, for ESA CCI SM such an approach would become very complex and of limited applicability because of the many satellites and different sensors involved, many of them with no or only limited temporal overlap. Therefore, the ESA CCI SM approach starts from publicly available Level 2 soil moisture data records, which are merged based on a thorough understanding of their error characteristics. This approach has the major advantage that the CDR production system benefits from the efforts by space agencies and other organisations to establish single-sensor soil moisture data records that are both internally and externally validated, while being computationally relatively lightweight.

The architecture for the ESA CCI SM Level 2 based merging framework was originally proposed by Liu et al (2011, 2012) and Wagner et al. (2012) and is – with some modifications – still being used today (Figure 1). Level 2 soil moisture products, produced outside the processing chain by various data providers, are used as input to the merging scheme. Currently, only active microwave soil moisture products generated with the TU Wien method (Naeimi et al. 2009; Wagner et al. 1999b) and passive microwave products produced with the Land Parameter Retrieval Model (LPRM; Owe et al. 2008) are being used because of their consistency in methodology across sensors (see Table 2). Level 2 soil moisture products from all available active and passive sensors are first mapped from their native observation times to a common daily time step (0:00 UTC ± 12 hours) using a nearest neighbour search in time. Then, the temporally rebinned Level 2 radiometer products are inter-calibrated using cumulative distribution function (CDF) matching (Liu et al. 2011) with AMSR-E soil moisture serving as a scaling reference, and merged into a radiometer-only (PASSIVE) product while taking into account the relative skill of the input products (Section 2.3). The same is done for the temporally rebinned Level 2 scatterometer products but with ASCAT soil moisture serving as a scaling reference. This results in a scatterometer-only (ACTIVE) product.

Subsequently, the systematic differences between ACTIVE and PASSIVE are corrected for by matching for the CDF of each pixel against long-term LSM-based soil moisture, which is currently provided by GLDAS-Noah v1 (Rodell et al. 2004). The choice of using a modelled soil moisture product and not one of the microwave-based products as scaling reference has been motivated by the fact that none of the latter has global coverage and spatially consistent quality (Liu et al. 2012). In the final step, the rescaled

ACTIVE and rescaled PASSIVE products are merged into the combined active+passive product (COMBINED), again based on their error characteristics. Given the native spatial resolutions of 25 to 50 km and revisit times of approximately 1 to 2 days of the Level 2 products, it was decided to provide a daily product with a grid spacing of 0.25°. Note, that the actual data availability of ESA CCI SM varies in space and time due to the varying spatial and temporal availability of the single-sensor Level 2 input products (Section 3). The units of measurement of ACTIVE is degree [%] of saturation while PASSIVE and COMBINED are provided in volumetric units [m^3m^{-3}].

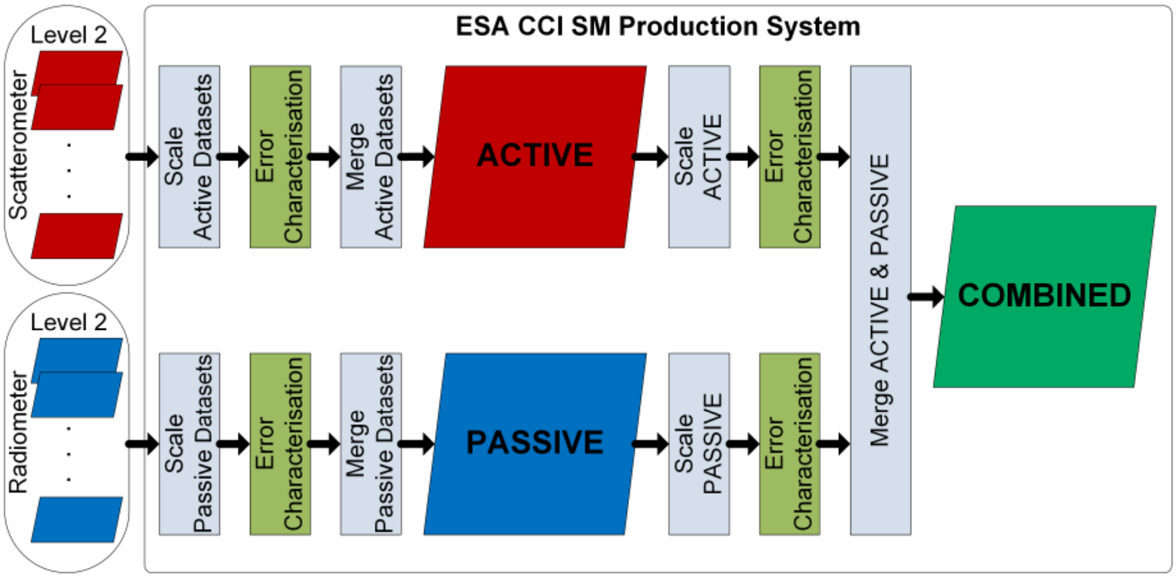

Figure 1 Schematic overview of ESA CCI SM production system. Modified from Wagner et al. (2012)

2.3 Product evolution and latest developments

The first ESA CCI SM product (v0.1, at that time referred to as ECV SM; Table 3) was released in 2012 and combined four radiometer and two scatterometer products into a single COMBINED dataset according to the methodology documented in Liu et al. (2012). Since then, the ESA CCI SM product was updated at regular intervals and complemented with the intermediate ACTIVE and PASSIVE products (Table 3). One of the major modifications of each subsequent release has been the continuous extension of ESA CCI SM into the near present, which was mainly facilitated by the introduction of new satellite sensors, i.e., Coriolis WindSat, GCOM-W1 AMSR2, SMOS MIRAS and MetOp-B ASCAT. Particularly, the integration of SMOS has been challenging because of its sensor characteristics, which differ significantly from earlier microwave radiometers. SMOS uses an interferometric radiometer instead of a scanning radiometer, and measures at a lower frequency (L-band) and over a wide range of incidence angles. While this offers new opportunities, also several challenges have to be overcome, especially with regard to the large impact of RFI over much of Eurasia (Oliva et al. 2012a), and the lack of simultaneous Ka-band observations which are commonly used in LPRM to estimate land surface temperatures. To overcome the latter, SMOS LPRM adopts an approach similar as for SMOS L3 and estimates the effective soil temperature from the skin and deeper soil temperatures provided by the Integrated Forecast System of the European Centre For Medium Range Weather Forecasts (ECMWF) (van der Schalie et al. 2016). Using LPRM-based SMOS retrievals instead of the official SMOS Level 3 product leads to a higher consistency with the other passive microwave products used in ESA CCI SM without significant loss of skill with regard to the latter (van der Schalie et al. in review). Besides, it also provides a solid base for future integration of SMAP-based LPRM retrievals (van der Schalie et al. 2016). In addition to the integration of new sensors, updates of Level 1 and Level 2 products that were already used in earlier ESA CCI SM releases are integrated in new ESA CCI SM releases. Notice, that the datasets are not updated until the near present to allow for using reprocessed data and making a thorough error assessment before public release.

Table 3 Specifications of ESA CCI SM public releases

	Version number			
	V0.1	V02.0 / v02.1*	V02.2	V03.2
Release date	June 2012	July 2014 / December 2014	December 2015	February 2017
Products provided	COMBINED	ACTIVE, PASSIVE, COMBINED	ACTIVE, PASSIVE, COMBINED	ACTIVE, PASSIVE, COMBINED
Scatterometer products included (algorithm + version)	ERS-1/2 AMI WS (TU Wien WARP 5.0), MetOp-A ASCAT (TU Wien/WARP 5.4)	ERS-1/2 AMI WS (TU Wien/WARP 5.0), MetOp-A ASCAT (TU Wien/WARP 5.4)	ERS-1 AMI WS (TU Wien/WARP 5.5), ERS-2 AMI WS (TU Wien/WARP5.4), MetOp-A ASCAT (H-SAF H25 / WARP5.5)	ERS-1/2 AMI WS (TU Wien/WARP 5.5), ERS-2 AMI WS (TU Wien/WARP5.4), MetOp-A+B ASCAT (H-SAF H109/H110 / WARP 5.6)
Radiometer products included (algorithm + version)	SMMR, SSM/I, TMI, AMSR-E (all VUA/NASA LPRM v3)	SMMR, SSM/I, TMI, AMSR-E, WindSat, AMSR2 (all VUA/NASA LPRM v5)	SMMR, SSM/I, TMI, AMSR-E, WindSat, AMSR2 (all VUA/NASA LPRM v5)	SMMR, SSM/I, TMI, WindSat (all VUA/NASA LPRM v5); AMSR-E, AMSR2, SMOS (all VanderSat LPRM v6)
Time period covered	1978/11 – 2010/12	1978/11-2013/12 (PASSIVE and COMBINED); 1991/08-2013/12 (ACTIVE)	1978/11-2014/12 (PASSIVE and COMBINED); 1991/08-2014/12 (ACTIVE)	1978/11-2015/12 (PASSIVE and COMBINED); 1991/08-2015/12 (ACTIVE)
Major algorithmic improvements with respect to forerunner	Original version as described in Liu et al. (2012). Noise estimates based on scaling and merging of single sensor error propagation estimates.	Data gaps in COMBINED (2003/02 – 2006/12) resulting from ERS-2 failure filled with AMSR-E data; improved CDF-scaling, spatial resampling of active data by Hamming window.	Improved flagging of spuriously low and high observations.	New weighted merging scheme for all three products based on signal-to-noise ratio of input datasets; random error estimates based on SNR
Ancillary data provided	Random error estimate for each observation; Flags for spurious observations (e.g. snow cover, frozen soil); Sensors used per period for each pixel	Random error estimate for each observation; Flags for spurious observations, day-/nighttime observation, ascending/descending mode; microwave frequency and sensor used for each soil moisture retrieval; original observation timestamp	Random error estimate for each observation; Flags for spurious observations; day-/nighttime observation; ascending/descending mode; microwave frequency and sensor used for each soil moisture retrieval; original observation timestamp	Random error estimate for each observation; Flags for spurious observations, day-/nighttime observation, ascending/descending mode; microwave frequency and sensor used for each soil moisture retrieval; original observation timestamp; SNR blending weights
File format	NetCDF-3 classic CF1.5	NetCDF-4 classic CF1.5	NetCDF-4 classic CF1.5	NetCDF-4 classic CF1.6

* v02.1 incorporated a few minor bug fixes and the product name change from ECV SM to ESA CCI SM.

Even though the core of the ESA CCI SM merging framework has basically remained unchanged since its first publication, individual components and data output have been continuously upgraded and expanded. Improvements were commonly triggered by feedback from users and scientific publications. For example, the inclusion of the intermediate ACTIVE and PASSIVE products in the product suite followed the wish of users to test alternative approaches for merging active and passive observations, or to assimilate these products separately into land surface or ecosystem models. The inclusion of ancillary data such as error estimates and flags for spurious retrievals should above all prevent from incorrect usage of the data (Wagner et al. 2014), but also allow for a more in-depth analysis of the dataset and the methods used to produce it, e.g. with regard to the different sensors, frequencies, satellite overpass times, and observation angles. For example, Dorigo et al. (2015b) showed that rebinning observations with different observation times to a common daily 00:00 UTC reference time had a negative impact on the quality of the merged product. Based on this result, it was decided to include also the original observation timestamp in the products, which also facilitates a more direct comparison against data with a sub-daily temporal resolution, like ground probe data, and allows the assimilation of the data in sub-daily model experiments (Miralles et al. 2016).

For the generation of ACTIVE and PASSIVE, the original merging framework (Liu et al. 2012) considered only the highest quality observations available during a certain period. For the COMBINED product, the decision on whether to use for a given pixel either ACTIVE, PASSIVE, or an average of both was based on their relative performance with respect to vegetation optical depth (VOD) obtained from AMSR-E C-band observations (Liu et al. 2012; Owe et al. 2001). However, in the case of sensor failure this led to reduced data coverage (Dorigo et al. 2015b). This issue was most dramatically illustrated by the absence of drought anomalies in the ESA CCI SM v0.1 dataset for the European heatwave of 2003 (Loew et al. 2013; Szczypta et al. 2014), which was caused by the failure of ERS-2, the sensor that was commonly used in this geographical region during that period. From v02.0 to v02.2 this was resolved by filling the data gaps caused by ERS failure with AMSR-E data. However, this resulted in a reduced quality for the gap-filled regions during this period. Moreover, using only the best performing individual dataset (for ACTIVE and PASSIVE) or dataset category (for COMBINED) is suboptimal from a merging perspective as it ignores the information contained in the retrievals that are not selected.

These issues motivated the development of a more rigorous blending scheme, which is for the first time implemented in ESA CCI SM v03.2 (Gruber et al. in review). In this scheme, the blending does not only consider the highest quality observations available during a certain period but uses a weighted average of measurements from all sensors that are available at a certain point in time to compute the merged soil moisture estimate. This results in a merged observation whose random errors are lower than those of each individual input dataset. The blending weight attributed to each dataset is defined as the reciprocal of its random error variance (Yilmaz et al. 2012), estimated separately for each blending period (see Section 3.1) using triple collocation analysis (Gruber et al. 2016b). The error variance is expressed as a signal-to-noise ratio (SNR), which relates the estimated error variance to the signal dynamics at the given location (Gruber et al. 2016b). The weights are obtained separately for each day from the SNR estimates of all datasets that provide a valid measurement on that day. If one or more datasets do not provide a valid measurement on a particular day, the decision whether or not to use the remaining datasets on that day is based on maximum error variance thresholds. This avoids degrading too severely the overall performance of the blended product by filling data gaps with input data that have too high random error variances. Note that this new blending scheme based on weighted averages is used to produce both the ACTIVE, PASSIVE, and COMBINED products. Figure 2 shows the blending weights that were used to produce the COMBINED product of v02.2 (top) and v03.2 (bottom) for the period when only ASCAT and AMSR2 are used (Section 3.1). The general weight patterns are in good agreement between the versions, but in v03.2 the areas that categorically exclude the least performing product are reduced, whilst the weights resolve the abrupt transitions between the active-only and passive-only regions of v02.2 by introducing a gradual transition.

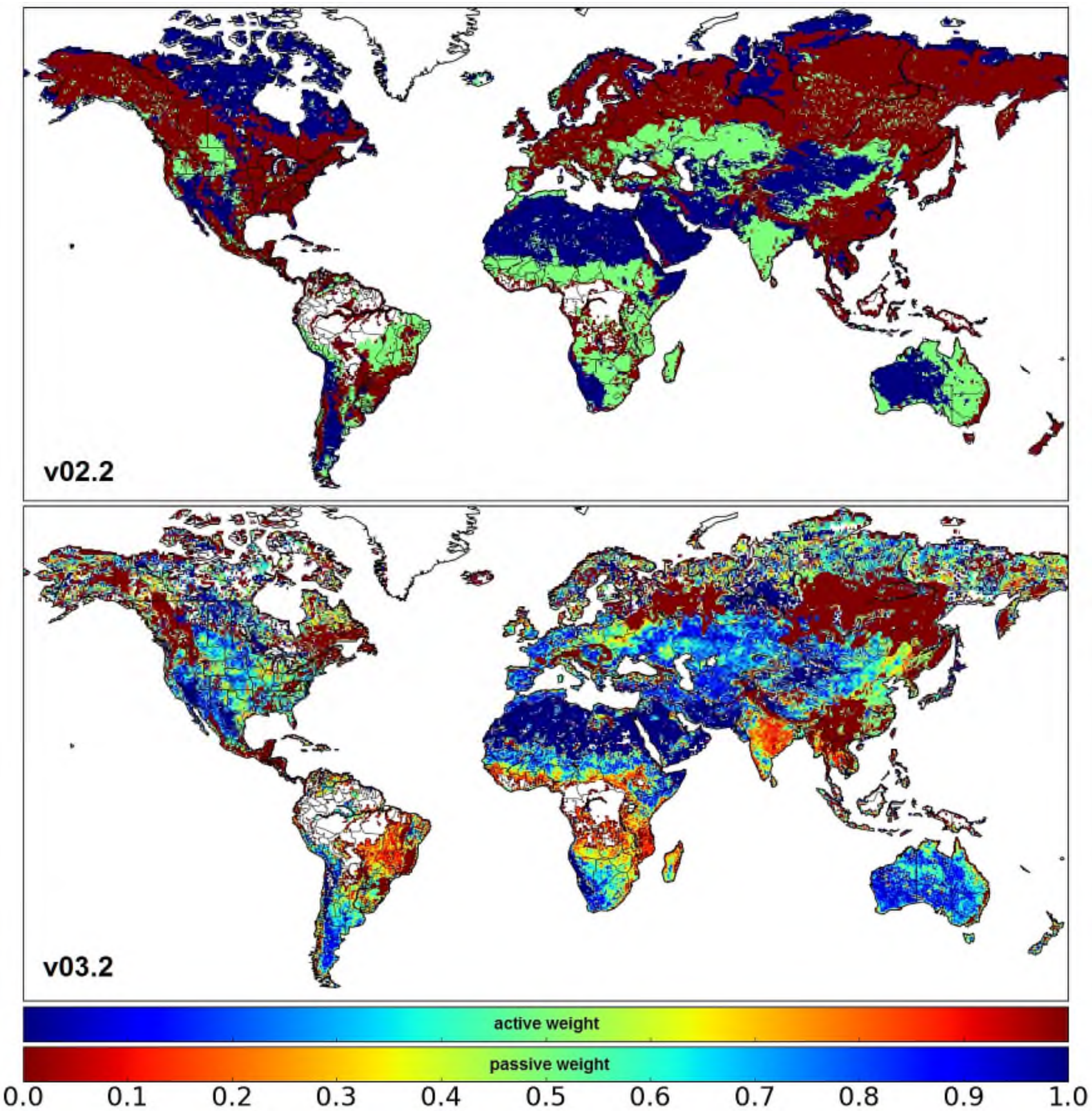

Figure 2 Blending weights attributed to ACTIVE and PASSIVE for the production of COMBINED in the period January-December 2014 when only ASCAT and AMSR2 are used for ESA CCI SM v02.2 (top) and ESA CCI SM v03.2 (bottom).

3 ESA CCI SM data characteristics and quality

3.1 Spatial-temporal coverage

Figure 3 shows the input Level 2 sensors that were used to produce the latest ESA CCI SM v03.2 products. Until October 2007, the sensors used for each period are similar to those used to generate v0.1 (Dorigo et al. 2015b), although all products based on these sensors have undergone algorithmic and/or calibration updates (Table 3). After this date, v03.2 diverges significantly from the earliest version: on the one hand, the products have been extended forward in time and now cover five more years of data (until December 2015). This has been facilitated by the inclusion of additional sensors like WindSat, SMOS, AMSR2 and MetOp-B ASCAT. On the other hand, advances in the blending procedure have facilitated the concurrent use of virtually any number of available datasets. This is reflected both in the ACTIVE and PASSIVE product, as well as in the COMBINED product, which blends up to four different Level 2 input products at the same time (Figure 3). Even more datasets may be simultaneously merged in the future, e.g., with the potential integration of SMAP.

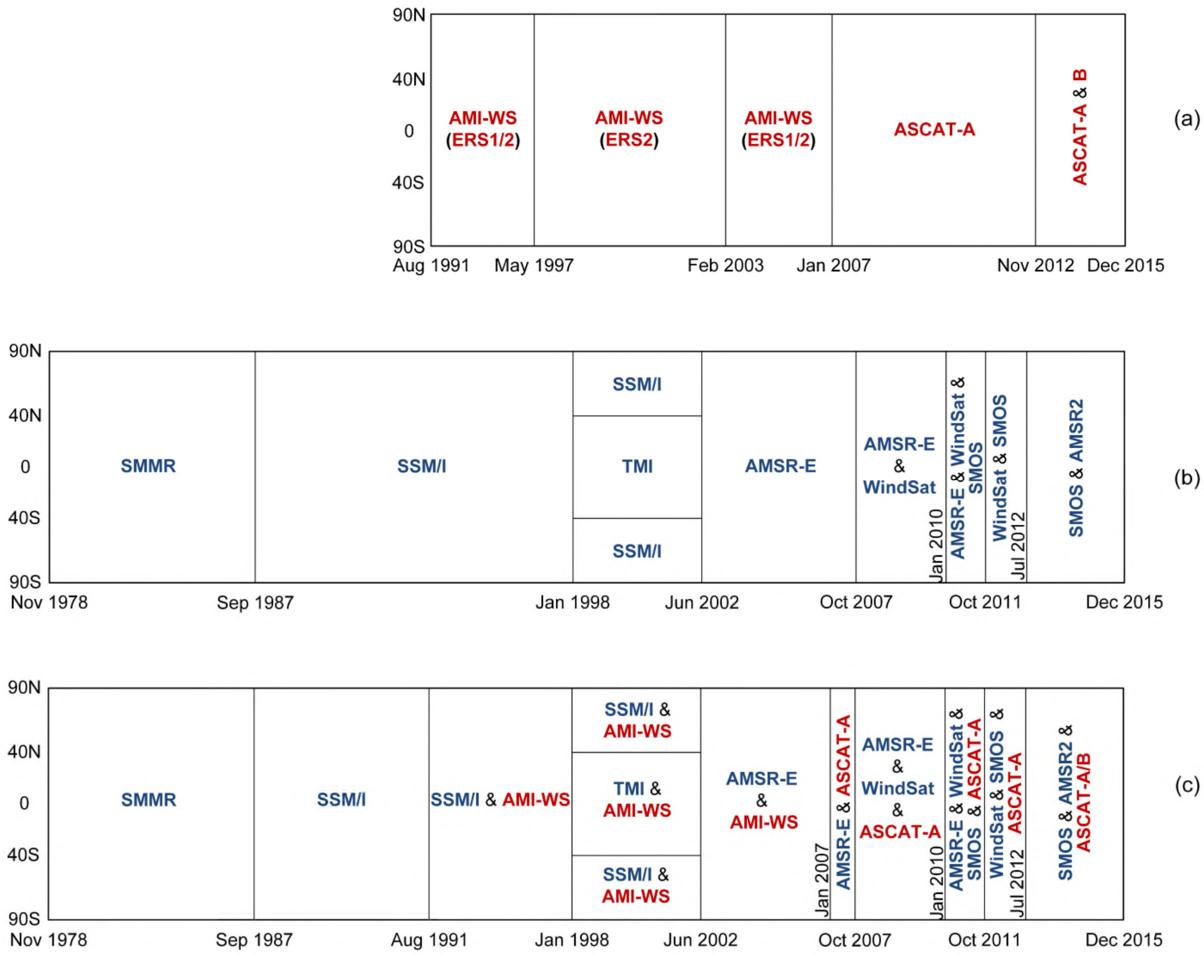

Figure 3 Spatial-temporal coverage of input products used to construct ESA CCI SM v03.2 (a) ACTIVE, (b) PASSIVE, (c) COMBINED. Blue colours indicate passive, red colours active microwave sensors. Modified from Dorigo et al. (2015b). The periods of unique sensor combinations are referred to as 'blending period'.

Combining two or more products increases the likelihood of having at least one observation for a given day and pixel, hence, reducing the number of data gaps. This is reflected by the average temporal observation density (Figure 4), which shows remarkable improvements from version to version: while version v0.1 for the period January 2007 – December 2010 only used MetOp-A ASCAT and AMSR-E data, v02.2 additionally includes WindSat. In version v03.2 also SMOS is introduced. This is visible e.g. for the eastern United States or eastern China, where the average observation frequency in this period has approximately doubled with respect to the first release.

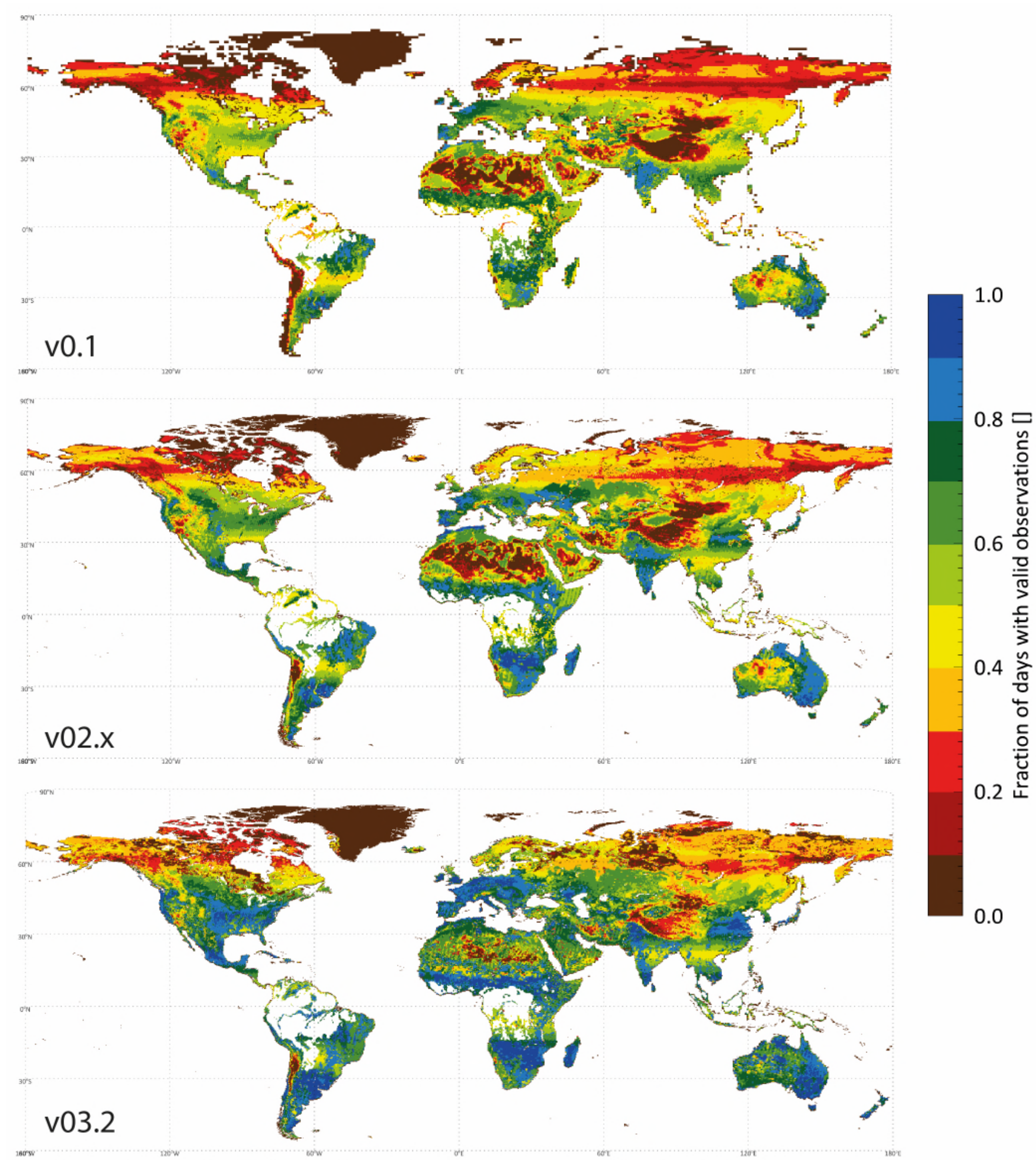

Figure 4 Fractional coverage of ESA CCI SM v0.1 (top), v02.0-v02.2 (middle), and v03.2 (bottom) for the period January 2007 – December 2010, expressed as the total number of daily observations per time period divided by the number of days spanning that time period.

For ESA CCI SM COMBINED v03.2 we observe a steady improvement in spatiotemporal coverage over time, approaching full coverage in more recent years (Figure 5). This directly coincides with the increasing number of satellites becoming available. Nevertheless, neither the increasing number of satellites nor the improved blending techniques are able to mitigate data gaps associated with the physical limitations of microwave observations for soil moisture retrieval (Section 3.2). Consequently, also in the latest product some areas still experience seasonal (e.g., northern latitudes) or even continuous (e.g., tropical rain forests) data gaps. In fact, for some northern regions the observation frequency has even slightly reduced over time due to improved masking of frozen conditions and snow (Figure 5).

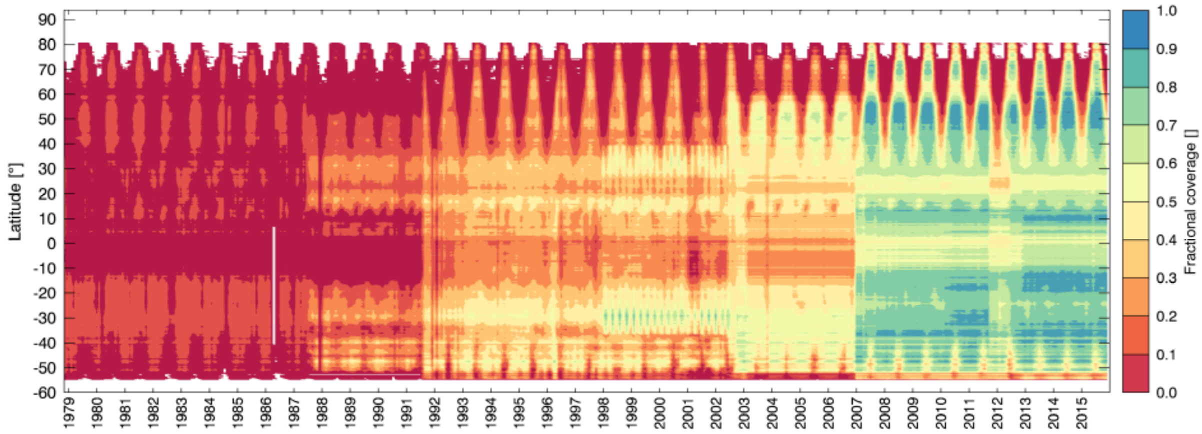

Figure 5 Fraction of days per month with valid (i.e., unflagged) observations of ESA CCI SM v03.2 COMBINED for each latitude and time period.

3.2 Data quality indicators

In both the Level 2 input products and the merged ESA CCI SM products, the quality of individual soil moisture observations is impacted by numerous factors, which can be roughly subdivided into five categories (Table 4): sensor properties, orbital characteristics, environmental conditions, algorithmic skill (e.g., methods used to correct for vegetation impacts), and post-processing (e.g., resampling). While some factors may homogeneously affect the entire globe during the lifetime of a satellite mission (e.g., observation wavelength) others may be variable through space (e.g., topography), time, or both (e.g., frozen soil conditions, vegetation cover). Some factors may entirely impede a realistic retrieval (e.g., snow/ice coverage) while the majority adds some degree of random error and bias to the obtained estimate, the amount of which depends on the nature, intensity, and subpixel area affected (e.g., by vegetation, open water).

Since no observation is free of error, the challenge is to mask only those observations that are below acceptable quality thresholds while providing reliable error estimates for the remainder. The active and passive microwave Level 2 processors flag for frozen soils, snow and ice cover probability, RFI, and failing retrieval. These flags are readily propagated into the ESA CCI SM products and complemented with additional flags and metadata (e.g. for sensor, frequency, ascending/descending mode, dense vegetation, and original observation timestamp). The Level 2 retrieval algorithms also produce uncertainty estimates based on the propagation of uncertainties related to instrument and observation specifications and methodological assumptions (Naeimi et al. 2009; Parinussa et al. 2011). However, combining and merging these error propagation estimates into ESA CCI SM is not trivial as they depend both on the retrieval and the error models used, and implicitly assume that the retrieval models themselves are free of error (Draper et al. 2013). Therefore, the random error estimates provided in ESA CCI SM are based on the triple collocation analysis (see Section 3.3 for details).

Table 4 Main sensor, observational, and environmental factors impacting the quality of the ESA CCI SM products.

Factor	Category	Affects active (A) or passive (P) observations	Impact on soil moisture retrieval	How it is handled in ESA CCI SM v03.2 + potential recommendation for use
Observation frequency / wavelength	Sensor	A,P	Shorter wavelengths (higher frequencies) are more sensitive to vegetation, theoretically causing higher errors. Different wavelengths have different soil penetration depths, and thus represent different surface soil moisture columns.	Preferential use of longer wavelengths when multiple frequencies are available. Indirectly accounted for by SNR-based weighting and indirectly quantified as part of the random error estimate (see below). The frequency and sensor that were used in ESA CCI SM are provided as ancillary data.
Instrument errors and noise	Sensor	A,P	Directly impacts the error of the single-sensor soil moisture retrieval	Included in total random error ESA CCI SM products assessed by triple collocation (see Section 3.3). Soil moisture random error provided as separate variable.
Local Incidence angle and azimuth	Sensor	A	Impacts backscatter signal strength and hence retrieved value	Accounted for by incidence angle and azimuthal correction in Level 2 retrieval. Remaining uncertainty is indirectly quantified as part of random error estimate.
Local observation time	Orbital	A,P	Vegetation water content changes during the day (Steele-Dunne et al. 2012), but this variability is not accounted for by the retrieval models. Early morning observations may be influenced by dew on soil and vegetation, thus leading to higher observed soil moisture. Solar irradiation causes discrepancies between canopy and soil temperatures which complicate the retrieval of soil moisture (Parinussa et al. 2016); see also "Land Surface Temperature" below Intra-daily variations because of convective precipitation and successive evaporation may be missed.	Partly addressed by excluding "day-time" radiometer observations. Remaining uncertainty is indirectly quantified as part of random error estimate.
Vegetation cover	Environmental	A,P	Reduces signal strength from soil and hence increases uncertainty of soil moisture retrieval	Included in total random error of ESA CCI SM products assessed by triple collocation (see Section 3.3). Dense vegetation is masked for passive Level 2 products according to sensor-specific VOD thresholds: Soil moisture random error is provided as a separate variable.
Topography	Environmental	A,P	Impacts backscatter signal strength; causes heterogeneous soil moisture conditions within the footprint	Not accounted for. Topography index is provided as metadata. A flagging of pixels with topography index > 10% is recommended.
Open water	Environmental	A,P	Impacts backscatter and brightness temperature signal strength	Not accounted for. Open water fraction is provided as metadata. A flagging of pixels with open water fraction > 10% is recommended
Urban areas, infrastructure	Environmental	A,P	Impacts backscatter and brightness temperature signal strength	Not directly accounted for. Uncertainty is indirectly quantified as part of random error estimate.
Ice and snow coverage	Environmental	A,P	Obstructs soil moisture information	Masked using radiometer-based land surface temperature observations (Holmes et al. 2009) and freeze/thaw detection (Naeimi et al. 2012) from Level 2 algorithms, and ancillary data from

				ERA-Interim and GLDAS-Noah in ESA CCI SM production. Flag provided as metadata.
Frozen soil water	Environmental	A,P	Strongly impacts observed backscatter / brightness temperatures causing a "false" reduction in soil moisture	Masked using radiometer-based land surface temperature observations (Holmes et al. 2009) and freeze/thaw detection (Naeimi et al. 2012) from Level 2 algorithms, and ancillary data from ERA-Interim and GLDAS-Noah in ESA CCI SM production. Flag provided as metadata.
Dry soil scattering	Environmental	A	Volume scattering causes unrealistic rises in retrieved soil moisture (Wagner et al. 2013b)	Not directly accounted for, but indirectly accounted for by low weight (related to high error) received in SNR-based blending.
Land surface temperature	Environmental	P	Errors in land surface temperature directly impact the quality of surface soil moisture retrievals	Partly addressed by excluding "day-time" radiometer observations. Remaining uncertainty is indirectly quantified as part of random error estimate.
Radio frequency interference (passive only)	Environmental	P	Artificially emitted radiance increases brightness temperatures and, hence, leads to a dry bias in retrieved soil moisture.	In the case of multi-frequency radiometers, a higher frequency channel (e.g. X-band) is used if RFI is detected. In other cases, the observation is masked.

3.3 Random error characteristics from triple collocation

The random error of an observation is – when expressed as SNR – a direct measure of its sensitivity to soil moisture changes (Gruber et al. 2016). Moreover, it defines the weight that the observation should receive when combined with other observations, e.g. through data assimilation (Gruber et al. 2015). The most common way of characterising random errors of satellite-based soil moisture estimates over large scales is triple collocation analysis (TCA), which provides estimates for the average error variance or SNR (e.g., Dorigo et al. 2010; Miralles et al. 2010; Scipal et al. 2008b; Stoffelen 1998). However, since TCA requires a large number of observations, it only provides a single error estimate for a larger time period and not for each observation individually (Zwieback et al. 2012). Moreover, TCA requires the availability of a dataset triplet with independent error structures, which is currently – on a global scale – only provided by a combination of an active microwave, a passive microwave, and an LSM-based soil moisture product. In the ESA CCI SM production, TCA is applied to estimate the error variances of the individual Level 2 input products (see Section 2.3) and - for each blending period separately – the error variances of ACTIVE and PASSIVE, respectively. Surface soil moisture estimates from the GLDAS-Noah v1 LSM provide the third dataset. Unfortunately, TCA cannot be used to evaluate the random error characteristics of COMBINED, since after blending ACTIVE and PASSIVE an additional dataset with independent error structures would be required to complement the triplet. To address this issue, a classical error propagation scheme (e.g., Parinussa et al. 2011) is used to propagate the TCA-based error variance estimates of ACTIVE and PASSIVE through the blending scheme to yield an estimate for the random error variance of the final COMBINED product (Gruber et al. in prep.):

$$var(\varepsilon_c) = w_a^2 var(\varepsilon_a) + w_p^2 var(\varepsilon_p) \qquad \text{(Eq. 1)}$$

where the superscripts denote the COMBINED (c), ACTIVE (a) and PASSIVE (p) datasets, respectively; $var(\varepsilon)$ denotes the error variances of the datasets; and w denotes the blending weights. Note, that similarly as for TCA, the error propagation notation in Eq. 1 assumes mutually independent error structures between ACTIVE and PASSIVE. From Eq. 1 it can be seen that the error variance of the blended product is typically smaller than the error variances of both input products unless they are very far apart, in which case the blended error variance may become equal to or only negligibly larger than that of the better input product.

However, the ACTIVE and PASSIVE input datasets of COMBINED are not perfectly collocated in time since the satellites do not provide measurements every day. Infact, there are days when either only ACTIVE or only PASSIVE provides a valid soil moisture estimate. As described in Section 2.3, we use such single-category observations to fill gaps in the blended product, but only if the error variance is below a certain threshold. Consequently, as inferred from Eq. 1, the random error variance of COMBINED on days with single-category observations is typically higher than that on days with blended multi-category observations. This results in an overall average random error variance of COMBINED that lies somewhere in between the random error variance of the single input datasets and the merged random error variance of all input products (estimated through error propagation) (Gruber et al. in review). How close the actual mean random error variance of COMBINED is to these boundaries depends on the number of days that have been filled with ACTIVE or PASSIVE only. To illustrate this, Figure 6 shows global maps of the estimated random error variances of ACTIVE, PASSIVE, and COMBINED in the period where MetOp-A/B ASCAT, AMSR2, and SMOS are jointly available (July 2012-December 2015). The comparison with VOD from AMSR2 C-band observations (Figure 6d) shows that at the global scale error patterns largely coincide with vegetation density.

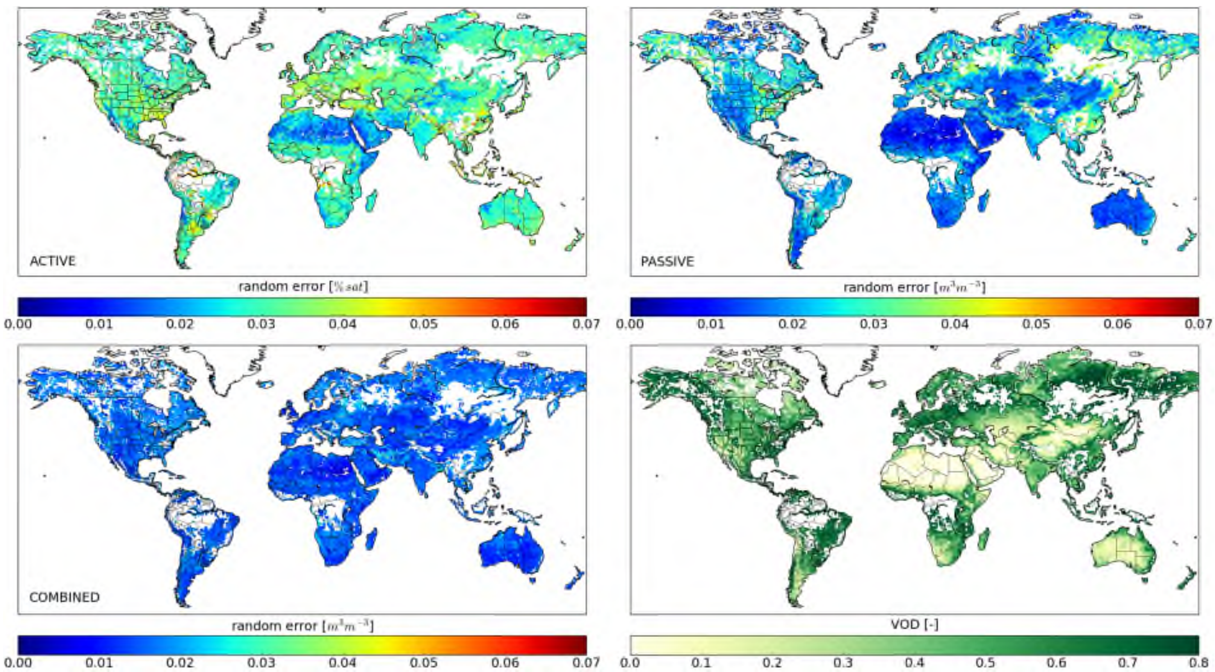

Figure 6 Average error variances of ESA CCI SM for ACTIVE, PASSIVE, and COMBINED estimated through triple collocation and error propagation for the period July 2012-December 2015. d) Long-term (July 2012-December 2015) VOD climatology from AMSR2 6.9 GHz observations.

3.4 Agreement with ground data

Traditionally, the skill of satellite-based soil moisture products is assessed by comparing them against ground-based observations, allwoing for the computation of statistics such as correlation, (unbiased) Root-Mean-Squared-Difference ((ub)RMSD), and bias. Numerous studies have validated the different ESA CCI SM product versions against in-situ soil moisture observations from various sites around the world. The most extensive evaluation of ESA CCI SM v0.1 was undertaken by Dorigo et al. (2015b), who employed all usable observations from the ISMN (Dorigo et al. 2011b; Dorigo et al. 2013) to assess the dataset performance for different regions and blending periods. They found that the dataset performance was slightly better during periods when lower frequency C-band observations are available. Nevertheless, tracking the temporal evolution of dataset performance based on in-situ information was severely hampered by the heterogeneity of the observations and a lack of permanent long-term monitoring sites of homogeneous quality in time (Dorigo et al. 2015b). In their study, Dorigo et al. (2015b) also confirmed that ESA CCI SM v0.1 had a performance which was similar or slightly better than the individual Level 2 input products, underlining the benefit of the merging approach. Albergel et al. (2013b) used several globally available in-situ networks with varying climatic conditions to put the ESA CCI SM v0.1 performance in relation to the skill of ERA-Interim/Land, a revised version of the land components of ERA-Interim (Balsamo et al. 2015) and MERRA-Land (Reichle et al. 2011). Similarly, Fang et al. (2016) performed a large-scale in-situ validation of all three ESA CCI SM v02.2 products and NLDAS2-Noah model simulations. Both studies showed that on average ESA CCI SM agrees well with in-situ observations but that for several networks the correlations still lack behind those obtained for the LSM simulations integrating observed precipitation. It has been suggested that, amongst other factors, this may be due to the discrepancy between the installation depth of the in-situ probes (typically 5 cm) and the typical depth of ~2 cm represented by the C- and X-band satellite products used until v02.2 (Albergel et al. 2013b; Dorigo et al. 2015b). However, a recent study showed that even for L-band microwave observations often this discrepancy exists and that the surface layer represented by the observations is shallower than previously suggested (Shellito et al. 2016).

Several regional and local studies analysed the performance of ESA CCI SM in regions characterised by different climates, land cover, and soil types. Pratola et al. (2014) obtained high correlations (>0.7) between ESA CCI SM v0.1 over various Irish grassland sites, characterized by a humid, temperate climate. Similar correlation values for v0.1 were obtained over grassland sites and agricultural fields in the United States, France, Spain, China, and Australia (Albergel et al. 2013b; An et al. 2016b). For non-grassland sites in China agreements are generally poorer (An et al. 2016b; Mao et al. 2017; Shen et al.

2016). The high altitude sites located on the Tibetan Plateau and in South-Western China, and the Tarim river basin in western China provide an exception. Here, various versions of ESA CCI SM COMBINED agree well with in-situ soil moisture and generally outperform LSM-based soil moisture products and other satellite-based SM products including Level 2 input products from ASCAT, AMSR-E/2, and SMOS (Albergel et al. 2013b; Peng et al. 2015; Su et al. 2016a; Zeng et al. 2015). Also for semi-arid areas, e.g. in Spain or Australia, where satellite observations typically show a high SNR (Gruber et al. 2016b), ESA CCI SM (v0.1) generally agrees well with in-situ observations (Albergel et al. 2013b; Dorigo et al. 2015b).

For certain regions, land cover types, or surface characteristics ESA CCI SM has reduced skill. Sathyanadh et al. (2016) found that over India LSM-based soil moisture products, specifically MERRA-Land, show higher correlations with in-situ data than ESA CCI SM v0.1. Moderate performance of ESA CCI SM v0.1 for this area was also found by Dorigo et al. (2015b). Further, generally poor correlations against in-situ data are found at high latitudes and in boreal forest environments for various versions of the COMBINED product (Dorigo et al. 2015b; Ikonen et al. 2016; Pratola et al. 2015). However, Ikonen et al. (2016) showed that with appropriate approaches to upscale the in-situ data to the satellite footprint - which take into account local information on soil, land cover, and sensor placement - a much better agreement between ground observations and ESA CCI SM can be obtained.

Apart from assessing a temporal and spatial agreement, in-situ data have also been used to assess more intricate properties of ESA CCI SM. Qiu et al. (2016) and Liu et al. (2015) concluded that in China trends in ESA CCI SM COMBINED (v0.1 and v02.1) generally reflected those observed in in-situ observations. In addition, Qiu et al. (2016) concluded that it better captures trends than ERA-Interim/Land and attributed this to the absence of irrigation modules in the latter. Su et al. (2016c) proposed a new methodology based on a large selection of in-situ stations in combination with various breakpoint detection techniques to identify and correct for inhomogeneities in the mean and variance in ESA CCI SM v02.2 related to changes in sensor constellations. The methodology works well for these in-situ stations, but the availability of long-term monitoring stations is too low to apply the method globally. However, Su et al. (2016c) showed that the method showed similar skill in detecting inhomogeneities when using a global LSM instead of in-situ data. For each transition between blending periods the authors observed inhomogeneities associated with sensor changes, although for more recent periods they are less frequent. Finally, Nicolai-Shaw et al. (2015) used a large number of sites over the United States to assess the spatial representativeness of ESA CCI SM v0.1. They concluded that, particularly for the temporal anomalies, ESA CCI SM better matches the spatial representativeness of in-situ observations than ERA-Interim/Land.

Based on the studies above, it can be concluded that the ESA CCI SM COMBINED products generally match relatively well with in-situ observations in temperate climates, over grassland and agricultural areas, and in semi-arid regions, but have difficulties in reflecting the temporal dynamics in the driest and wettest areas. This may be both due to a generally lower SNR of the satellite data over such areas (Gruber et al. 2016b) as well as a reduced skill of certain in-situ probes in extreme conditions (Cosh et al. 2016; Dorigo et al. 2011b). Most of the reported studies focused on temporal correlation (either applied to the soil moisture values directly or to its anomalies) as a comparison metric, which is justifiable, being closely related to metrics such as the (ub)RMSD) (Entekhabi et al. 2010b; Gruber et al. 2016b). Dorigo et al. (2015b) pointed out that one should not use metrics like bias and RMSD to assess the skill of the COMBINED product, as the scaling step involved to combine active and passive observations (See Section 2.2) imposes the dynamic range of the GLDAS-Noah LSM on the ESA CCI SM COMBINED products. In addition, the gap in spatial representativeness of the in-situ point measurement and the coarse satellite footprint introduces additional error to the metrics of agreement, which ideally should be corrected for when using in-situ data for satellite validation (Gruber et al. 2013).

3.5 Comparison against land surface models and gridded precipitation

Since in-situ soil moisture measurements are limited in space, time, and representativeness (Dorigo et al. 2015b), complementary evaluations based on the comparison with independent soil moisture products (e.g. from LSMs, land surface reanalysis) are fundamental for a thorough assessment of the skill of ESA CCI SM as well as to steer algorithmic improvements (Albergel et al. 2013a). Particularly land surface reanalysis products, which in regions with high quality forcing data adequately capture the temporal dynamics of soil moisture (Albergel et al. 2013b), are well suited for this purpose due to their comparable spatial resolution, uniform configuration over time, and global availability. Also comparisons against gridded datasets of climate variables with a close physical link to soil moisture, e.g. precipitation and evaporation, are expected to provide valuable insight into the dataset performance (e.g., Meng et al. 2017).

Several studies compared intra- and inter-annual soil moisture dynamics of ESA CCI SM with various land surface reanalysis products, including ERA-Interim (Dee et al. 2011), ERA-Interim/Land, MERRA-Land, and GLDAS-Noah, as well as with long-term satellite precipitation products such as the Global Precipitation Climatology Project (GPCP; Huffman et al. 2009). In general, good temporal agreement between LSM soil moisture and various versions of ESA CCI SM COMBINED was found in the (sub-)tropics (with the exception of densely vegetated areas like the Amazon or Congo basins) and in central Eurasia (Albergel et al. 2013a; Albergel et al. 2013b; Chakravorty et al. 2016; Dorigo et al. 2012; Loew et al. 2013). ESA CCI SM COMBINED v02.2 showed a skill in capturing wet and dry extreme events over

Eastern Africa comparable to the Variable Infiltration Capacity model and the Noah LSM forced with precipitation from CHIRPS and the remaining meteorological input from MERRA (McNally et al., 2016), while ESA CCI SM COMBINED v02.1 showed a similar soil moisture response to weak monsoon phases in India and Myanmar as the Climate Forecast System Reanalysis (CFSR) produced by NCEP (Shrivastava et al. 2016). Better correlations between ESA CCI SM COMBINED and LSMs are usually obtained in the presence of a significant fraction of bare soil. Also, the latest ESA CCI SM COMBINED v03.2 product generally shows high positive correlations with ERA-Interim/Land, except for parts of the tundra regions, where the two products show a strong anticyclical behaviour (Figure 7a). Comparison with long-term precipitation from GPCP (Figure 7c) shows positive correlations with ESA CCI SM COMBINED over these areas. This suggests that negative correlations may stem from issues in ERA-Interim/Land rather than in ESA CCI SM. However, long-term soil moisture anomalies of ESA CCI SM COMBINED v03.2 and ERA-Interim/Land in the tundra regions mostly do correlate positively (Figure 7b), which may point to a deficiency of ERA-Interim/Land in representing the seasonal cycle.

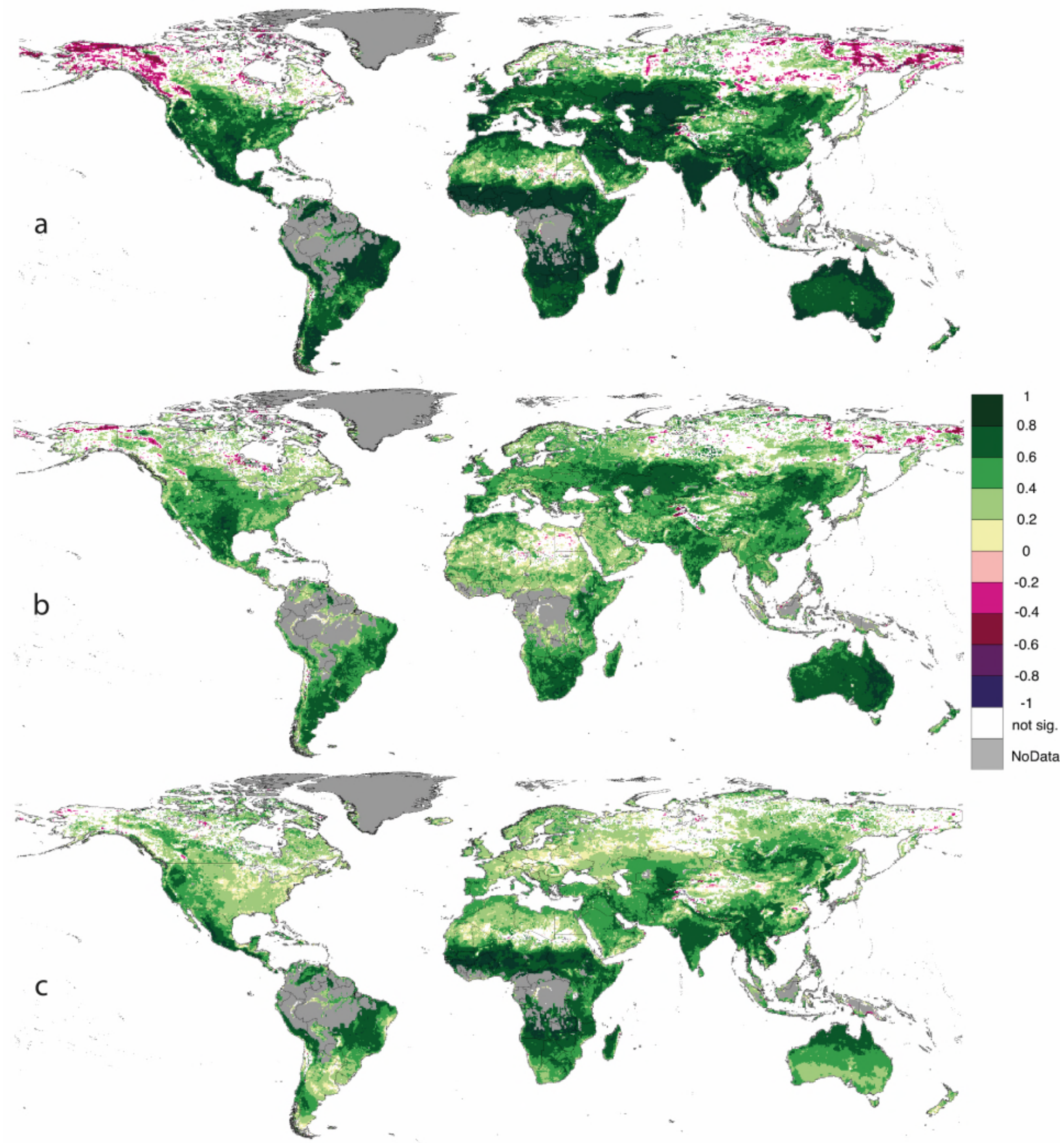

Figure 7 Pearson correlation over the period 1997-2013 of a) ESA CCI SM COMBINED v03.2 and ERA-Interim/Land 0-7 cm soil moisture, b) long-term anomalies of ESA CCI SM COMBINED v03.2 and ERA-Interim/Land 0-7 cm soil moisture, and c) ESA CCI SM COMBINED v03.2 soil moisture and GPCP 1DD precipitation. White areas indicate pixels for which correlations are not significant (p>0.05).

LSM products may be used to assess trend behaviour and dataset stability, even though the forcing used to generate these products often contains inhomogeneities (Ferguson and Mocko 2017). Dorigo et al. (2012) assessed trends in the ESA CCI SM v0.1 combined product for the period 1988–2010, and compared them with trends in soil moisture from LSMs (GLDAS-Noah and ERA-Interim), in satellite-based Normalised Difference Vegetation Index (NDVI) data, and in the GPCP precipitation product. The broad correspondence in trends between ESA CCI SM and the other products lends confidence in the dataset's capability of capturing long-term systematic changes. Albergel et al. (2013a) found that the observed trends in ESA CCI SM v0.1 were also in line with trends in ERA-Interim/Land but deviated more strongly from those in MERRA-Land. Su et al. (2016c) used MERRA-Land to identify discontinuities related to sensor blending periods in ESA CCI SM v02.2 and assessed their potential impact on trend statistics. Even though inconsistencies were detected, trends between ESA CCI SM and MERRA-Land largely agreed. Moreover, Albergel et al. (2013a) tested the consistency of the ESA CCI SM v0.1 over time by correlating it with ERA-Interim/Land surface soil moisture estimates for different sub-periods of the entire data record. They found a slight increase in correlation over time, with the exception of the years dominated by retrievals from Ku-band observations of the SSM/I sensor, which are more sensitive to vegetation. They also highlighted the large effect changes in spatial data coverage can have on global statistics on temporal stability (Albergel et al. 2013a).

Comparing ESA CCI SM to LSM simulations may help to guide future algorithmic updates. For example, Szczypta et al. (2014) compared ESA CCI SM v0.1 to surface soil moisture from the CO_2-responsive version of the ISBA Land Surface Model (Gibelin et al. 2006) over 1991-2008. Simulated surface soil moisture (0-1 cm) generally agreed well with ESA CCI SM and helped to highlight regions where ESA CCI SM had reduced skill, e.g. over the Turkish Tauros mountain chain. This information was used to improve the initial blending scheme over vegetated mountain ranges (Section 2.3). Fang et al. (2016) compared the three products of ESA CCI SM v02.2 against simulated soil moisture from the Noah LSM (Ek et al. 2003) forced with National Land Data Assimilation System (NLDAS)-2 atmospheric forcing over the United States for the period 2000-2013. Considering soil moisture anomaly time series, ESA CCI SM COMBINED v02.2 presented higher correlations with the Noah LSM than ACTIVE or PASSIVE, which highlights the added value of combining active and passive observations using the ESA CCI SM blending technique. Chakravorty et al. (2016) found that ESA CCI SM v02.1 ACTIVE and COMBINED show a similar level of correlation with soil moisture from MERRA-Land. When applying the triple collocation to the three datasets in order to investigate the spatial distribution of random errors, ACTIVE on average has lower random errors than PASSIVE and COMBINED, with exception of the arid desert regions of western India. These results suggest that, at least for this region, the blending of ACTIVE and PASSIVE into COMBINED based on VOD thresholds in v02.1 did not optimally exploit the information contained in the input datasets. This observation provided an important motivation for revising the blending methodology scheme as described in Section 2.3

Another advanced (indirect) validation technique relies on assimilating satellite soil moisture product into a simple water balance model (Crow 2007) or a more sophisticated LSM (Albergel et al. 2017). The obtained updated dataset accounts for the synergies of the various upstream products and provides statistics, which can be used to monitor the quality of the assimilated observations. The French Meteorological service (CNRM, Météo-France) is in the process of implementing an LDAS at both continental and global scale (Albergel et al. 2017; Barbu et al. 2014; Fairbairn et al. 2017). The long-term LDAS statistics can be analysed to detect possible drifts in the quality of the products: innovations (observations vs. model forecast), residuals (observations vs. analysis) and increments (analysis vs. model forecast).

Finally, the possibility to use precipitation data for the assessment of the ESA CCI SM products is currently investigated (Ciabatta et al. 2016). Ciabatta et al. (subm.) used the SM2RAIN algorithm for estimating precipitation from ESA CCI SM data (see Section 4.4). The estimated precipitation data are then compared with ground-observed datasets, e.g., GPCC, characterised by a much larger spatial-temporal coverage than in-situ soil moisture observations, to indirectly assess the quality of the ESA CCI SM products.

3.6 Tracking dataset quality among releases

Evaluating the quality of ESA CCI SM should be continuously repeated once a new dataset version becomes available to assess the potential impact of improved calibrations and algorithmic changes. In this section, we present various methods that are being adopted to assess the impact of product updates. Figure 8 shows the distributions of the correlations between the different ESA CCI SM COMBINED versions and globally available in-situ soil moisture measurements obtained from the ISMN, the North American Soil Moisture Database (Quiring et al. 2015), and the Swiss Soil Moisture Experiment network (Mittelbach and Seneviratne 2012) for the 1991-2010 time period. To comply with the topsoil moisture represented by ESA CCI SM we considered only in-situ measurements down to a maximum of 5 cm depth. For those stations that provide at least two years of data, we calculated the correlation between the daily in-situ measurements and the corresponding grid cell for the longest available time period, while only time steps were used that provide data for all ESA CCI SM versions. Correlations between these stations and ERA-Interim/Land layer 1 (0-7 cm) are provided as reference. Figure 8 shows that on average the data set quality is stable across versions, with a slight tendency towards improved correlations for more recent releases. This confirms that changes in the methodology and input data used generally have a positive impact. Note, that these results are based only on regions where in-situ soil moisture data are available, hence restricting the analysis mainly to the United States and Europe (Dorigo et al. 2015b). Besides, the inclusion of v0.1 limits the common analysis period to end in 2010. Figure S1 in the Supplement shows that generally correlations are higher for more recent periods (2011-2013) in which additional Level 2 input products are integrated (e.g. SMOS, AMSR2, MetOp-B ASCAT).

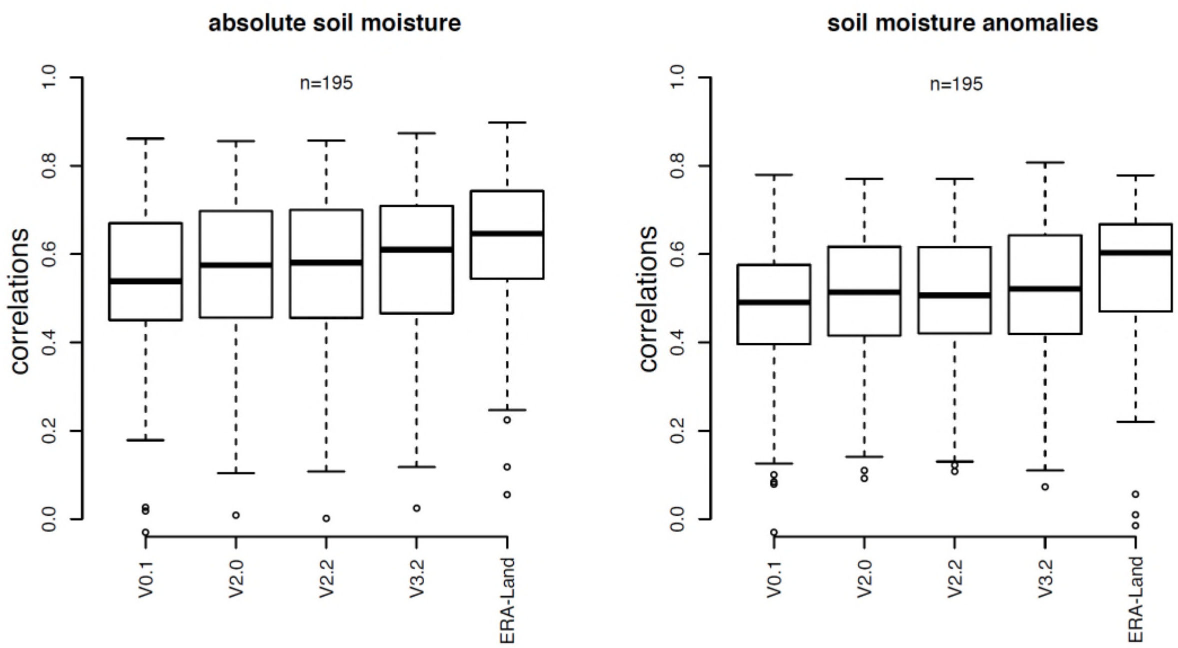

Figure 8 *Boxplots (displaying median, inter-quartile range (IQR), upper (lower) quartile plus (minus) 1.5 times the IQR, and outliers) of the correlations of the publicly released versions of ESA CCI SM COMBINED and ERA-Interim/Land with globally available in-situ probe observations down to a maximum depth of 5 cm, both for absolute values and long-term soil moisture anomalies. Only observations within the period 1991-2010 were considered.*

As an alternative to the in-situ-based skill tracking, which has a strong regional and temporal bias (Dorigo et al. 2015b), changes between dataset releases can be assessed by comparing them to a fixed global reference, e.g. provided by an LSM. Figure 9 plots the correlations between two versions of ESA CCI SM COMBINED (v0.1 and v02.2) and the first layer (0-7 cm) of ERA-Interim/Land. Each triangle represents the median global correlation over a 3-year sub-period within the period 1979-2010, similarly as in Albergel et al. (2013a). Only locations that show a significant correlation for each 3-year sub-period in both versions are considered. For both absolute soil moisture values (left) and anomalies (right) all symbols fall below the 1:1 line. Since error correlations between any of the ESA CCI SM datasets and ERA-Interim/Land are expected to be close to zero (Gruber et al. 2016a), all increases in the correlation can be reliably interpreted as an increase in the SNR for the newer ESA CCI SM product. Differences between the two versions are smaller in the most recent sub-periods, which may be related to the fact that algorithmic updates, i.e., a change from LPRM v3 to v5 (see Table 3) and filtering of spurious observations herein have had a larger impact on the Level 2 radiometer products used before 2002 (the year in which AMSR-E was introduced) than on the relatively high quality products used after this date.

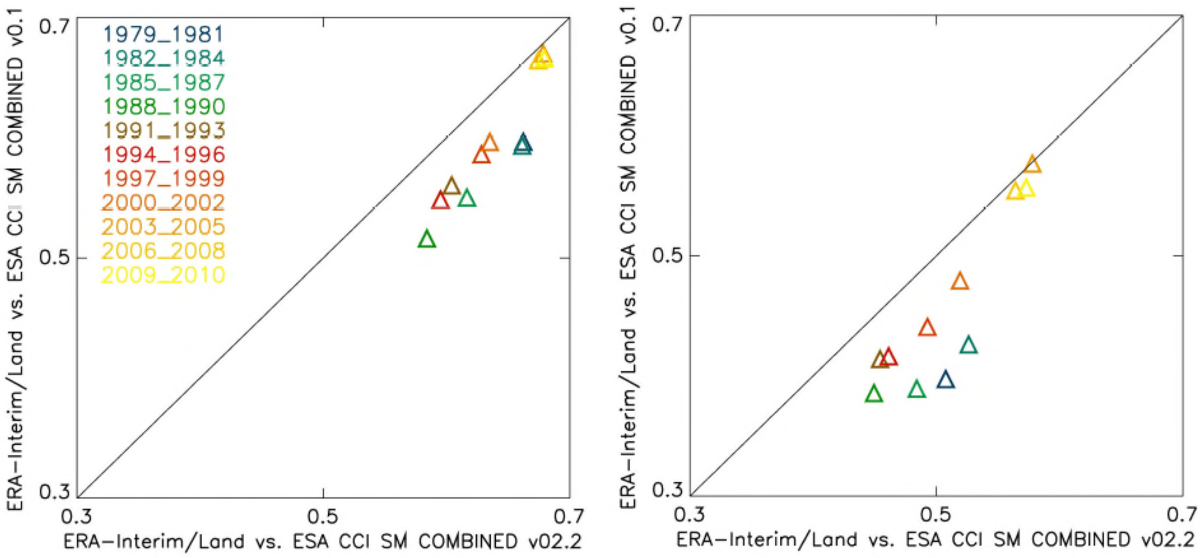

Figure 9. Correlations between soil moisture from the first soil layer (0-7 cm) of ERA-Interim/Land and ESA CCI SM COMBINED v0.1 (y-axis) and v02.2 (x-axis), respectively. The left image shows the results for absolute values, the right image for anomalies from a 35-day moving window. Each triangle represents the median global correlation over a 3-year period, similar as in (Albergel et al. 2013a). Only pixels that show significant correlations (p<0.05) for both product versions and for all periods were used in the computation of the global median values.

Figure 10 shows the differences in correlation between soil moisture from the first soil layer (0-7 cm) of ERA-Interim/Land and ESA CCI SM COMBINED of v02.1 and v03.2, respectively. Figures S2 and S3 in the Supplement show the changes in correlation for the intermediate product updates and reveal that the most prominent changes occur between v02.2 and v03.2, illustrating the impact of the new merging scheme (Section 2.3). The figures show that most areas and land cover types, particularly moderately vegetated areas, experienced an overall improvement in correlation, both for absolute values and anomalies. In contrast, in desert areas correlations are lower for the latest product release, which is most likely related to the filling of temporal gaps in the passive microwave time series with lower quality active microwave observations (Dorigo et al. 2010). Thus, in these areas the increase in fractional coverage observed in Figure 4 goes at the cost of the product accuracy. It should be noted however that a decrease in correlation with ERA-Interim/Land does not always indicate a reduction in product skill, as ERA-Interim/Land may not capture all soil moisture variations correctly (e.g. Figure 7). Hence, assessing changes in product skill over time should entail a combination of methods and reference datasets.

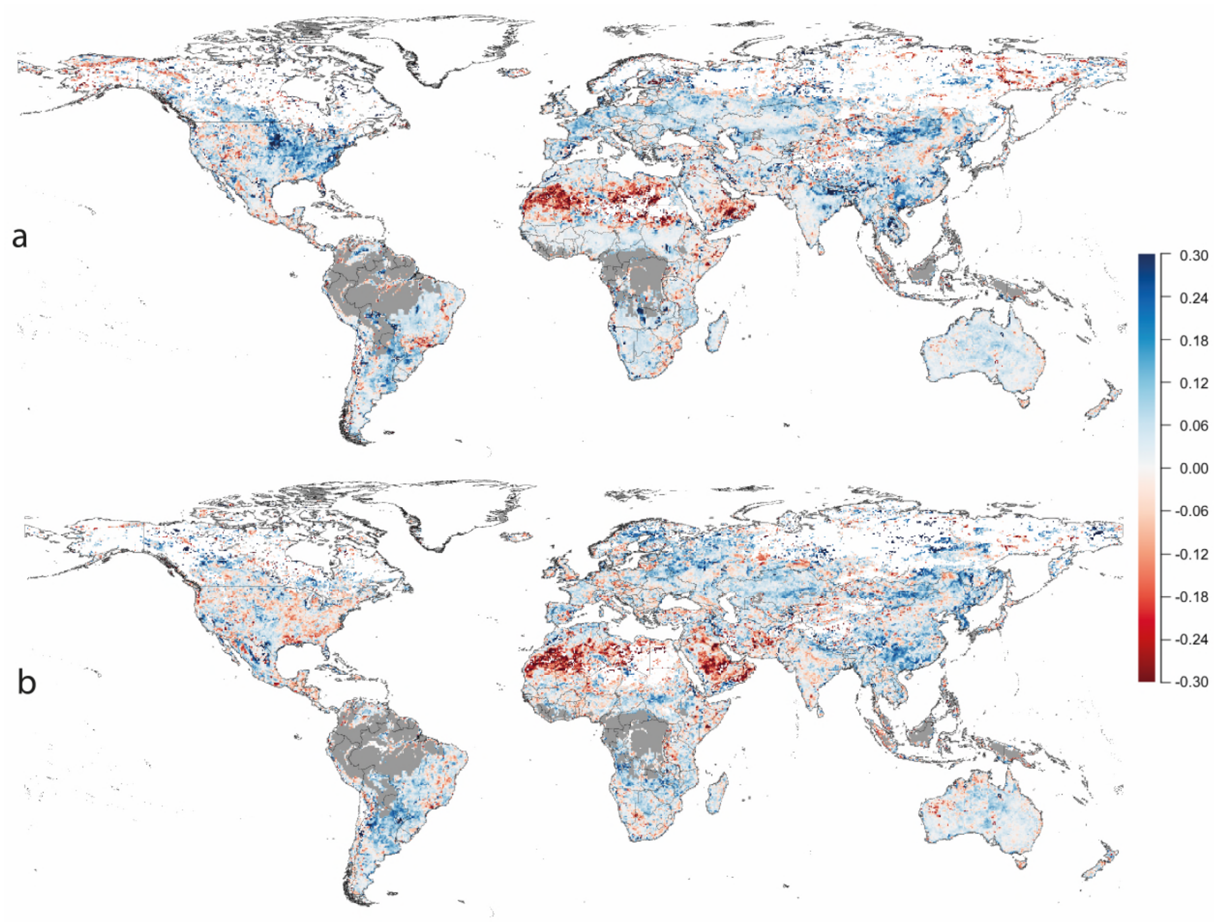

Figure 10. Differences in correlation between soil moisture from the first soil layer (0-7 cm) of ERA-Interim/Land and ESA CCI SM COMBINED v03.2 and v02.1, respectively for a) absolute soil moisture; b) long-term soil moisture anomalies. Blue colours denote an increase in correlation from v02.1 to v03.2, red colours a decrease, grey colours no change, and white colours areas where no significant correlations (p<0.05) were observed for one or both product versions. Correlations were computed for the period 1997-2013.

4 ESA CCI SM in Earth system applications

A wide variety of studies have explored the potential of ESA CCI SM product for improving our understanding of Earth system processes, in particular with respect to climate variability and change (Table 5). Even though the application fields are seemingly different, in all of them ESA CCI SM plays a central role in benchmarking, calibrating, or providing an alternative to the land surface hydrology in dedicated models. The following sections will provide an extensive synthesis of how ESA CCI SM has been used in the different application areas, the motivation of each study for using this product in particular, and the main drawbacks encountered when using the ESA CCI SM data. A synthesis of the limitations and the unexploited potential of the dataset is given in Section 5. For our assessment, we reviewed all scientific papers that correctly cite any of the key publications on the dataset (i.e., Dorigo et al. 2012; Dorigo et al. 2015b; Liu et al. 2012; Liu et al. 2011; Wagner et al. 2012) and were listed either in Scopus (http://scopus.com/) or Google Scholar (https://scholar.google.com) as of June 22, 2017.

Table 5: Applications where ESA CCI SM has been used to improve our Earth system understanding. Modified from Dorigo and De Jeu (2016).

Application area	Main purpose	References	Motivation for using ESA CCI SM	Limitations identified
Climate variability and change	Long-term trends in soil moisture	Albergel et al. (2013b); An et al. (2016b); Dorigo et al. (2012); Feng and Zhang (2015); Li et al. (2015); Qiu et al. (2016); Rahmani et al. (2016); Su et al. (2016c); Wang et al. (2016); Zheng et al. (2016)	Long-term coverage needed for robust trend assessment	No global coverage; no representation of root-zone; data quality changes over time
	Assessment of drivers of soil moisture trends	Chen et al. (2017); Feng (2016); Liu et al. (2015); Meng et al. (2017); Zhan et al. (in press)	Long-term coverage for robust driver assessment	Data gaps in time and space
	Soil moisture as driver of multi-annual variability in land evaporation	Miralles et al. (2014b)	Independent evidence of long-term trends and variability in modelled soil moisture, constraining errors in water balance model	Not mentioned
	Impact of ocean atmosphere system on soil moisture variability	Bauer-Marschallinger et al. (2013); Miralles et al. (2014b); Nicolai-Shaw et al. (2016)	Long-term dataset required for assessing low impact of frequency climate oscillations	Data periods with reduced spatial coverage
	Soil moisture as indicator of global climate variability and change	De Jeu et al. (2011); De Jeu et al. (2012); Dorigo et al. (2014); Dorigo et al. (2015a); Dorigo et al. (2016); Dorigo et al. (accepted); Parinussa et al. (2013)	Assess actual soil moisture condition with respect to historical context	Lack of global coverage hampers assessment of mean global and hemispherical trends
	Impact of soil moisture on trends in aerosols	Klingmüller et al. (2016)	Long-term coverage required for robust trend and driver assessment	Not mentioned
	Validation of ESMs and climate models (mean fields, spatial patterns, temporal variability, trends)	Agrawal and Chakraborty (2016); Du et al. (2016); Huang et al. (2016); Lauer et al. (in press); Pieczka et al. (2016); Ruosteenoja et al. (2017); van den Hurk et al. (2016); Yuan and Quiring (2017)	Potential for assessing long-term climatology, variability, and trends	Layer thickness not consistent among models and satellite observations; ESA CCI SM uncertainties are larger than the RMSE of many of the models; data gaps due to frozen soils, snow, and dense vegetation.
	Validation and sensitivity analysis of regional climate models	Pieczka et al. (2016); Unnikrishnan et al. (2017)	Potential for assessing long-term climatology, variability, and trends	Evaluation of absolute values not possible; discrepancy in layer thickness represented.

	Assimilation in regional climate model	Paxian et al. (2016)	Not mentioned	Not mentioned
	Variability of precipitation and soil moisture during South Asian Monsoon	Shrivastava et al. (2016, 2017)	Convergence of evidence together with reanalysis soil moisture and precipitation, robust assessment of inter-annual variability	Temporal data gaps during monsoon season
Land atmosphere interactions	Improved understanding of soil moisture feedbacks on precipitation	Guillod et al. (2014); Guillod et al. (2015) (indirectly, through assimilation of ESA CCI SM into GLEAM)	Constraining errors in water balance model over long period	Not mentioned
	Feedback of antecedent soil moisture on Tibetan and Indian monsoon intensity	Zhou et al. (2016); (KanthaRao and Rakesh)	Long-term dataset for robust statistics	Dataset not suitable due to large data gaps in winter
	Identifying role of soil moisture on temperature variability and heatwaves	Casagrande et al. (2015); Hirschi et al. (2014); Miralles et al. (2014a)	Constraining errors in water balance model over long period by data assimilation; long period provides robust coupling statistics	No representation of root-zone soil moisture; lacking information about exact sampling depth
	Observation-based land-atmosphere coupling (to evaluate coupling of LSM products and ensembles)	Catalano et al. (2016); Knist et al. (2017); Li et al. (2016); Li et al. (2017)	Independent reference for long period.	Spatial data gaps; seasonal variation in spatial coverage
	Improved modelling of land evaporation	Martens et al. (2017); Miralles et al. (2014b); Park et al. (2017)	Constraining errors in water balance model over long period by data assimilation	Negative impact in very dry areas and areas where quality of precipitation is high
	Explaining trends in evapotranspiration	Rigden and Salvucci (2017); Zeng et al. (2014)	Long-term availability for trend assessment	Not mentioned
	Impact of soil moisture (among other drivers) on dust aerosol dynamics	Klingmüller et al. (2016); Xi and Sokolik (2015)	Long-term coverage required for robust trend and driver assessment	Not mentioned
Global biogeochemical cycles and ecology	Evaluation of global vegetation models	Sato et al. (2016); Szczypta et al. (2014); Traore et al. (2014) Willeit and Ganopolski (2016)	Long-term coverage for robust statistics	Poor performance for some mountain ranges; No data available for densely vegetated areas; seasonal variation in spatial coverage
	Impact of soil moisture dynamics on vegetation productivity	Barichivich et al. (2014); Chen et al. (2014); Cissé et al. (2016); Ghazaryan et al. (2016); Liu et al. (2017b); McNally et al. (2016); Muñoz et al. (2014); Nicolai-Shaw et al. (in press); Papagiannopoulou et al. (2016); Papagiannopoulou et al. (2017); Szczypta et	Long-term coverage for robust assessment of drivers	Poor data quality and data gaps for densely vegetated areas, frozen conditions, and mountain areas; temporal data gaps

		al. (2014); Wu et al. (2016)		
	Validation of dry season intensity indicator	Murray-Tortarolo et al. (2016)	Lon-term dataset required for robust evaluation	Not mentioned
	Impact of large-scale re-vegetation on soil moisture	Jiao et al. (2016a)	Long-term coverage allows for trend assessment	Not mentioned
	Connecting trends in soil moisture and vegetation productivity	Dorigo et al. (2012); Feng (2016)	Long-term coverage required for trend assessment	Spatial data gaps, ESA CCI SM has trend removed before 1987
	Assessing ecosystem water use efficiency	He et al. (2017)	Long-term data availability for robust statistics	Reduced quality over densely vegetated areas; high uncertainty for earlier periods
	Improved crop modelling	Park et al. (2017); Sakai et al. (2016); Wang et al. (2016); Wang et al. (2017)	Complementarity of active and passive microwave soil moisture for different land cover types; assessment of long-term links between soil moisture and vegetation	Poor performance along coasts; differences in spatial scale; representativeness for fragmented landscapes; impact of irrigation; spatiotemporal data gaps
	Assessing drivers of fire activity	Forkel et al. (2016); Ichoku et al. (2016)	Long-term availability is essential for assessing dynamics and drivers of infrequent fire activity	No coverage for dense vegetation, temporal gaps
	Potential for constraining terrestrial carbon cycle simulations by data assimilation	Kaminski et al. (2013); Scholze et al. (2017)	Long-term data availability	Accurate description of random error for each observation; Does not provide estimate of root-zone soil moisture
	Assessment of satellite-observed carbon fluxes	Detmers et al. (2015)	Long-term availability	Not mentioned
	Forcing for simulating global atmospheric CH_4 uptake by soils	Murguia-Flores et al. (2017)	Long-term availability	Data gaps for dense vegetation
	Soil moisture as driver of animal species migration	Madani et al. (2016)	Long-term dataset required for robust pattern assessment	Coarse resolution
	Impact of wind farms on environmental conditions for vegetation growth	Tang et al. (2017)	Long-term availability	Not mentioned
Hydrological and land surface modelling	Evaluating model *states* in hydrological models and LSMs	Du et al. (2016); Fang et al. (2016); Lai et al. (2016); Lauer et al. (in press); Loew et al. (2013); Mao et al. (2017); Okada et al. (2015); Rakovec et al. (2015); Schellekens et al. (2017); Spennemann et al. (2015); Szczypta et al. (2014) Ghosh et al. (2016); Mishra et al.	Robust statistics based on long comparison period	Not suited for validating absolute values (bias, root-mean-square-difference); discrepancy between model and observation layer depths; different dataset characteristics for different periods (variance, data gaps);

		(2014); Mueller and Zhang (2016); Parr et al. (2015)		spatiotemporal data gaps.
	Evaluating model *processes* in hydrological models and LSMs (e.g. dry down)	Chen et al. (2016b)	More realistic dry down characteristics than LSM-based soil moisture	None
	Assimilated to constrain coupled LSM and hydrological simulations	Albergel et al. (2017)	Long-term availability	No impact on deeper soil layers
	Used to estimate the error covariance matrix of an ensemble of LSM simulations in order to optimally merge them.	Crow et al. (2015)	Long data record length essential for reducing sampling errors	large temporal variations in temporal frequency, actual spatial resolution, and accuracy; dependency on GLDAS-Noah as scaling reference; differences in vertical measurement support between models and observations
	Persistence and prediction of soil moisture anomalies in LSMs	Nicolai-Shaw et al. (2016)	Long-term dataset required for robust statistics	Exact vertical measurement support unknown
	Improving runoff predictions and flood (risk) modelling	Massari et al. (2015); Tramblay et al. (2014)	Not specified	Not mentioned
	Calibrating Soil and Water Assessment Tool hydrological model	Kundu et al. (in press)	Not specified	Only few model parameters sensitive to surface soil moisture
	Improved water budget modelling	Abera et al. (2016); Allam et al. (2016)	Long-term availability for more robust statistics	Vertical measurement support too shallow to provide indication of changes in soil and ground water storage
	Computing changes in groundwater storage	Asoka et al. (2017)	Long-term availability for trends assessment	Not mentioned
	Modelling surface water dynamics	Heimhuber et al. (2017)	Long-term availability for more robust statistics	Not mentioned
	Assessing irrigation	Kumar et al. (2015); Qiu et al. (2016)	Long-term data required for trend-based method of Qiu et al. (2015)	Coarse spatial resolution for detecting fine scale irrigation
	Assessing the impact of agricultural intensification on soil moisture	Liu et al. (2015)	Long-term data coverage needed for long-term impacts	Spatial gaps
	Trigger of landslides	Dahigamuwa et al. (2016)	Long-term availability	Not mentioned
	Improving satellite rainfall retrievals	Bhuiyan et al. (in review-a); Bhuiyan et al. (in review-b); Kumar et al. (2015); Qiu et al. (2016)	Data record spans multiple satellite precipitation missions	Not mentioned
	Computing cumulative precipitation amounts	Ciabatta et al. (subm.); Ciabatta et al. (2016); Liu et al. (2015)	Long data record needed for generation of long-	Too low signal-to-noise ratio in some areas; spatial and temporal data gaps

			term precipitation dataset	
	Validating soil moisture products derived from precipitation	Dahigamuwa et al. (2016); Das and Maity (2015)	Long-term availability for robust statistics	Not mentioned
Drought applications	Validation of drought indices	van der Schrier et al. (2013) Liu et al. (2017a)	Lon-term dataset required for robust assessment	Reduced temporal coverage before 1991
	Development of new drought monitoring index	Carrão et al. (2016); Enenkel et al. (2016b); Rahmani et al. (2016)	Long-term dataset required for robust computation of normal soil moisture distributions	Variable data availability in time; reduced data quality over densely vegetated areas; not available in near-real-time
	Improved detection of agricultural droughts	Liu et al. (2015); Padhee et al. (2017); Yuan et al. (2015a)	Long-term dataset required for robust long-term statistics	Because of temporal data gaps extreme events may not be captured; reduced skill of COMBINED compared to ACTIVE in densely vegetated areas
	Probabilistic drought forecasting	Asoka and Mishra (2015); Linés et al. (2017); Yan et al. (2017)	Long-term dataset required for robust computation of normal soil moisture distributions	Coarse resolution; data gaps
	Soil moisture for integrated drought monitoring and assessment	Cammalleri et al. (2017); Enenkel et al. (2016b); McNally et al. (2016); (Nicolai-Shaw et al. in press); Rahmani et al. (2016)	Long-term dataset required for robust long-term statistics	Poor spatio-temporal coverage prior to 1992; spatial data gaps; lack of root-zone soil moisture
	Evaluation of drought forecasting systems	McNally et al. (2017); Shah and Mishra (2016); Yuan et al. (2015b)	Long-term availability for robust evaluation. Sensitivity to wetlands (which are not represented LSMs).	Poor spatio-temporal coverage prior to 1992; differences in representative depth
(Hydro)meteorological applications	NWP model evaluation	Arnault et al. (2015)	Not mentioned	Discrepancy in scale
	Supporting NWP land surface scheme improvements	This study (Section 4.6)	Long-term dataset required for robust evaluation of land surface scheme	Spatial data gaps for densely vegetated areas
	Assimilation into NWP model	Zhan et al. (2016)	Reducing uncertainties in temperature and humidity	Not mentioned

4.1 Climate variability and change

As soil moisture is an integrative component of the Earth system, any large scale variability or change in our climate should manifest itself in globally observed soil moisture patterns. In this role, ESA CCI SM has made a significant contribution to the body of evidence of natural and human-induced climate variability and change. Indicative for this, is the contribution of ESA CCI SM to the State of the Climate

Reports that are issued every year by National Oceanic and Atmospheric Administration (e.g., Blunden and Arndt 2016). Several studies have shown a clear relationship between major oceanic-atmospheric modes of variability in the climate system, e.g. El Niño Southern Oscillation (ENSO), and variations in ESA CCI SM (Bauer-Marschallinger et al. 2013; Dorigo et al. 2016; Miralles et al. 2014b); Nicolai-Shaw et al. (2016). By applying enhanced statistical methods to the multi-decadal ESA CCI SM v0.1 dataset over Australia, Bauer-Marschallinger et al. (2013) were able to disentangle the portion of soil moisture variability that is driven by the major climate oscillations affecting this continent, i.e., ENSO, the Indian Ocean Dipole and the Antarctic Oscillation, from other modes of short-term and long-term variability. Miralles et al. (2014b) showed that inter-annual soil moisture variability as observed by ESA CCI SM COMBINED v02.2 largely drives the observed large-scale variability in continental evaporation.

ESA CCI SM has been widely used to assess global trends in soil moisture, mostly in combination with LSMs. Based on ESA CCI SM v0.1, Dorigo et al. (2012) revealed that for the period 1988–2010 27% of the area covered by the dataset showed significant trends, of which almost three quarters were drying trends. A similar conclusion was drawn by Feng and Zhang (2015) based on ESA CCI SM COMBINED v02.1. The strong tendency towards drying was largely confirmed by trends computed for the same period from ERA-Interim and GLDAS-Noah (Dorigo et al. 2012), and ERA-Interim/Land and MERRA-Land (Albergel et al. 2013b), although the spatial trend patterns were not everywhere congruent between datasets. The agreement in trends between a newer version of ESA CCI SM (v02.2) and MERRA-Land were recently confirmed by Su et al. (2016c). Trend analyses performed on a more regional scale, but for different time periods (e.g., An et al. 2016b; Li et al. 2015; Rahmani et al. 2016; Wang et al. 2016; Zheng et al. 2016) generally confirmed the results obtained at the global scale, while providing a more detailed view on the impact of local land management practices, e.g. irrigation, on observed trends (Qiu et al. 2016), and the impact of soil moisture trends on regional climate (Klingmüller et al. 2016). Feng (2016) assessed the drivers of trends in ESA CCI SM COMBINED v02.2 and concluded that at the global scale climate change is by far the most important driver of long-term changes in soil moisture, although at the regional level land cover and land use change may play a significant role. Similar conclusions were drawn by regional studies over China (Chen et al. 2017; Liu et al. 2015; Meng et al. 2017). Other studies analysed the variability and trends in ESA CCI SM in relation to other atmospheric variables and circulation patterns over Asia (Shrivastava et al. 2016, 2017; Zhan et al. in press). Nevertheless, given the limited data record length, the impact of low-frequency climate oscillations on trends should first be carefully addressed before any robust conclusion about the sign and magnitude of perpetual changes can be drawn (Miralles et al. 2014b). Likewise, the potential impact of dataset artefacts should be carefully quantified and corrected for (Su et al. 2016c).

ESA CCI SM has been widely used as a reference for evaluating model states and trends in global and regional climate simulations. Different versions of ESA CCI SM COMBINED were used to systematically evaluate soil moisture states, trends, and dynamics of models participating in the latest Coupled Model Intercomparison Project (CMIP5) (Du et al. 2016; Huang et al. 2016; Lauer et al. in press; Yuan and Quiring 2017). At the regional scale, various studies used ESA CCI SM COMBINED to assess the sensitivity to soil moisture of various processes in global and regional climate models (Agrawal and Chakraborty 2016; Pieczka et al. 2016; Unnikrishnan et al. 2017) or to improve climate simulations by assimilating ESA CCI SM directly (Paxian et al. 2016). Even though most studies report positive experiences, the use of ESA CCI SM for climate model evaluations is primarily limited by discrepancies in surface layer thickness between models and satellite observations, the existence of spatial data gaps, and the fact that it does not provide an independent reference for evaluating absolute values. Despite these limitations, ESA CCI SM has been proposed (together with other land-based products) as an official reference for validating the land surface components of the CMIP6 models (van den Hurk et al. 2016).

4.2 Land-atmosphere interactions

As soil moisture is essential in partitioning the fluxes of water and energy at the land surface, it can affect the dynamics of humidity and temperature in the planetary boundary layer. This control of soil moisture on evapotranspiration is important for the intensity and persistence of heatwaves, as the depletion of soil moisture and the resulting reduction in evaporative cooling may trigger an amplified increase in air temperature (Fischer et al. 2007; Hirschi et al. 2011; Miralles et al. 2014a; Seneviratne et al. 2006b). While many studies on soil moisture–evapotranspiration and soil moisture–temperature coupling are based on modelling results or use precipitation-based drought indices as a proxy for soil moisture, ESA CCI SM enables analyses based on long-term observed soil moisture estimates (Casagrande et al. 2015; Hirschi et al. 2014; Miralles et al. 2014a). Therefore, ESA CCI SM in combination with other large-scale observations has been widely used to evaluate the coupling diagnostics found in models (Catalano et al. 2016; Knist et al. 2017; Li et al. 2016; Li et al. 2017; Zhou et al. 2016).

Limitations with respect to the depth of the soil moisture retrievals (i.e., reporting the content of moisture in the first few centimetres as opposed to the entire root depth affecting transpiration) have triggered some debate about the appropriateness of ESA CCI SM to investigate evapotranspiration dynamics and atmospheric feedbacks (Hirschi et al. 2014). Hirschi et al. (2014) showed that the strength of the relationship between soil moisture and temperature extremes appears underestimated with ESA CCI SM compared to estimates based on the Standardized Precipitation Index (SPI; McKee et al. 1993; Stagge et al. 2015), which seems to be related to an underestimation of the temporal dynamics and of large dry/wet anomalies within ESA CCI SM. This effect is enhanced under extreme dry conditions and may lead to a decoupling of the surface layer from deeper layers and from atmospheric fluxes (and resulting temperatures). Thus the added value of root-zone soil moisture is likely more important for applications dealing with extreme conditions, while for mean climatological applications the information content in the surface layer appears adequate. The assimilation of remote sensing surface soil moisture into a land surface model (e.g., Albergel et al. 2017; Lannoy and Reichle 2016) provides a possible alternative here. In fact, root zone soil moisture estimates by the satellite-based Global Land Evaporation Amsterdam Model (GLEAM; Miralles et al. 2011) have been improved by the assimilation of ESA CCI SM, while the overall quality of evaporation estimates remains similar after assimilation (Martens et al. 2017). Also, the assimilation of ESA CCI SM COMBINED v02.1 helped interpreting global land evaporation patterns and multi-annual variability in response to the El Niño Southern Oscillation (Miralles et al. 2014b). The obvious link between soil moisture and evaporation has motivated several studies to use ESA CCI SM COMBINED (v0.1 and v02.1) to attribute trends observed for evaporation (Rigden and Salvucci 2017; Zeng et al. 2014).

Soil moisture also affects precipitation through evapotranspiration. Yet, the effect of soil moisture on precipitation is much more debated than for air temperature. Studies report both positive or negative feedbacks, and even no feedback. Using a precursor of ESA CCI SM, Taylor et al. (2012) identified a spatially negative feedback of soil moisture on convective precipitation regarding the location, i.e., that afternoon rain is more likely over relatively dry soils due to mesoscale circulation effects. Guillod et al. (2015) revisited the soil moisture effect on precipitation using GLEAM root-zone soil moisture with ESA CCI SM COMBINED v02.1 assimilated, and showed that spatial and temporal correlations with opposite signs may coexist within the same region: precipitation events take place preferentially during wet periods (moisture recycling), but within the area have a preference to fall over comparatively drier patches (local, spatially negative feedbacks).

A more indirect but potentially strong soil moisture – atmosphere feedback was found by Klingmüller et al. (2016), who were able to link an observed positive trend in Aerosol Optical Depth (AOD) in the Middle East to a negative trend in ESA CCI SM COMBINED v02.1. As lower soil moisture translates into enhanced dust emissions, their results suggested that increasing temperature and decreasing relative humidity in the last decade have promoted soil drying, leading to increased dust emissions and AOD. Also Xi and Sokolik (2015) found significant correlations between the variability in AOD and soil moisture. These changes in atmospheric composition again may have considerable impact on radiative forcing and precipitation initiation (Ramanathan et al. 2001) and as such impact the energy and water cycles in the area.

4.3 Global biogeochemical cycles and ecosystems

Soil moisture is a regulator for various processes in terrestrial ecosystems such as plant phenology, photosynthesis, biomass allocation, turnover, and mortality, and the accumulation and decomposition of carbon in soils (Carvalhais et al. 2014; Nemani et al. 2003; Reichstein et al. 2013; Richardson et al. 2013). Low soil moisture during drought reduces photosynthesis, enhances ecosystem disturbances such as insect infestations or fires, and thus causes plant mortality and accumulation of dead biomass in litter and soils (Allen et al. 2010; McDowell et al. 2011; Thurner et al. 2016). The release of carbon from soils to the atmosphere through respiration is also controlled by soil moisture (Reichstein and Beer, 2008). Consequently, soil moisture is a strong control on variations in the global carbon cycle (Ahlström et al. 2013; Poulter et al. 2014; van der Molen et al. 2012).

Despite the importance of soil moisture for the global carbon cycle, satellite-derived soil moisture data are currently under-explored in carbon cycle and ecosystem research. Because long-term soil moisture observations were lacking until recently, most studies on the effects of soil moisture on vegetation relied on precipitation estimates (Du et al. 2013; Poulter et al. 2013), indirect drought indices (Hogg et al. 2013; Ji and Peters 2003), or soil moisture estimates from land surface models (Forkel et al. 2015; Rahmani et al. 2016). More recently, studies used ESA CCI SM to assess impacts of water availability and droughts on plant phenology and productivity based on satellite-derived vegetation indices and variables such as the NDVI or the Leaf Area Index (LAI), or directly of vegetation productivity (Murray-Tortarolo et al. 2016). For example, Szczypta et al. (2014) used ESA CCI SM v0.1, modelled soil moisture, and LAI over the Euro-Mediterranean zone to evaluate two land surface models and to predict LAI anomalies over cropland. LAI was predictable from ESA CCI SM in large homogeneous cropland regions, e.g. in Southern Russia (Szczypta et al. 2014). Strong positive relationships between ESA CCI SM COMBINED and NDVI and/or LAI were also found for Australia (Chen et al. 2014; v0.1; Liu et al. 2017b; v02.1), for croplands in North China (Wang et al. 2016; v0.1; Wang et al. 2017; v02.1) and the Ukraine (Ghazaryan et al. 2016; v02.1), for East Africa (McNally et al. 2016; v02.1; Wu et al. 2016; v02.0), and Senegal (Cissé et al. 2016; v0.1). Generally, many regions with positive (greening) or negative (browning) trends in NDVI show also positive and negative trends in ESA CCI SM v0.1, respectively (Dorigo et al. 2012). This co-occurrence of soil moisture and NDVI trends reflects the strong water control on vegetation phenology and productivity. Interestingly, soil moisture from ESA CCI SM v0.1 was also correlated with NDVI in some boreal forests, which are primarily temperature-controlled (Barichivich et al. 2014). In these regions, soil moisture and vegetation productivity were controlled by variations in the accumulation and thawing of winter snow packs (Barichivich et al. 2014). However, some water-limited regions showed negative ESA CCI SM v0.1 soil moisture trends with no corresponding trend in NDVI (Dorigo et al. 2012). In these cases, the positive relation between surface soil moisture and vegetation is likely modified by vegetation type and vegetation density (Feng, 2016; McNally et al., 2016). For example, densely vegetated areas in East Africa show stronger correlations between ESA CCI SM COMBINED v02.1 soil moisture and NDVI than sparsely vegetated areas (McNally et al., 2016). Regional differences in the response of ecosystems to soil moisture variability have also been attributed to differences in water use efficiency (He et al. 2017). Novel data-driven approaches enable quantification of the share of ESA CCI SM in controlling NDVI variability as opposed to other water and climate drivers (Papagiannopoulou et al. 2016; Papagiannopoulou et al. 2017). Figure 11 shows the correlation between the latest ESA CCI SM COMBINED (v03.2) product and NDVI GIMMS 3G (Tucker et al. 2005) with a lag time of soil moisture preceding NDVI of 16 days. In most regions and especially in water-limited areas such as the Sahel, there is a strong and direct response of NDVI to soil moisture. On the other hand, correlations are negative in many temperate regions. This is likely because NDVI is highest in summer months when soil moisture decreases. This demonstrates that vegetation productivity in temperate regions is primarily temperature-controlled and strongly affected by human activities through agriculture or forest management (Forkel et al. 2015; Papagiannopoulou et al. 2017).

Apart from the analysis of relations with vegetation indices, the ESA CCI SM datasets have been used in other ecosystem studies. For example, Muñoz et al. (2014) investigated tree ring chronologies of conifers in the Andeans in conjunction with soil moisture variability from ESA CCI SM v0.1. The study revealed a previously unobserved relation between tree growth and summer soil moisture (Muñoz et al., 2014). While most studies have looked at the impact of soil moisture on vegetation, only very few studies have assessed the opposite, i.e. the impact of vegetation on soil moisture. One such example is the study of Jiao et al. (2016b) who looked at the impact of large-scale reforestation on soil moisture in China. Indirect links between soil moisture and ecosystem dynamics have been the studies of Madani et al. (2016), who used ESA CCI SM COMBINED v0.1 as one of the predictors of Emu migrations in Australia and of Tang et al. (2017) who assessed the impact of wind farms on ESA CCI SM COMBINED v02.2 and vegetation productivity.

Furthermore, ESA CCI SM v0.1 and vegetation data were used to evaluate ecosystem models (Sato et al. 2016; Szczypta et al. 2014; Traore et al. 2014; Willeit and Ganopolski 2016). Thereby, the results of Traore et al. (2014) demonstrate that a model that best performs for soil moisture does not necessarily best perform for plant productivity. This demonstrates the need to jointly use soil moisture and vegetation or carbon cycle observations to improve global ecosystem/carbon cycle models (Kaminski et al. 2013; Scholze et al. 2016). The use of the ESA CCI SM in such an analysis could potentially constrain model uncertainties regarding the long-term hydrological control on vegetation productivity and ecosystem respiration (Detmers et al. 2015; Scholze et al. 2017). However, a major source of uncertainty about the future terrestrial carbon cycle is related to how global ecosystem models represent carbon turnover, vegetation dynamics, and disturbances such as fires (Friend et al. 2014). It was previously shown that variations in satellite-derived soil moisture are related to extreme fire events in boreal forests (Bartsch et al. 2009; Forkel et al. 2012). Consequently, the ESA CCI SM COMBINED dataset has been used together with climate, vegetation, and socio-economic data to assess controls on fire activity globally and to identify appropriate model physics structures for global fire models (Forkel et al. 2016; Ichoku et al. 2016). Because of the role of soil moisture on microbial activity, ESA CCI SM v0.1 has been used as one of the forcings to simulate global atmospheric methane uptake by soils (Murguia-Flores et al. 2017).

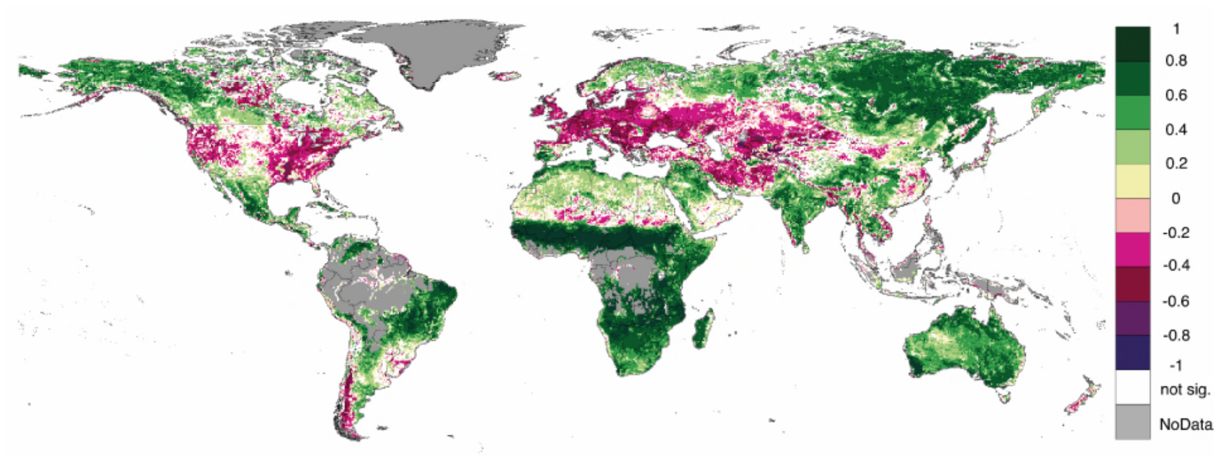

Figure 11: Mean Pearson correlation coefficient R between ESA CCI soil moisture v03.2 and GIMMS NDVI3g for the period 1991 to 2013 for a lag time of soil moisture preceding NDVI by 16 days. White areas indicate pixels for which correlations are not significant (p>0.05).

4.4 Hydrological and land surface modelling

As soil moisture drives processes like runoff, flooding, evaporation, infiltration, and ground water recharge, it is important that hydrological models accurately map soil moisture states. The potential of using ESA CCI SM to validate surface soil moisture fields in state-of-the-art LSMs, reanalysis products, and large-scale hydrological models has been largely recognized (Fang et al. 2016; Ghosh et al. 2016; Lai et al. 2016; Loew et al. 2013; Mao et al. 2017; Mishra et al. 2014; Mueller and Zhang 2016; Okada et al. 2015; Parr et al. 2015; Rakovec et al. 2015; Spennemann et al. 2015; Szczypta et al. 2014). Schellekens et al. (2017) exploited the long-term availability of ESA CCI SM COMBINED v02.2 to validate according to the standardised International Land Model Benchmarking (ILAMB) protocol the soil moisture fields of ten global hydrological and land surface models, all forced with the same meteorological forcing dataset for the period 1979-2012. New insights in the model representation of hydrological processes like infiltration have been offered by comparing the memory length (Chen et al. 2016b; Lauer et al. in press) and the frequency domains (Polcher et al. 2016) between LSMs and remote sensing products, including ESA CCI SM COMBINED v02.3. Crow et al. (2015) utilized ESA CCI

SM v0.1 to estimate the error covariance matrix for an ensemble of LSM simulations of surface soil moisture in order to optimally merge them. The authors claim that the long period covered by the ESA CCI SM product is essential for removing sampling error in these estimates. Similarly as for climate model evaluations, the use of ESA CCI SM for hydrological model evaluations is hampered by discrepancies in surface layer thickness between models and satellite observations, the existence of spatial data gaps, heterogeneity of data properties over time, and the dependency of the absolute values in an LSM (Table 5).

Satellite soil moisture data can bring important benefits in runoff modelling and forecasting both through an improved initialisation of rainfall-runoff models and through data assimilation techniques that allow for updating the soil moisture states. Several studies have shown the positive impact on flood and runoff prediction through assimilation of single sensor Level 2 products used in ESA CCI SM, e.g. obtained from ASCAT (Brocca et al. 2010), AMSR-E (Sahoo et al. 2013), and SMOS (Lievens et al. 2015). Wanders et al. (2014) and Alvarez-Garreton et al. (2015) showed the improved skill of runoff predictions when jointly assimilating multiple soil moisture products (SMOS, ASCAT and AMSR-E), resulting mainly from improved temporal sampling. Long-term homogeneous soil moisture products like ESA CCI SM become important in flood modelling studies that require a multi-year period for the calibration and validation of model parameters. Assimilating the ESA CCI SM COMBINED v02.2 product over the Upper Niger River basin improved runoff predictions even though the simulation of the rainfall-runoff model was already good (Massari et al. 2015). Tramblay et al. (2014) used ESA CCI SM v0.1 to better constrain model parameters, and hence reduce uncertainties, of a parsimonious hydrological model in the Mono River basin (Africa), with the goal to evaluate the impact of climate change on extreme events. Further studies are clearly needed to assess the full potential of ESA CCI SM product for runoff modelling and forecasting. For example, even a simple model based only on persistence allows for the prediction of soil moisture (Nicolai-Shaw et al. 2016), and exploiting this characteristic could contibute to improved early warning systems. At the local scale, Dahigamuwa et al. (2016) used ESA CCI SM v0.1 in combination with vegetation cover to improve the prediction of landslide ocurrence.

ESA CCI SM products have been used for improving the quantification of the different components of the hydrological cycle, i.e. evaporation (Allam et al. 2016; Martens et al. 2017; Miralles et al. 2014b), groundwater storage (Asoka et al. 2017), and rainfall (Bhuiyan et al. in review-a; Bhuiyan et al. in review-b; Ciabatta et al. 2016). Soil moisture contains information on antecedent precipitation. This principle is being exploited by the SM2RAIN method (Brocca et al. 2014; Brocca et al. 2013), which uses an inversion of the soil-water balance equation to obtain a simple analytical relationship for estimating precipitation accumulations from the knowledge of a soil moisture time-series. The method has been tested on a wide range of Level 2 satellite soil moisture products and ESA CCI SM COMBINED v02.2 (Brocca et al. 2014; Ciabatta et al. 2016). SM2RAIN realistically reproduces daily precipitation amounts when compared to gauge observations and in certain regions may even outperform direct satellite-based estimates of precipitation, even though its performance hinges on the quality of the soil moisture product used as input (Brocca et al. 2014; Ciabatta et al. 2016). Its application to ESA CCI SM COMBINED provides an independent global climatology of precipitation from 1979 onwards. Abera et al. (2016) used the SM2RAIN precipitation product from ESA CCI SM (Ciabatta et al. subm.; Ciabatta et al. 2016) to quantify the space-time variability of rainfall, evaporation, runoff and water storage for the Upper Blue Nile river basin in Africa.

Heimhuber et al. (2017) used ESA CCI SM (version unknown) in a statistical framework to predict the dynamics in surface water in south-eastern Australia. ESA CCI SM has also been used to map large-scale irrigation, which is largely unquantified on a global scale and, consequently, not included in most large scale hydrological and/or land surface models (Qiu et al. 2016). By comparing modelled and satellite soil moisture data, irrigated areas can be detected when satellite data and modelled data (the latter do not include irrigation) show different temporal dynamics. Kumar et al. (2015) used satellite soil moisture observations from ESA CCI SM COMBINED v02.1, ASCAT, AMSR-E, SMOS, and WindSat for dtecting irrigation over the United States. Similarly, Qiu et al. (2016) detected irrigated areas in China by evaluating the differences in trends between ESA CCI SM COMBINED v02.1 and precipitation. Liu et al. (2015) used ESA CCI SM v0.1 to support the attribution of negative trends in soil moisture in Northern China to agricultural intensification.

4.5 Drought applications

Soil moisture droughts, also referred to as agricultural droughts, may be driven by a lack of precipitation and/or increased evapotranspiration (Seneviratne et al. 2012). In addition to natural variability, human land modification and water management can contribute to agricultural drought (Liu et al. 2015; Van Loon et al. 2016). Prior to the availability of global satellite-based soil moisture datasets, precipitation and temperature gridded datasets were favoured for developing drought monitoring indices. Well-known examples, although primarily indicative of meteorological drought rather than agricultural drought, are the SPI and the Palmer Drought Severity Index (PDSI; Palmer 1965). ESA CCI SM has been repeatedly used to evaluate the performance of such indices (Liu et al. 2017a; van der Schrier et al. 2013).

ESA CCI SM can be used to directly monitor agricultural drought, or help to set up alternative drought indicators. For example, Carrão et al. (2016) and Rahmani et al. (2016) used ESA CCI SM COMBINED (v02.0 and v02.1, respectively) to develop a drought index comparable to SPI but based on actual soil moisture observations instead of precipitation, naming them the Empirical Standardized Soil Moisture

Index (ESSMI) and Standardized Soil Moisture Index (SSI), respectively. Carrão et al. (2016) found high correlations between ESSMI and maize, soybean, and wheat crop yields in Latin America and with this index could accurately describe the severe and extreme drought intensities in north-eastern Brazil in 1993, 2012, and 2013. Based on SSI, Rahmani et al. (2016) were able to identify a severe drought event that started in December 2012 in the northern part of Iran. The Enhanced Combined Drought Index (ECDI) proposed by Enenkel et al. (2016b) combines ESA CCI SM COMBINED v02.2 with satellite-derived observations of rainfall, land surface temperature and NDVI for the detection of drought events, and has been successfully used to detect large-scale drought events in Ethiopia between the years 1992-2014.

McNally et al. (2016) specifically evaluated the use of ESA CCI SM COMBINED v02.2 for agricultural drought and food security monitoring in East Africa, and found that ESA CCI SM is a valuable addition to a 'convergence of evidence' framework for drought monitoring. Like Dorigo et al. (2015b) they emphasize that users should be aware of the spatial and temporal differences in data quality caused for example by significant data gaps prior to 1992, the lack of overlap between sensors, or difficulties with soil moisture retrievals over certain terrains such as heavily vegetated areas. Post 1992, McNally et al. (2016) generally found good agreement between ESA CCI SM and other soil moisture products as well as with NDVI in East Africa. Yuan et al. (2015a) assessed the skill of ESA CCI SM v02.1 in capturing short-term soil moisture droughts over China. They found that the PASSIVE and COMBINED products have better drought detection skills over the sparsely vegetated regions in north-western China while ACTIVE worked best in the more densely vegetated areas of eastern China.

At the global scale, Miralles et al. (2014b) identified the effect of El Niño-driven droughts in soil moisture, NDVI and evaporation, using GLEAM and ESA CCI SM COMBINED v02.1. This in combination with the high persistence of soil moisture (Nicolai-Shaw et al. 2016; Seneviratne et al. 2006a) makes the ESA CCI SM dataset valuable for the monitoring and prediction of drought events. Hence, various versions of ESA CCI SM COMBINED have been used as a piece of evidence for probabilistic drought monitoring and forecasting in India (Asoka and Mishra 2015; Padhee et al. 2017), Spain (Linés et al. 2017), and the United States (Yan et al. 2017). Recently, ESA CCI SM COMBINED v02.2 was used to validate the predictions of process-based drought forecasting models applied in Sub-Saharan Africa (McNally et al. 2017) and India (Shah and Mishra 2016).

4.6 (Hydro)meteorological applications

Numerical Weather Prediction (NWP) involves the use of computer models of the Earth system to simulate how the state of the Earth system is likely to evolve over a period of a few hours up to 1-2 weeks ahead. It also considers longer timescales (seasonal and climate) through the notion of seamless prediction (Palmer et al. 2008). A number of studies provide strong support for the notion that high skill in short- and medium-range forecasts of air temperature and humidity over land requires proper initialization of soil moisture (Beljaars et al. 1996; Douville et al. 2000; Drusch and Viterbo 2007; van den Hurk et al. 2012). There is evidence also of a similar impact from soil moisture on seasonal forecasts (Dirmeyer and Halder 2016; Koster et al. 2011; Koster et al. 2004; Weisheimer et al. 2011).

Remotely sensed soil moisture datasets like ESA CCI SM can serve NWP by offering a long-term, consistent, and independent reference against which NWP output fields can be evaluated. This may eventually improve meteorological forecasts through a better representation of the land surface and of the fluxes between the land surface and the atmosphere in the NWP (see Section 4.2). For example, Arnault et al. (2015) used ESA CCI SM (version unknown) to evaluate soil moisture predicted with a Weather Research and Forecast (WRF)-Hydro Coupled Modeling System for West Africa. Recently, ECMWF made an offline development in its Land Surface Model HTESSEL (Balsamo et al. 2015; Balsamo et al. 2009), making it possible to add extra layers of soil as well as changing their thickness (Mueller et al. 2016). An experiment was run which increases the number of soil layers from four to nine and reduces the thickness of the upper soil layer from seven (0-7 cm) to one (0-1) centimetre. One of the rationales for having this thin topsoil layer is having a surface layer that is closer to the depth sampled by existing satellite observations and thus allowing for a better assimilation of these observations. Soil moisture from the first layer of two offline experiments, forced by ERA-Interim reanalysis, and considering either a 1 cm depth (GE8F) or a 7 cm depth (GA89) layer was compared to the ESA CCI SM COMBINED v02.2 over the period 1979-2014. Correlations were computed for absolute soil moisture and anomaly time series from a 35-day moving average (Dorigo et al. 2015b). We illustrate differences in correlation between the two experiments in Figure 12. The red colours illustrate that in most areas using a 1 cm instead of a 7 cm surface layer depth leads to a better match with the ESA CCI SM COMBINED dataset. Positive differences frequently reach values higher than 0.2, particularly for correlations on anomaly time series, which shows that a thinner model layer better mimics satellite-observed surface soil moisture variations, as was expected.

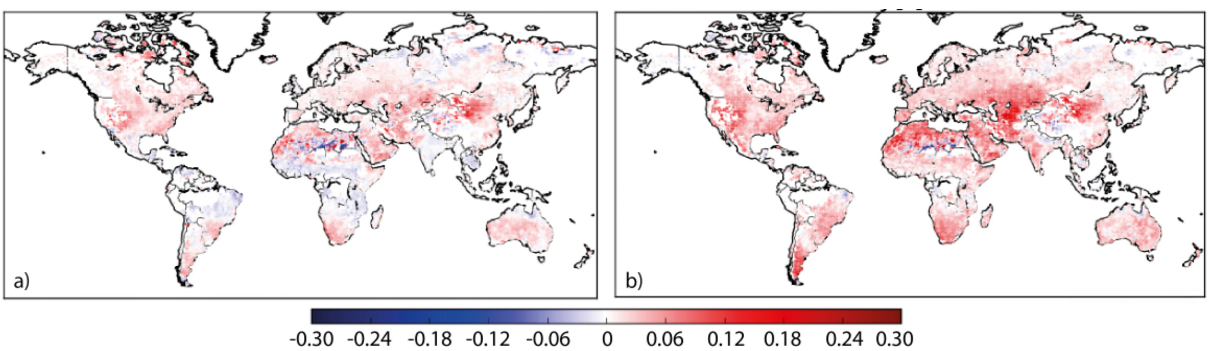

Figure 12 Differences in correlations of absolute soil moisture values (left) and anomalies (right) differences between ESA CCI SM COMBINED v02.2 and soil moisture from the first layer of soil of two offline experiments over 1979-2014. Experiment GE8F has a first layer of soil of 1 cm depth (0-1cm), GA89 of 7 cm depth (0-7cm). Differences are only shown for pixels that provide significant correlations (p<0.05) for both experiments. Pixels where these conditions are not met have been left blank.

Few studies have assimilated remotely sensed soil moisture directly into NWPs and climate models to update their soil moisture fields. Even though this mostly leads to a significant improvement of the model's soil moisture fields, its impact on the meteorological forecast itself, e.g. on 2 metre air (T2m) temperature (Bisselink et al. 2011), screen temperature or relative humidity predictions (de Rosnay et al. 2013; Dharssi et al. 2011; Scipal et al. 2008a), is typically limited in areas with dense coverage of the ground-based meteorological observing network and difficult to evaluate in poorly observed areas. We are only aware of one study that assimilated ESA CCI SM (version unknown) directly into an NWP to update its soil moisture field (Zhan et al. 2016). This study showed that assimilating ESA CCI SM into the NASA Unified WRF model coupled with NASA Land Information System could decrease the RMSEs of near-surface air temperature and humidity for certain forecasts and decrease the biases of NUWRF model longer term rainfall forecasts more significantly than those of the shorter term forecasts.

5 Closing the gap between Earth system research requirements and observations

Our overview of product characteristics in Section 3 shows that the ESA CCI SM products are able to overcome several of the drawbacks that single-sensor products have with respect to their applicability in a climate context, particularly concerning the dataset length and revisit times. Even though ESA CCI SM is approaching the requirements outlined in the 2015 GCOS Status Report our analysis also shows that these characteristics vary significantly through space and time. Thus, it is often not meaningful to capture certain dataset characteristics in a single statistical number. Besides, the GCOS requirements present only a high-level consensus view on what is required to meet the increasing and more varied needs for climate data and information (GCOS-200 2016). Therefore, our review of validation and application studies is crucial for identifying more specific requirements and the degree to which these are currently met by ESA CCI SM. It reveals that not all applications have the same requirements: for example, while for flood forecasting a high observation density appears to be of ultimate importance, this may be less crucial when studying long-term global trends in mean soil moisture. Based on our review we see the following research priorities for improving ESA CCI SM and soil moisture CDRs in general.

Higher spatial resolutions

Higher spatial resolutions are required to serve more regional applications, e.g., to map the impact of irrigation on local water budgets or to assess the impacts of local soil moisture variability on atmospheric instability (Taylor et al. 2013). Higher spatial resolutions of ESA CCI SM can be either achieved by including observations with higher native resolution (e.g. SAR, thermal infrared) or by applying appropriate downscaling techniques to the coarse scale observations (An et al. 2016a; Peng et al. 2016).

Filling data gaps and improved temporal sampling

Many users and applications have difficulties in dealing with intermittent data. A way to address this would be the creation of gap-filled time series, which would improve the nominal observation density. At the same time, increasing the actual (real) observation density prior to 2002 to a daily resolution would be required to have a significant impact on data assimilation, e.g. in hydrological models or land surface reanalyses (Alvarez-Garreton et al. 2015). This may be partly overcome by improved blending approaches, although data density will remain insufficient in the earliest periods due to a lack of appropriate satellites. Sub-daily resolutions would be necessary to capture the high-frequency components of the soil moisture signal which in the temporal domain are driven mainly by precipitation and the diurnal cycle of solar radiation (Dorigo et al. 2013). A denser temporal sampling is also crucial to better quantify land-atmosphere interactions, e.g., soil moisture controls on convective precipitation (Guillod et al. 2014; Taylor et al. 2012). Fortunately, the current constellation of coarse-scale microwave satellites is capable of providing measurements several times per day (SMOS and SMAP at around 6:00 am and pm, ASCAT at 9:30 am and pm, and AMSR2 at 1:30 am and pm). At the same time, due to physical limitations of microwave remote sensing in providing useful information below snow/ice cover, under frozen conditions, or underneath dense vegetation, spatial data gaps will remain an issue also in the future.

Improved product accuracy

Section 3 showed that there is still considerable room for reducing errors. Especially for Level 2 products from scatterometers a lot could still be gained by an improved modelling of vegetation effects and sub-surface scattering effects in dry soils (Liu et al. 2016; Morrison 2013; Wagner et al. 2013a). Passive microwave Level 2 products would benefit from an improved modelling of the effect of diurnal temperature variations on soil moisture retrievals (Parinussa et al. 2016) and a better quantification of the actual soil depths sampled by the different microwave frequencies (Wilheit 1978). Both the active and passive Level 2 products would profit from an improved characterization of the sub-daily behaviour of soil and canopy moisture and the application of de-noising methods (Su et al. 2015). These improved Level 2 products would in turn contribute to reduced errors in the ESA CCI SM products. Not only product errors themselves need to be improved, but also their characterisation in space and time and their communication to the users. As suggested earlier, providing a single error estimate for the entire dataset is impractical and insufficient. Applications based on data assimilation only profit maximally if the product errors are accurately and dynamically characterized at the level of individual observations (Lahoz and Schneider 2014).

Improved blending methods

Some studies observed a reduced skill of COMBINED with respect to the ACTIVE or PASSIVE products (Chakravorty et al. 2016; Szczypta et al. 2014; Yuan et al. 2015a). Even though this issue has been largely resolved for the reported study areas in the latest version (Figure 13), there remain some areas where the merging of ACTIVE and PASSIVE into COMBINED leads to a reduction of skill. In-depth analyses are needed to reveal whether this is related to the scaling of the remote sensing products against an LSM-based climatology or to the merging strategy itself. Also, the temporal gap filling of the best performing product with lower quality observations has a negative impact on the overall skill of COMBINED (Gruber et al. in prep.). Thus, the challenge of the merging procedure is to find an optimum trade-off between increased spatial-temporal coverage and maintaining acceptable data quality. A potential way to optimise the current merging methodology may be to assess errors and merge datasets at different temporal scales (Su et al. 2016b). In addition, it may be worthwhile looking into alternative merging approaches, e.g. machine learning approaches (Kolassa et al. 2016; Rodríguez-Fernández et al. 2015) or data assimilation frameworks (Kolassa et al. 2017).

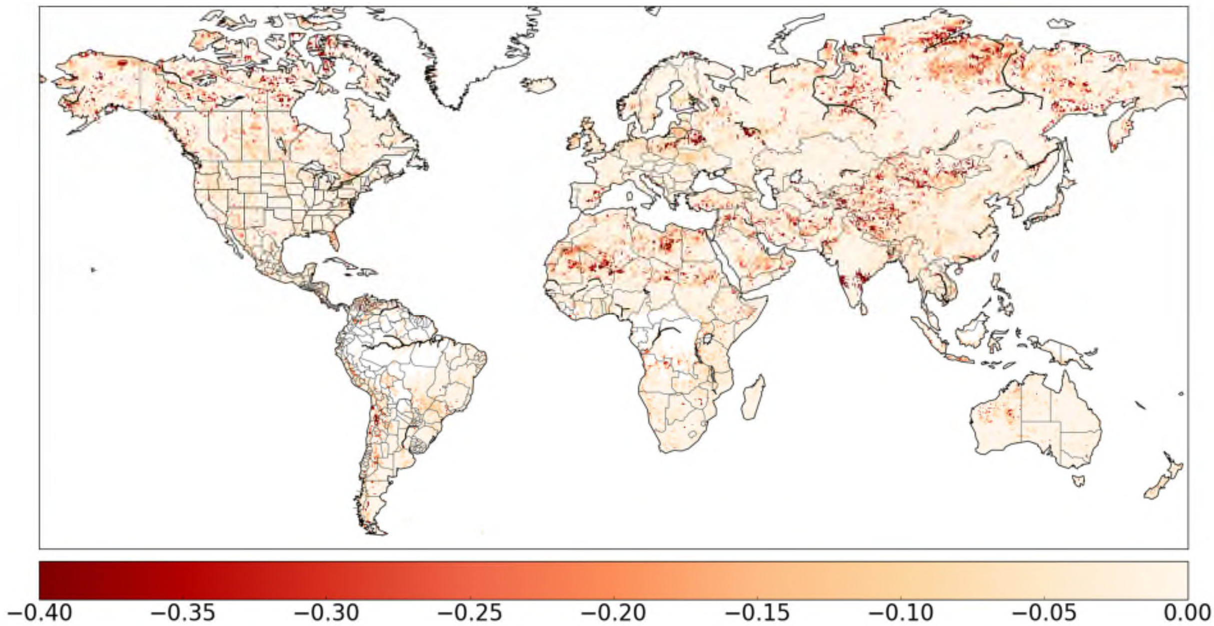

Figure 13 Differences in correlation between ERA-Interim/Land and ESA CCI SM v03.2 COMBINED on the one hand, and ERA/Interim-Land and the best performing ESA CCI SM v03.2 product (either COMBINED, ACTIVE, or PASSIVE) on the other. Differences close or equal to zero indicate that COMBINED merges the input products without a substantial loss in skill, while negative values indicate that either ACTIVE or PASSIVE outperforms COMBINED.

Improved temporal consistency

For climate change applications it is of utmost importance that the trend signal contained in the ESA CCI SM products have a geophysical meaning and are not introduced, e.g., by changes in sensor constellation. Assessing, and possibly correcting for such potential artefacts should therefore receive high priority in future product releases (Su et al. 2016c). However, despite the potential detection and correction of more obvious inhomogeneities like changes in the mean or variance, more intricate inhomogeneities, e.g. changes in data quality and spatiotemporal coverage, may be easily overlooked. Yet, these may have considerable impact on several applications, e.g. the attribution of the frequency of extreme events (Loew et al. 2013; Padhee et al. 2017; Yuan et al. 2015a) or the assessment of mean global trends (Dorigo et al. 2012). Long-term missions with consistent specifications, e.g., as provided by the ERS and MetOp satellites, are crucial for supporting homogenisation and intercalibration efforts.

Shorter latency times between data acquisition and data availability

Short latency times are required for embedding the ESA CCI SM product in operational services. While monitoring services, e.g. drought monitors, would already profit from a latency of ten days, operational flood forecasting and the initialisation of boundary conditions in NWP models require a near-real-time availability of the product. Enenkel et al. (2016a) demonstrated the feasibility of producing an ESA CCI SM near-real-time dataset, although they also showed that such a service is constrained by the latency and quality of available Level 2 products. Operational production and updating of the dataset with a maximum latency of 10 days is foreseen to take place within the Copernicus Climate Change Services (C3S; https://climate.copernicus.eu/) from June 2017 onwards. ESA CCI SM v03.2 will form the basis for this service.

Independency of LSMs

To optimally serve model benchmarking activities, especially regarding the assessment of biases, the ESA CCI SM COMBINED product should become entirely independent of any LSM. Even though the current scaling against the GLDAS -Noah reference LSM hardly affects trends and temporal dynamics in the product, it does make the ESA CCI SM COMBINED dataset impractical for assessing model biases. Globally available L-band observations from SMOS and SMAP may be considered as an alternative scaling reference in the future.

Creation of a root-zone soil moisture product

Root-zone soil moisture is required for a complete assessment of land-atmosphere interactions, for better linking soil moisture variability to ecosystem and agricultural drought dynamics, and for hydrological modelling. Although this is seemingly unattainable without the intervention of an LSM to propagate surface soil moisture observations to the root-zone, simplified approaches such as the Soil Water Index method (Albergel et al. 2008; Wagner et al. 1999b) may already be useful (Brocca et al. 2012).

One should be aware that user requirements on satellite soil moisture will continue to change, reflecting advances in Earth system research and evolving societal needs. As regards climate applications, the latest GCOS Implementation Plan (GCOS-200 2016) already addresses a couple of the new top-level requirements identified in this study, including improvements in the spatial resolution and the need to provide subsidiary variables to better characterize the quality of the surface soil moisture data. The required subsidiary variables are the freeze/thaw status, surface inundation, VOD and root-zone soil moisture. Freeze/thaw status and surface inundation are needed to flag environmental conditions when the retrieval of soil moisture data from microwave measurements is not possible due to fundamental physical reasons (Zwieback et al. 2015).

Even with consolidated user requirements for soil moisture CDRs, the main challenge remains to determine to what degree these requirements are actually met by long-term products like ESA CCI SM. This requires standardised strategies based on commonly agreed reference datasets, methodologies, and metrics. Some examples of potential methods were adopted in this study but these need to be further elaborated. Apart from statistical approaches like the triple collocation, all other evaluation methods to some degree suffer from a general data sparsity in several regions of the world, e.g. the tropical forests or the sub-arctic. In these regions, there is not only a lack of in-situ soil moisture stations (Ochsner et al. 2013) but also of meteorological monitoring stations. Thus, also the precipitation and LSM products used in various evaluation approaches have larger uncertainties here. For example, Albergel et al. (2013a) showed that the trends in two reanalysis datasets widely diverged in these areas. Therefore, to date, data-rich areas dominate in the evaluation process. One of the main priorities of the international community should therefore be to establish in-situ networks in data-poor regions and guarantee the continuation of existing long-term monitoring sites to assess stability and trends over a wide range of land surface conditions. A good starting point may be offered by the globally well-distributed and error-characterised SMAP core validation sites (Colliander et al. 2017).

6 Conclusion and outlook

In this study, we provided a comprehensive overview of the specifications of the ESA CCI SM product suite and the Earth system applications that have made use of these datasets either to benchmark or to improve current process understanding as captured in state-of-the-art models. The strong user interest in the soil moisture CDRs is reflected by the wide variety of science communities who have exploited the potential of these products. The main motivation for using the ESA CCI SM products over existing single-sensor products is its unique long period of coverage, which makes it potentially suitable to assessing long-term variability and change, although users should confirm data homogeneity for their region of application.

ESA CCI SM products have already led to numerous publications, which were used in this study to review the capabilities and shortcomings of the products for Earth system applications and provide valuable information for shaping the priorities of new product releases. Yet, the full potential of ESA

CCI SM remains underexploited. This is partly due to the complexity and limitations of the data, e.g., the varying dataset quality through space and time, and the occurrence of data gaps, which makes it difficult for users to integrate the data in their applications. Such limitations can be partly addressed by continuing efforts to improve Level 2 retrievals and merging methodologies, and through the introduction of new, high-quality sensors like SMAP in the merged products. However, it will not be possible to mitigate all issues related to the creation of an entirely homogeneous dataset from 1978 onwards. These issues relate to the absence of suitable sensors in the early decades and the physical limitations of the microwave signal in general. Thus, to exploit the full potential of the ESA CCI SM datasets, future efforts should not only focus on algorithmic improvements but also on clearly communicating the dataset characteristics to expert and non-expert users alike.

Finally, the acceptance of the ESA CI SM products by a broad user community and integration into operational applications strongly hinges on its long-term sustainability. For the coming years, it is very likely that ESA will continue to support the scientific development of ESA CCI SM. At the same time, operational reprocessing, software maintenance, and near-real-time updating of ESA CCI SM v03.2 is foreseen to take place within the Copernicus Climate Change Services from June 2017 onwards. However, a successful continuation of ESA CCI SM also requires sustenance of the input missions. Currently, the risk of failing missions is relatively low: From the active microwave side two almost identical MetOp-A and MetOp-B ASCAT scatterometers are currently operated by EUMETSAT, while MetOp-C ASCAT will be launched in 2018 to replace MetOp-A (Lin et al. 2016). From that time, MetOp-A will remain in orbit to serve as backup in case of failure of one of the other MetOp satellites. Continuation beyond the current MetOp program will be provided by the approved MetOp Second Generation (MetOp-SG) program, which will start in 2021/22 and has the goal to provide continuation of C-band scatterometer and other systematic observations for another 21 years, i.e., at least until 2042. Also for the passive microwave part there is currently a redundancy of suitable missions: AMSR2 C-band observations, ASMR2, GPM GMI, and Fengyun 1B X-band radiometers, and of course the dedicated L-band missions SMOS and SMAP. GPM GMI, Fengyun 1B, and SMAP are currently not exploited in ESA CCI SM, so there is even potential to further improve the quality and coverage of the merged ESA CCI SM products. In case of failure of one of these missions, there is enough potential backup to reduce the impact of satellite failure on the short to mid-term. More worrying is the long-term continuation of L-band and C-band radiometer missions, since neither SMOS, nor SMAP nor AMSR2 has confirmed continuation. Nevertheless, the planned Water Cycle Observation Mission (WCOM) of the Chinese Academy of Sciences has the potential to bridge the looming gap in L- and C-band observation time series from 2020 onwards (Shi et al. 2016). Yet, a strong commitment of space agencies worldwide to provide continuation of single sensor missions and ESA CCI SM is needed to bolster the acceptance of satellite-derived soil moisture by a large user community in general.

7 Acknowledgements and data access

The development and evolution of the ESA CCI SM datasets as well as the authors have been supported by the ESA STSE Water Cycle Multi-mission Observation Strategy (WACMOS) project (Contract no. 22086/08/1-EC), ESA's Climate Change Initiative for Soil Moisture (Contract No. 4000104814/11/I-NB and 4000112226/14/I-NB) and the European Union's FP7 EartH2Observe "Global Earth Observation for Integrated Water Resource Assessment" project (grant agreement number 331 603608). Wouter Dorigo is supported by the "TU Wien Science Award 2015", a personal grant awarded by the Vienna University of Technology. The data used in this study can be accessed through the ESA CCI SM project site (http://www.esa-soilmoisture-cci.org/), ESA's CCI open data portal (http://cci.esa.int/data), and the Earth2Observe Water Cycle Integrator (https://wci.earth2observe.eu/).

8 References

Abelen, S., & Seitz, F. (2013). Relating satellite gravimetry data to global soil moisture products via data harmonization and correlation analysis. *Remote Sensing of Environment, 136*, 89-98

Abera, W., Formetta, G., Brocca, L., & Rigon, R. (2016). Water budget modelling of the Upper Blue Nile basin using the JGrass-NewAge model system and satellite data. *Hydrol. Earth Syst. Sci. Discuss., 2016*, 1-28

Agrawal, S., & Chakraborty, A. (2016). Role of surface hydrology in determining the seasonal cycle of Indian summer monsoon in a general circulation model. *Hydrol. Earth Syst. Sci. Discuss., 2016*, 1-33

Ahlström, A., Smith, B., Lindström, J., Rummukainen, M., & Uvo, C.B. (2013). GCM characteristics explain the majority of uncertainty in projected 21st century terrestrial ecosystem carbon balance. *Biogeosciences, 10*, 1517-1528

Al-Yaari, A., Wigneron, J.P., Kerr, Y., de Jeu, R., Rodriguez-Fernandez, N., van der Schalie, R., Al Bitar, A., Mialon, A., Richaume, P., Dolman, A., & Ducharne, A. (2016). Testing regression equations to derive long-term global soil moisture datasets from passive microwave observations. *Remote Sensing of Environment, 180*, 453-464

Albergel, C., de Rosnay, P., Gruhier, C., Muñoz-Sabater, J., Hasenauer, S., Isaksen, L., Kerr, Y., & Wagner, W. (2012). Evaluation of remotely sensed and modelled soil moisture products using global ground-based in situ observations. *Remote Sensing of Environment, 118*, 215-226

Albergel, C., Dorigo, W., Balsamo, G., Muñoz-Sabater, J., de Rosnay, P., Isaksen, L., Brocca, L., de Jeu, R., & Wagner, W. (2013a). Monitoring multi-decadal satellite earth observation of soil moisture products through land surface reanalyses. *Remote Sensing of Environment, 138*, 77-89

Albergel, C., Dorigo, W., Reichle, R., Balsamo, G., Rosnay, P.d., Muñoz-Sabater, J., Isaksen, L., Jeu, R.d., & Wagner, W. (2013b). Skill and global trend analysis of soil moisture from reanalyses and microwave remote sensing. *Journal of Hydrometeorology, 14*, 1259–1277

Albergel, C., Munier, S., Leroux, D.J., Dewaele, H., Fairbairn, D., Barbu, A.L., Gelati, E., Dorigo, W., Faroux, S., Meurey, C., Le Moigne, P., Decharme, B., Mahfouf, J.F., & Calvet, J.C. (2017). Sequential assimilation of satellite-derived vegetation and soil moisture products using SURFEX_v8.0: LDAS-

Monde assessment over the Euro-Mediterranean area. *Geoscientific Model Development Discussions, in review*

Albergel, C., Rüdiger, C., Pellarin, T., Calvet, J.C., Fritz, N., Froissard, F., Suquia, D., Petitpa, A., Piguet, B., & Martin, E. (2008). From near-surface to root-zone soil moisture using an exponential filter: An assessment of the method based on in-situ observations and model simulations. *Hydrology and Earth System Sciences, 12*, 1323-1337

Allam, M.M., Jain Figueroa, A., McLaughlin, D.B., & Eltahir, E.A.B. (2016). Estimation of evaporation over the upper Blue Nile basin by combining observations from satellites and river flow gauges. *Water Resources Research*, n/a-n/a

Allen, C.D., Macalady, A.K., Chenchouni, H., Bachelet, D., McDowell, N., Vennetier, M., Kitzberger, T., Rigling, A., Breshears, D.D., Hogg, E.H., Gonzalez, P., Fensham, R., Zhang, Z., Castro, J., Demidova, N., Lim, J.-H., Allard, G., Running, S.W., Semerci, A., & Cobb, N. (2010). A global overview of drought and heat-induced tree mortality reveals emerging climate change risks for forests. *Forest Ecology and Management, 259*, 660-684

Alvarez-Garreton, C., Ryu, D., Western, A.W., Su, C.H., Crow, W.T., Robertson, D.E., & Leahy, C. (2015). Improving operational flood ensemble prediction by the assimilation of satellite soil moisture: comparison between lumped and semi-distributed schemes. *Hydrology and Earth System Sciences, 19*, 1659-1676

An, R., Wang, H.-L., You, J.-j., Wang, Y., Shen, X.-j., Gao, W., Wang, Y.-n., Zhang, Y., Wang, Z., Quaye-Ballardd, J.A., & Chen, Y. (2016a). Downscaling soil moisture using multisource data in China. In (pp. 100041Z-100041Z-100014)

An, R., Zhang, L., Wang, Z., Quaye-Ballard, J.A., You, J., Shen, X., Gao, W., Huang, L., Zhao, Y., & Ke, Z. (2016b). Validation of the ESA CCI soil moisture product in China. *International Journal of Applied Earth Observation and Geoinformation, 48*, 28-36

Arnault, J., Wagner, S., Rummler, T., Fersch, B., Bliefernicht, J., Andresen, S., & Kunstmann, H. (2015). Role of Runoff–Infiltration Partitioning and Resolved Overland Flow on Land–Atmosphere Feedbacks: A Case Study with the WRF-Hydro Coupled Modeling System for West Africa. *Journal of Hydrometeorology, 17*, 1489-1516

Asoka, A., Gleeson, T., Wada, Y., & Mishra, V. (2017). Relative contribution of monsoon precipitation and pumping to changes in groundwater storage in India. *Nature Geosci, 10*, 109-117

Asoka, A., & Mishra, V. (2015). Prediction of vegetation anomalies to improve food security and water management in India. *Geophysical Research Letters, 42*, 5290-5298

Balsamo, G., Albergel, C., Beljaars, A., Boussetta, S., Brun, E., Cloke, H., Dee, D., Dutra, E., Muñoz-Sabater, J., Pappenberger, F., de Rosnay, P., Stockdale, T., & Vitart, F. (2015). ERA-Interim/Land: a global land surface reanalysis data set. *Hydrology and Earth System Sciences, 19*, 389-407

Balsamo, G., Viterbo, P., Beljaars, A., van den Hurk, B., Hirschi, M., Betts, A.K., & Scipal, K. (2009). A Revised Hydrology for the ECMWF Model: Verification from Field Site to Terrestrial Water Storage and Impact in the Integrated Forecast System. *Journal of Hydrometeorology, 10*, 623-643

Barbu, A.L., Calvet, J.C., Mahfouf, J.F., & Lafont, S. (2014). Integrating ASCAT surface soil moisture and GEOV1 leaf area index into the SURFEX modelling platform: a land data assimilation application over France. *Hydrology and Earth System Sciences, 18*, 173-192

Barichivich, J., Briffa, K.R., Myneni, R., Van der Schrier, G., Dorigo, W., Tucker, C.J., Osborn, T., & Melvin, T. (2014). Temperature and Snow-Mediated Moisture Controls of Summer Photosynthetic Activity in Northern Terrestrial Ecosystems between 1982 and 2011. *Remote Sensing, 6*, 1390-1431

Bartsch, A., Baltzer, H., & George, C. (2009). The influence of regional surface soil moisture anomalies on forest fires in Siberia observed from satellites. *Environmental Research Letters, 4*, 45021-45021

Bauer-Marschallinger, B., Dorigo, W.A., Wagner, W., & van Dijk, A.I.J.M. (2013). How oceanic oscillation drives soil moisture variations over mainland Australia: An analysis of 32 years of satellite observations. *Journal of Climate, 26*, 10159–10173

Beljaars, A.C.M., Viterbo, P., Miller, M.J., & Betts, A.K. (1996). The Anomalous Rainfall over the United States during July 1993: Sensitivity to Land Surface Parameterization and Soil Moisture Anomalies. *Monthly Weather Review, 124*, 362-383

Bhuiyan, M.A.E., Anagnostou, E.N., & Kirstetter, P.-E. (in review-a). A Non-Parametric Statistical Technique for Modeling Overland TMI (2A12) Rainfall Retrieval Error. *IEEE Geoscience and Remote Sensing Letters*

Bhuiyan, M.A.E., Nikolopoulos, E.I., Anagnostou, E.N., Quintana-Seguí, P., & Barella-Ortiz, A. (in review-b). A Nonparametric Statistical Technique for Combining Global Precipitation Datasets: Development and Hydrological Evaluation over the Iberian Peninsula. *Hydrology and Earth System Sciences*

Bisselink, B., Van Meijgaard, E., Dolman, A.J., & De Jeu, R.A.M. (2011). Initializing a regional climate model with satellite-derived soil moisture. *Journal of Geophysical Research D: Atmospheres, 116*

Blunden, J., & Arndt, D.S. (2016). State of the Climate in 2015. *Bulletin of the American Meteorological Society, 97*, S1–S27

Brocca, L., Ciabatta, L., Massari, C., Moramarco, T., Hahn, S., Hasenauer, S., Kidd, R., Dorigo, W., Wagner, W., & Levizzani, V. (2014). Soil as a natural raingauge: estimating global rainfall from satellite soil moisture data. *Journal of Geophysical Research D: Atmospheres, 119*, 5128–5141

Brocca, L., Melone, F., Moramarco, T., Wagner, W., Naeimi, V., Bartalis, Z., & Hasenauer, S. (2010). Improving runoff prediction through the assimilation of the ASCAT soil moisture product. *Hydrology and Earth System Sciences, 14*, 1881-1893

Brocca, L., Moramarco, T., Melone, F., & Wagner, W. (2013). A new method for rainfall estimation through soil moisture observations. *Geophysical Research Letters, 40*, 853-858

Brocca, L., Moramarco, T., Melone, F., Wagner, W., Hasenauer, S., & Hahn, S. (2012). Assimilation of Surface- and Root-Zone ASCAT Soil Moisture Products Into Rainfall–Runoff Modeling. *Geoscience and Remote Sensing, IEEE Transactions on, 50*, 2542-2555

Cammalleri, C., Vogt, J.V., Bisselink, B., & de Roo, A. (2017). Comparing soil moisture anomalies from multiple independent sources over different regions across the globe. *Hydrol. Earth Syst. Sci. Discuss., 2017*, 1-34

Carrão, H., Russo, S., Sepulcre-Canto, G., & Barbosa, P. (2016). An empirical standardized soil moisture index for agricultural drought assessment from remotely sensed data. *International Journal of Applied Earth Observation and Geoinformation, 48*, 74-84

Carvalhais, N., Forkel, M., Khomik, M., Bellarby, J., Jung, M., Migliavacca, M., Mu, M., Saatchi, S., Santoro, M., Thurner, M., Weber, U., Ahrens, B., Beer, C., Cescatti, A., Randerson, J.T., & Reichstein, M. (2014). Global covariation of carbon turnover times with climate in terrestrial ecosystems. *Nature, 514*, 213-217

Casagrande, E., Mueller, B., Miralles, D.G., Entekhabi, D., & Molini, A. (2015). Wavelet correlations to reveal multiscale coupling in geophysical systems. *Journal of Geophysical Research: Atmospheres, 120*, 7555-7572

Catalano, F., Alessandri, A., De Felice, M., Zhu, Z., & Myneni, R.B. (2016). Observationally based analysis of land–atmosphere coupling. *Earth Syst. Dynam., 7*, 251-266

Chakravorty, A., Chahar, B.R., Sharma, O.P., & Dhanya, C.T. (2016). A regional scale performance evaluation of SMOS and ESA-CCI soil moisture products over India with simulated soil moisture from MERRA-Land. *Remote Sensing of Environment, 186*, 514-527

Chen, F., Crow, W.T., Colliander, A., Cosh, M.H., Jackson, T.J., Bindlish, R., Reichle, R.H., Chan, S.K., Bosch, D.D., Starks, P.J., Goodrich, D.C., & Seyfried, M.S. (2016a). Application of Triple Collocation in Ground-Based Validation of Soil Moisture Active/Passive (SMAP) Level 2 Data Products. *IEEE Journal of Selected Topics in Applied Earth Observations and Remote Sensing, PP*, 1-14

Chen, T., de Jeu, R.A.M., Liu, Y.Y., van der Werf, G.R., & Dolman, A.J. (2014). Using satellite based soil moisture to quantify the water driven variability in NDVI: A case study over mainland Australia. *Remote Sensing of Environment, 140*, 330-338

Chen, T., McVicar, T., Wang, G., Chen, X., de Jeu, R., Liu, Y., Shen, H., Zhang, F., & Dolman, A. (2016b). Advantages of Using Microwave Satellite Soil Moisture over Gridded Precipitation Products and Land Surface Model Output in Assessing Regional Vegetation Water Availability and Growth Dynamics for a Lateral Inflow Receiving Landscape. *Remote Sensing, 8*, 428

Chen, X., Liu, X., Liu, Z., Zhou, P., Zhou, G., Liao, J., & Liu, L. (2017). Spatial clusters and temporal trends of seasonal surface soil moisture across China in responses to regional climate and land cover changes. *Ecohydrology, 10*, n/a-n/a

Ciabatta, L., Massari, C., Brocca, L., Gruber, A., Reimer, C., Hahn, S., Paulik, C., Dorigo, W., Kidd, R., & Wagner, W. (subm.). Long-term (1998-2015) ESA CCI soil moisture derived rainfall dataset through SM2RAIN. *Earth System Science Data*

Ciabatta, L., Massari, C., Brocca, L., Reimer, C., Hann, S., Paulik, C., Dorigo, W., & Wagner, W. (2016). Using Python® language for the validation of the CCI soil moisture products via SM2RAIN. *PeerJ Preprints, 4*, e2131v2134

Ciais, P., Reichstein, M., Viovy, N., Granier, A., Ogee, J., Allard, V., Aubinet, M., Buchmann, N., Bernhofer, C., Carrara, A., Chevallier, F., De Noblet, N., Friend, A.D., Friedlingstein, P., Grunwald, T., Heinesch, B., Keronen, P., Knohl, A., Krinner, G., Loustau, D., Manca, G., Matteucci, G., Miglietta, F., Ourcival, J.M., Papale, D., Pilegaard, K., Rambal, S., Seufert, G., Soussana, J.F., Sanz, M.J., Schulze, E.D., Vesala, T., & Valentini, R. (2005). Europe-wide reduction in primary productivity caused by the heat and drought in 2003. *Nature, 437*, 529-533

Cissé, S., Eymard, L., Ottlé, C., Ndione, J., Gaye, A., & Pinsard, F. (2016). Rainfall Intra-Seasonal Variability and Vegetation Growth in the Ferlo Basin (Senegal). *Remote Sensing, 8*, 66

Colliander, A., Jackson, T.J., Bindlish, R., Chan, S., Das, N., Kim, S.B., Cosh, M.H., Dunbar, R.S., Dang, L., Pashaian, L., Asanuma, J., Aida, K., Berg, A., Rowlandson, T., Bosch, D., Caldwell, T., Caylor, K., Goodrich, D., al Jassar, H., Lopez-Baeza, E., Martínez-Fernández, J., González-Zamora, A., Livingston, S., McNairn, H., Pacheco, A., Moghaddam, M., Montzka, C., Notarnicola, C., Niedrist, G., Pellarin, T., Prueger, J., Pulliainen, J., Rautiainen, K., Ramos, J., Seyfried, M., Starks, P., Su, Z., Zeng, Y., van der Velde, R., Thibeault, M., Dorigo, W., Vreugdenhil, M., Walker, J.P., Wu, X., Monerris, A., O'Neill, P.E., Entekhabi, D., Njoku, E.G., & Yueh, S. (2017). Validation of SMAP surface soil moisture products with core validation sites. *Remote Sensing of Environment, 191*, 215-231

Colliander, A., Jackson, T.J., Bindlish, R., Chan, S., Kim, S.B., Cosh, M.H., Dunbar, R.S., Dang;, L., Pashaian;, L., Asanuma;, J., Berg;, A.A., Rowlandson;, T., Bosch;, D., Caldwell;, T., Caylor;, K., Goodrich;, D., Jassar;, H.a., Lopez-Baeza;, E., Martinez-Fernandez;, J., Gonzalez-Zamora;, A., Livingston;, S., McNairn;, H., Pacheco;, A., Moghaddam;, M., Montzka;, C., Notarnicola;, C., Niedrist;, G., Pellarin;, T., Prueger;, J., Pulliainen;, J., Rautiainen;, K., Ramos;, J., Seyfried;, M., Starks;, P., Su;, Z., Zeng;, Y., Velde;, R.v.d., Thibeault;, M., Dorigo;, W., Vreugdenhil;, M., Walker;, J.P., Wu;, X., Monerris;, A., O'Neill;, P.E., Entekhabi;, D., Njoku;, E.G., & Yueh, S.H. (2016). Validation of SMAP Surface Soil Moisture Products with Core Validation Sites. *Remote Sensing of Environemnt, in review*

Cosh, M.H., Ochsner, T.E., McKee, L., Dong, J., Basara, J.B., Evett, S.R., Hatch, C.E., Small, E.E., Steele-Dunne, S.C., Zreda, M., & Sayde, C. (2016). The Soil Moisture Active Passive Marena, Oklahoma, In Situ Sensor Testbed (SMAP-MOISST): Testbed Design and Evaluation of In Situ Sensors. *Vadose Zone Journal, 15*

Crow, W.T. (2007). A novel method for quantifying value in spaceborne soil moisture retrievals. *Journal of Hydrometeorology, 8*, 56-67

Crow, W.T., Su, C.H., Ryu, D., & Yilmaz, M.T. (2015). Optimal averaging of soil moisture predictions from ensemble land surface model simulations. *Water Resources Research, 51*, 9273-9289

Dahigamuwa, T., Yu, Q., & Gunaratne, M. (2016). Feasibility Study of Land Cover Classification Based on Normalized Difference Vegetation Index for Landslide Risk Assessment. *Geosciences, 6*, 45

Das, S.K., & Maity, R. (2015). Potential of Probabilistic Hydrometeorological Approach for Precipitation-Based Soil Moisture Estimation. *Journal of Hydrologic Engineering, 20*

De Jeu, R., & Dorigo, W. (2016). On the importance of satellite observed soil moisture. *International Journal of Applied Earth Observation and Geoinformation, 45, Part B*, 107-109

De Jeu, R., Dorigo, W., Wagner, W., & Liu, Y. (2011). [Global Climate] Soil Moisture [in: State of the Climate in 2010]. *Bulletin of the American Meteorological Society, 92*, S52-S53

De Jeu, R.A.M., Dorigo, W.A., Parinussa, R.M., Wagner, W., & Chung, D. (2012). [Global Climate] Sol Moisture [in: State of the Climate in 2011]. *Bulletin of the American Meteorological Society, 93*, S30-S34

de Rosnay, P., Drusch, M., Vasiljevic, D., Balsamo, G., Albergel, C., & Isaksen, L. (2013). A simplified Extended Kalman Filter for the global operational soil moisture analysis at ECMWF. *Quarterly Journal of the Royal Meteorological Society, 139*, 1199-1213

Dee, D.P., Uppala, S.M., Simmons, A.J., Berrisford, P., Poli, P., Kobayashi, S., Andrae, U., Balmaseda, M.A., Balsamo, G., Bauer, P., Bechtold, P., Beljaars, A.C.M., van de Berg, L., Bidlot, J., Bormann, N., Delsol, C., Dragani, R., Fuentes, M., Geer, A.J., Haimberger, L., Healy, S.B., Hersbach, H., Hólm, E.V., Isaksen, L., Kållberg, P., Köhler, M., Matricardi, M., McNally, A.P., Monge-Sanz, B.M., Morcrette, J.J., Park, B.K., Peubey, C., de Rosnay, P., Tavolato, C., Thépaut, J.N., & Vitart, F. (2011). The ERA-Interim reanalysis: Configuration and performance of the data assimilation system. *Quarterly Journal of the Royal Meteorological Society, 137*, 553-597

Detmers, R.G., Hasekamp, O., Aben, I., Houweling, S., van Leeuwen, T.T., Butz, A., Landgraf, J., Köhler, P., Guanter, L., & Poulter, B. (2015). Anomalous carbon uptake in Australia as seen by GOSAT. *Geophysical Research Letters, 42*, 8177-8184

Dharssi, I., Bovis, K.J., Macpherson, B., & Jones, C.P. (2011). Operational assimilation of ASCAT surface soil wetness at the Met Office. *Hydrology and Earth System Sciences, 15*, 2729-2746

Dirmeyer, P.A., & Halder, S. (2016). Application of the Land–Atmosphere Coupling Paradigm to the Operational Coupled Forecast System, Version 2 (CFSv2). *Journal of Hydrometeorology, 18*, 85-108

Dorigo, W., Chung, D., Parinussa, R.M., Reimer, C., Hahn, S., Liu, Y.Y., Wagner, W., de Jeu, R.A.M., Paulik, C., & Wang, G. (2014). [Global Climate] Soil Moisture [in: “State of the Climate in 2013”]. *Bulletin American Meteorological Society, 95*, S25-S26

Dorigo, W., & De Jeu, R. (2016). Satellite soil moisture for advancing our understanding of earth system processes and climate change. *International Journal of Applied Earth Observation and Geoinformation, 48*, 1-4

Dorigo, W., De Jeu, R., Chung, D., Parinussa, R., Liu, Y., Wagner, W., & Fernandez-Prieto, D. (2012). Evaluating global trends (1988-2010) in homogenized remotely sensed surface soil moisture. *Geophysical Research Letters, 39*, L18405

Dorigo, W., Reimer, C., Chung, D., Parinussa, R.M., Melzer, T., Wagner, W., de Jeu, R.A.M., & Kidd, R. (2015a). [Hydrological cyce] Soil Moisture [in: “State of the Climate in 2014”]. *Bulletin American Meteorological Society, 96*, S28-S29

Dorigo, W., Van Oevelen, P., Wagner, W., Drusch, M., Mecklenburg, S., Robock, A., & Jackson, T. (2011a). A New International Network for in Situ Soil Moisture Data. *EOS Transactions of AGU, 92*, 141-142

Dorigo, W.A., Chung, D., Gruber, A., Hahn, S., Mistelbauer, T., Parinussa, R.M., Paulik, C., Reimer, C., van der Schalie, R., de Jeu, R.A.M., & Wagner, W. (2016). Soil Moisture [in: “State of the Climate in 2015”]. *Bulletin American Meteorological Society, 97*, S31-S32

Dorigo, W.A., Chung, D., Gruber, A., Hahn, S., Mistelbauer, T., Parinussa, R.M., Reimer, C., van der Schalie, R., de Jeu, R.A.M., & Wagner, W. (accepted). Soil Moisture [in: “State of the Climate in 2016”]. *Bulletin American Meteorological Society*

Dorigo, W.A., Gruber, A., De Jeu, R.A.M., Wagner, W., Stacke, T., Loew, A., Albergel, C., Brocca, L., Chung, D., Parinussa, R.M., & Kidd, R. (2015b). Evaluation of the ESA CCI soil moisture product using ground-based observations. *Remote Sensing of Environment, 162*, 380-395

Dorigo, W.A., Scipal, K., Parinussa, R.M., Liu, Y.Y., Wagner, W., de Jeu, R.A.M., & Naeimi, V. (2010). Error characterisation of global active and passive microwave soil moisture data sets. *Hydrology and Earth System Sciences, 14*, 2605-2616

Dorigo, W.A., Wagner, W., Hohensinn, R., Hahn, S., Paulik, C., Xaver, A., Gruber, A., Drusch, M., Mecklenburg, S., van Oevelen, P., Robock, A., & Jackson, T. (2011b). The International Soil Moisture Network: a data hosting facility for global in situ soil moisture measurements. *Hydrology and Earth System Sciences, 15*, 1675-1698

Dorigo, W.A., Xaver, A., Vreugdenhil, M., Gruber, A., Hegyiová, A., Sanchis-Dufau, A.D., Wagner, W., & Drusch, M. (2013). Global automated quality control of in-situ soil moisture data from the International Soil Moisture Network. *Vadose Zone Journal, 12*

Douville, H., Viterbo, P., Mahfouf, J.-F., & Beljaars, A.C.M. (2000). Evaluation of the Optimum Interpolation and Nudging Techniques for Soil Moisture Analysis Using FIFE Data. *Monthly Weather Review, 128*, 1733-1756

Draper, C., Reichle, R., de Jeu, R., Naeimi, V., Parinussa, R., & Wagner, W. (2013). Estimating root mean square errors in remotely sensed soil moisture over continental scale domains. *Remote Sensing of Environment, 137*, 288-298

Drusch, M., & Viterbo, P. (2007). Assimilation of screen-level variables in ECMWF's integrated forecast system: A study on the impact on the forecast quality and analyzed soil moisture. *Monthly Weather Review, 135*, 300-314

Du, E., Vittorio, A.D., & Collins, W.D. (2016). Evaluation of hydrologic components of community land model 4 and bias identification. *International Journal of Applied Earth Observation and Geoinformation, 48*, 5-16

Du, L., Tian, Q., Yu, T., Meng, Q., Jancso, T., Udvardy, P., & Huang, Y. (2013). A comprehensive drought monitoring method integrating MODIS and TRMM data. *International Journal of Applied Earth Observation and Geoinformation, 23*, 245-253

Ek, M.B., Mitchell, K.E., Lin, Y., Rogers, E., Grunmann, P., Koren, V., Gayno, G., & Tarpley, J.D. (2003). Implementation of Noah land surface model advances in the National Centers for Environmental Prediction operational mesoscale Eta model. *Journal of Geophysical Research: Atmospheres, 108*, n/a-n/a

Enenkel, M., Reimer, C., Dorigo, W., Wagner, W., Pfeil, I., Parinussa, R., & De Jeu, R. (2016a). Combining satellite observations to develop a global soil moisture product for near-real-time applications. *Hydrology and Earth System Sciences, 20*, 4191-4208

Enenkel, M., Steiner, C., Mistelbauer, T., Dorigo, W., Wagner, W., See, L., Atzberger, C., Schneider, S., & Rogenhofer, E. (2016b). A Combined Satellite-Derived Drought Indicator to Support Humanitarian Aid Organizations. *Remote Sensing, 8*, 340

Entekhabi, D., Njoku, E.G., O'Neill, P.E., Kellogg, K.H., Crow, W.T., Edelstein, W.N., Entin, J.K., Goodman, S.D., Jackson, T.J., Johnson, J., Kimball, J., Piepmeier, J.R., Koster, R.D., Martin, N., McDonald, K.C., Moghaddam, M., Moran, S., Reichle, R., Shi, J.C., Spencer, M.W., Thurman, S.W., Tsang, L., & Van Zyl, J. (2010a). The soil moisture active passive (SMAP) mission. *Proceedings of the IEEE, 98*, 704-716

Entekhabi, D., Reichle, R.H., Koster, R.D., & Crow, W.T. (2010b). Performance Metrics for Soil Moisture Retrievals and Application Requirements. *Journal of Hydrometeorology, 11*, 832-840

Fairbairn, D., Barbu, A.L., Napoly, A., Albergel, C., Mahfouf, J.F., & Calvet, J.C. (2017). The effect of satellite-derived surface soil moisture and leaf area index land data assimilation on streamflow simulations over France. *Hydrology and Earth System Sciences, 21*, 2015-2033

Fang, L., Hain, C.R., Zhan, X., & Anderson, M.C. (2016). An inter-comparison of soil moisture data products from satellite remote sensing and a land surface model. *International Journal of Applied Earth Observation and Geoinformation, 48*, 37-50

Feng, H. (2016). Individual contributions of climate and vegetation change to soil moisture trends across multiple spatial scales. *Scientific Reports, 6*, 32782

Feng, H., & Zhang, M. (2015). Global land moisture trends: drier in dry and wetter in wet over land. *Scientific Reports, 5*, 18018

Ferguson, C.R., & Mocko, D.M. (2017). Diagnosing an Artificial Trend in NLDAS-2 Afternoon Precipitation. *Journal of Hydrometeorology, 18*, 1051-1070

Findell, K.L., Gentine, P., Lintner, B.R., & Guillod, B.P. (2015). Data Length Requirements for Observational Estimates of Land–Atmosphere Coupling Strength. *Journal of Hydrometeorology, 16*, 1615-1635

Findell, K.L., Gentine, P., Lintner, B.R., & Kerr, C. (2011). Probability of afternoon precipitation in eastern United States and Mexico enhanced by high evaporation. *Nature Geosci, 4*, 434-439

Fischer, E.M., Seneviratne, S.I., Lüthi, D., & Schär, C. (2007). Contribution of land-atmosphere coupling to recent European summer heat waves. *Geophysical Research Letters, 34*, n/a-n/a

Forkel, M., Dorigo, W., Lasslop, G., Teubner, I., Chuvieco, E., & Thonicke, K. (2016). Identifying required model structures to predict global fire activity from satellite and climate data. *Geoscientific Model Development Discussions, in review*

Forkel, M., Migliavacca, M., Thonicke, K., Reichstein, M., Schaphoff, S., Weber, U., & Carvalhais, N. (2015). Co-dominant water control on global inter-annual variability and trends in land surface phenology and greenness. *Global Change Biology*, n/a-n/a

Forkel, M., Thonicke, K., Beer, C., Cramer, W., Bartalev, S., & Schmullius, C. (2012). Extreme fire events are related to previous-year surface moisture conditions in permafrost-underlain larch forests of Siberia. *Environmental Research Letters, 7*, 044021

Friend, A.D., Lucht, W., Rademacher, T.T., Keribin, R., Betts, R., Cadule, P., Ciais, P., Clark, D.B., Dankers, R., Falloon, P.D., Ito, A., Kahana, R., Kleidon, A., Lomas, M.R., Nishina, K., Ostberg, S., Pavlick, R., Peylin, P., Schaphoff, S., Vuichard, N., Warszawski, L., Wiltshire, A., & Woodward, F.I. (2014). Carbon residence time dominates uncertainty in terrestrial vegetation responses to future climate and atmospheric CO2. *Proceedings of the National Academy of Sciences, 111*, 3280-3285

Gao, H., Wood, E.F., Jackson, T.J., Drusch, M., & Bindlish, R. (2006). Using TRMM/TMI to retrieve surface soil moisture over the southern United States from 1998 to 2002. *Journal of Hydrometeorology, 7*, 23-38

GCOS-138 (2010). Implementation Plan for the Global Observing System for Climate in support of the UNFCCC - 2010 Update. In: World Meteorological Organization

GCOS-200 (2016). The Global Observing System for Climate: Implementation Needs. GCOS 2016 Implementation Plan.

Ghazaryan, G., Dubovyk, O., Kussul, N., & Menz, G. (2016). Towards an Improved Environmental Understanding of Land Surface Dynamics in Ukraine Based on Multi-Source Remote Sensing Time-Series Datasets from 1982 to 2013. *Remote Sensing, 8*, 617

Ghosh, S., Vittal, H., Sharma, T., Karmakar, S., Kasiviswanathan, K.S., Dhanesh, Y., Sudheer, K.P., & Gunthe, S.S. (2016). Indian Summer Monsoon Rainfall: Implications of Contrasting Trends in the Spatial Variability of Means and Extremes. *PLoS ONE, 11*, e0158670

Gibelin, A.-L., Calvet, J.-C., Roujean, J.-L., Jarlan, L., & Los, S.O. (2006). Ability of the land surface model ISBA-A-gs to simulate leaf area index at the global scale: Comparison with satellites products. *Journal of Geophysical Research: Atmospheres, 111*, n/a-n/a

Greve, P., & Seneviratne, S.I. (2015). Assessment of future changes in water availability and aridity. *Geophysical Research Letters, 42*, 5493-5499

Gruber, A., Crow, W., Dorigo, W., & Wagner, W. (2015). The potential of 2D Kalman filtering for soil moisture data assimilation. *Remote Sensing of Environment, 171*, 137-148

Gruber, A., Dorigo, W., Crow, W., & Wagner, W. (in review). Triple collocation based merging of active and passive satellite soil moisture retrievals. *IEEE Transactions on Geoscience and Remote Sensing*

Gruber, A., Dorigo, W., van der Schalie, R., de Jeu, R., & Wagner, W. (in prep.). Improved blending of multi-satellite products into the ESA CCI soil moisture climate data record

Gruber, A., Dorigo, W., Zwieback, S., Xaver, A., & Wagner, W. (2013). Characterizing coarse-scale representativeness of in-situ soil moisture measurements from the International Soil Moisture Network. *Vadose Zone Journal, 12*

Gruber, A., Su, C.H., Crow, W.T., Zwieback, S., Dorigo, W.A., & Wagner, W. (2016a). Estimating error cross-correlations in soil moisture data sets using extended collocation analysis. *Journal of Geophysical Research: Atmospheres, 121*, 1208-1219

Gruber, A., Su, C.H., Zwieback, S., Crow, W.T., Wagner, W., & Dorigo, W. (2016b). Recent advances in (soil moisture) triple collocation analysis. *International Journal of Applied Earth Observation and Geoinformation, 45, Part B*, 200-211

Guillod, B.P., Orlowsky, B., Miralles, D., Teuling, A.J., Blanken, P.D., Buchmann, N., Ciais, P., Ek, M., Findell, K.L., Gentine, P., Lintner, B.R., Scott, R.L., Van den Hurk, B., & I. Seneviratne, S. (2014). Land-surface controls on afternoon precipitation diagnosed from observational data: uncertainties and confounding factors. *Atmos. Chem. Phys., 14*, 8343-8367

Guillod, B.P., Orlowsky, B., Miralles, D.G., Teuling, A.J., & Seneviratne, S.I. (2015). Reconciling spatial and temporal soil moisture effects on afternoon rainfall. *Nature Communications, 6*

He, B., Wang, H., Huang, L., Liu, J., & Chen, Z. (2017). A new indicator of ecosystem water use efficiency based on surface soil moisture retrieved from remote sensing. *Ecological Indicators, 75*, 10-16

Heimhuber, V., Tulbure, M.G., & Broich, M. (2017). Modeling multidecadal surface water inundation dynamics and key drivers on large river basin scale using multiple time series of Earth-observation and river flow data. *Water Resources Research, 53*, 1251-1269

Hirschi, M., Mueller, B., Dorigo, W., & Seneviratne, S.I. (2014). Using remotely sensed soil moisture for land–atmosphere coupling diagnostics: The role of surface vs. root-zone soil moisture variability. *Remote Sensing of Environment, 154*, 246-252

Hirschi, M., Seneviratne, S.I., Alexandrov, V., Boberg, F., Boroneant, C., Christensen, O.B., Formayer, H., Orlowsky, B., & Stepanek, P. (2011). Observational evidence for soil-moisture impact on hot extremes in southeastern Europe. *Nature Geoscience, 4*, 17-21

Hogg, E.H., Barr, A.G., & Black, T.A. (2013). A simple soil moisture index for representing multi-year drought impacts on aspen productivity in the western Canadian interior. *Agricultural and Forest Meteorology, 178–179*, 173-182

Holmes, T.R.H., De Jeu, R.A.M., Owe, M., & Dolman, A.J. (2009). Land surface temperature from Ka band (37 GHz) passive microwave observations. *Journal of Geophysical Research D: Atmospheres, 114*

Huang, Y., Gerber, S., Huang, T., & Lichstein, J.W. (2016). Evaluating the drought response of CMIP5 models using global gross primary productivity, leaf area, precipitation, and soil moisture data. *Global Biogeochemical Cycles, 30*, 1827-1846

Huffman, G.J., Adler, R.F., Bolvin, D.T., & Gu, G. (2009). Improving the global precipitation record: GPCP Version 2.1. *Geophysical Research Letters, 36*

Ichoku, C., Ellison, L.T., Willmot, K.E., Matsui, T., Dezfuli, A.K., Gatebe, C.K., Wang, J., Wilcox, E.M., Lee, J., Adegoke, J., Okonkwo, C., Bolten, J., Policelli, F.S., & Habib, S. (2016). Biomass burning, land-cover change, and the hydrological cycle in Northern sub-Saharan Africa. *Environmental Research Letters, 11*

Ikonen, J., Vehviläinen, J., Rautiainen, K., Smolander, T., Lemmetyinen, J., Bircher, S., & Pulliainen, J. (2016). The Sodankylä in situ soil moisture observation network: an example application of ESA CCI soil moisture product evaluation. *Geosci. Instrum. Method. Data Syst., 5*, 95-108

Jackson, T.J. (1993). Measuring surface soil moisture using passive microwave remote sensing. *Hydrological Processes, 7*, 139-152

Ji, L., & Peters, A.J. (2003). Assessing vegetation response to drought in the northern Great Plains using vegetation and drought indices. *Remote Sensing of Environment, 87*, 85-98

Jiao, Q., Li, R., Wang, F., Mu, X., Li, P., & An, C. (2016a). Impacts of Re-Vegetation on Surface Soil Moisture over the Chinese Loess Plateau Based on Remote Sensing Datasets. *Remote Sensing, 8*

Jiao, Q., Li, R., Wang, F., Mu, X., Li, P., & An, C. (2016b). Impacts of Re-Vegetation on Surface Soil Moisture over the Chinese Loess Plateau Based on Remote Sensing Datasets. *Remote Sensing, 8*, 156

Jones, L.A., Ferguson, C.R., Kimball, J.S., Zhang, K., Chan, S.T.K., McDonald, K.C., Njoku, E.G., & Wood, E.F. (2010). Satellite Microwave Remote Sensing of Daily Land Surface Air Temperature Minima and Maxima From AMSR-E. *IEEE Journal of Selected Topics in Applied Earth Observations and Remote Sensing, 3*, 111-123

Kaminski, T., Knorr, W., Schürmann, G., Scholze, M., Rayner, P.J., Zaehle, S., Blessing, S., Dorigo, W., Gayler, V., Giering, R., Gobron, N., Grant, J., Heimann, M., Hooker-Strout, A., Houweling, S., Kato, T., Kattge, J., Kelley, D., Kemp, S., Koffi, E.N., Kostler, C., Mathieu, P.P., Pinty, B., Reick, C., Rödenbeck, C., Schnur, R., Scipal, K., Sebald, C., Stacke, T., Terwisscha van Scheltinga, A., Vossbeck, M., Widmann, H., & Ziehn, T. (2013). The BETHY/JSBACH Carbon Cycle Data Assimilation System: experiences and challenges. *Journal of Geophysical Research: Biogeosciences, 118*, 1414-1426

KanthaRao, B., & Rakesh, V. (2017). Observational evidence for the relationship between spring soil moisture and June rainfall over the Indian region. *Theoretical and Applied Climatology*, 1-15

Kerr, Y.H., Al-Yaari, A., Rodriguez-Fernandez, N., Parrens, M., Molero, B., Leroux, D., Bircher, S., Mahmoodi, A., Mialon, A., Richaume, P., Delwart, S., Al Bitar, A., Pellarin, T., Bindlish, R., Jackson, T.J., Rüdiger, C., Waldteufel, P., Mecklenburg, S., & Wigneron, J.P. (2016). Overview of SMOS performance in terms of global soil moisture monitoring after six years in operation. *Remote Sensing of Environment, 180*, 40-63

Kerr, Y.H., Waldteufel, P., Richaume, P., Wigneron, J.P., Ferrazzoli, P., Mahmoodi, A., Bitar, A.A., Cabot, F., Gruhier, C., Juglea, S.E., Leroux, D., Mialon, A., & Delwart, S. (2012). The SMOS Soil Moisture Retrieval Algorithm. *IEEE Transactions on Geoscience and Remote Sensing, 50*, 1384-1403

Kerr, Y.H., Waldteufel, P., Wigneron, J.P., Delwart, S., Cabot, F., Boutin, J., Escorihuela, M.J., Font, J., Reul, N., Gruhier, C., Juglea, S.E., Drinkwater, M.R., Hahne, A., Marti, n-Neira, M., & Mecklenburg, S. (2010). The SMOS Mission: New Tool for Monitoring Key Elements ofthe Global Water Cycle. *Proceedings of the IEEE, 98*, 666-687

Klingmüller, K., Pozzer, A., Metzger, S., Stenchikov, G.L., & Lelieveld, J. (2016). Aerosol optical depth trend over the Middle East. *Atmospheric Chemistry and Physics, 16*, 5063-5073

Knist, S., Goergen, K., Buonomo, E., Christensen, O.B., Colette, A., Cardoso, R.M., Fealy, R., Fernández, J., García-Díez, M., Jacob, D., Kartsios, S., Katragkou, E., Keuler, K., Mayer, S., van Meijgaard, E., Nikulin, G., Soares, P.M.M., Sobolowski, S., Szepszo, G., Teichmann, C., Vautard, R., Warrach-Sagi, K., Wulfmeyer, V., & Simmer, C. (2017). Land-atmosphere coupling in EURO-CORDEX evaluation experiments. *Journal of Geophysical Research: Atmospheres, 122*, 79-103

Koike, T., Nakamura, Y., Kaihotsu, I., Davva, N., Matsuura, N., Tamagawa, K., & Fujii, H. (2004). Development of an Advanced Microwave Scanning Radiometer (AMSR-E) Algorithm of Soil Moisture and Vegetation Water Content. *Annual Journal of Hydraulic Engineering, JSCE, 48*, 217-222

Kolassa, J., Gentine, P., Prigent, C., & Aires, F. (2016). Soil moisture retrieval from AMSR-E and ASCAT microwave observation synergy. Part 1: Satellite data analysis. *Remote Sensing of Environment, 173*, 1-14

Kolassa, J., Reichle, R.H., & Draper, C.S. (2017). Merging active and passive microwave observations in soil moisture data assimilation. *Remote Sensing of Environment, 191*, 117-130

Koster, R.D., Mahanama, S.P.P., Livneh, B., Lettenmaier, D.P., & Reichle, R.H. (2010). Skill in streamflow forecasts derived from large-scale estimates of soil moisture and snow. *Nature Geosci, 3*, 613-616

Koster, R.D., Mahanama, S.P.P., Yamada, T.J., Balsamo, G., Berg, A.A., Boisserie, M., Dirmeyer, P.A., Doblas-Reyes, F.J., Drewitt, G., Gordon, C.T., Guo, Z., Jeong, J.H., Lee, W.S., Li, Z., Luo, L., Malyshev, S., Merryfield, W.J., Seneviratne, S.I., Stanelle, T., van den Hurk, B.J.J.M., Vitart, F., & Wood, E.F. (2011). The Second Phase of the Global Land–Atmosphere Coupling Experiment: Soil Moisture Contributions to Subseasonal Forecast Skill. *Journal of Hydrometeorology, 12*, 805-822

Koster, R.D., Suarez, M.J., Liu, P., Jambor, U., Berg, A., Kistler, M., Reichle, R., Rodell, M., & Famiglietti, J. (2004). Realistic Initialization of Land Surface States: Impacts on Subseasonal Forecast Skill. *Journal of Hydrometeorology, 5*, 1049-1063

Kumar, S.V., Peters-Lidard, C.D., Santanello, J.A., Reichle, R.H., Draper, C.S., Koster, R.D., Nearing, G., & Jasinski, M.F. (2015). Evaluating the utility of satellite soil moisture retrievals over irrigated areas and the ability of land data assimilation methods to correct for unmodeled processes. *Hydrology and Earth System Sciences, 19*, 4463-4478

Kundu, D., Vervoort, R.W., & van Ogtrop, F.F. (in press). The value of remotely sensed surface soil moisture for model calibration using SWAT. *Hydrological Processes*, n/a-n/a

Lahoz, W.A., & Schneider, P. (2014). Data assimilation: making sense of Earth Observation. *Frontiers in Environmental Science, 2*

Lai, X., Wen, J., Cen, S., Huang, X., Tian, H., & Shi, X. (2016). Spatial and Temporal Soil Moisture Variations over China from Simulations and Observations. *Advances in Meteorology, 2016*, 14

Lannoy, G.J.M.D., & Reichle, R.H. (2016). Global Assimilation of Multiangle and Multipolarization SMOS Brightness Temperature Observations into the GEOS-5 Catchment Land Surface Model for Soil Moisture Estimation. *Journal of Hydrometeorology, 17*, 669-691

Lauer, A., Eyring, V., Righi, M., Buchwitz, M., Defourny, P., Evaldsson, M., Friedlingstein, P., de Jeu, R., de Leeuw, G., Loew, A., Merchant, C.J., Müller, B., Popp, T., Reuter, M., Sandven, S., Senftleben, D., Stengel, M., Van Roozendael, M., Wenzel, S., & Willén, U. (in press). Benchmarking CMIP5 models with a subset of ESA CCI Phase 2 data using the ESMValTool. *Remote Sensing of Environment*

Li, L., Gaiser, P.W., Gao, B.C., Bevilacqua, R.M., Jackson, T.J., Njoku, E.G., Rüdiger, C., Calvet, J.C., & Bindlish, R. (2010). WindSat global soil moisture retrieval and validation. *IEEE Transactions on Geoscience and Remote Sensing, 48*, 2224-2241

Li, L., Schmitt, R.W., Ummenhofer, C.C., & Karnauskas, K.B. (2016). North Atlantic salinity as a predictor of Sahel rainfall. *Science Advances, 2*

Li, M., Ma, Z., Gu, H., Yang, Q., & Zheng, Z. (2017). Production of a combined land surface data set and its use to assess land-atmosphere coupling in China. *Journal of Geophysical Research: Atmospheres, 122*, 948-965

Li, X., Gao, X., Wang, J., & Guo, H. (2015). Microwave soil moisture dynamics and response to climate change in Central Asia and Xinjiang Province, China, over the last 30 years. *Journal of Applied Remote Sensing, 9*, 096012-096012

Lievens, H., Tomer, S.K., Al Bitar, A., De Lannoy, G.J.M., Drusch, M., Dumedah, G., Hendricks Franssen, H.J., Kerr, Y.H., Martens, B., Pan, M., Roundy, J.K., Vereecken, H., Walker, J.P., Wood, E.F., Verhoest, N.E.C., & Pauwels, V.R.N. (2015). SMOS soil moisture assimilation for improved hydrologic simulation in the Murray Darling Basin, Australia. *Remote Sensing of Environment, 168*, 146-162

Lin, C.C., Lengert, W., & Attema, E. (2016). Three Generations of C-Band Wind Scatterometer Systems From ERS-1/2 to MetOp/ASCAT, and MetOp Second Generation. *IEEE Journal of Selected Topics in Applied Earth Observations and Remote Sensing, PP*, 1-25

Linés, C., Werner, M., & Bastiaanssen, W. (2017). The predictability of reported drought events and impacts in the Ebro Basin using six different remote sensing data sets. *Hydrol. Earth Syst. Sci. Discuss., 2017*, 1-24

Liu, M., Xu, X., Xu, C., Sun, A.Y., Wang, K., Scanlon, B.R., & Zhang, L. (2017a). A new drought index that considers the joint effects of climate and land surface change. *Water Resources Research*, n/a-n/a

Liu, N., Harper, R.J., Dell, B., Liu, S., & Yu, Z. (2017b). Vegetation dynamics and rainfall sensitivity for different vegetation types of the Australian continent in the dry period 2002–2010. *Ecohydrology, 10*, n/a-n/a

Liu, P.-W., Judge, J., DeRoo, R.D., England, A.W., Bongiovanni, T., & Luke, A. (2016). Dominant backscattering mechanisms at L-band during dynamic soil moisture conditions for sandy soils. *Remote Sensing of Environment, 178*, 104-112

Liu, Y., Pan, Z., Zhuang, Q., Miralles, D.G., Teuling, A.J., Zhang, T., An, P., Dong, Z., Zhang, J., He, D., Wang, L., Pan, X., Bai, W., & Niyogi, D. (2015). Agriculture intensifies soil moisture decline in Northern China. *Scientific Reports, 5*, 11261

Liu, Y.Y., Dorigo, W.A., Parinussa, R.M., De Jeu, R.A.M., Wagner, W., McCabe, M.F., Evans, J.P., & Van Dijk, A.I.J.M. (2012). Trend-preserving blending of passive and active microwave soil moisture retrievals. *Remote Sensing of Environment, 123*, 280-297

Liu, Y.Y., Parinussa, R.M., Dorigo, W.A., De Jeu, R.A.M., Wagner, W., Van Dijk, A.I.J.M., McCabe, M.F., & Evans, J.P. (2011). Developing an improved soil moisture dataset by blending passive and active microwave satellite-based retrievals. *Hydrology and Earth System Sciences, 15*, 425-436

Loew, A. (2013). Terrestrial satellite records for climate studies: How long is long enough? A test case for the Sahel. *Theoretical and Applied Climatology, 115*, 427-440

Loew, A., Stacke, T., Dorigo, W., de Jeu, R., & Hagemann, S. (2013). Potential and limitations of multidecadal satellite soil moisture observations for selected climate model evaluation studies. *Hydrology and Earth System Sciences, 17*, 3523-3542

Madani, N., Kimball, J.S., Nazeri, M., Kumar, L., & Affleck, D.L.R. (2016). Remote Sensing Derived Fire Frequency, Soil Moisture and Ecosystem Productivity Explain Regional Movements in Emu over Australia. *PLoS ONE, 11*, e0147285

Mao, Y., Wu, Z., He, H., Lu, G., Xu, H., & Lin, Q. (2017). Spatio-temporal analysis of drought in a typical plain region based on the soil moisture anomaly percentage index. *Science of the Total Environment, 576*, 752-765

Martens, B., Miralles, D.G., Lievens, H., Van der Schalie, R., De Jeu, R.A.M., Fernandez-Prieto, D., Beck, H.E., Dorigo, W.A., & Verhoest, N.E.C. (2017). GLEAM v3.0: satellite-based land evaporation and root-zone soil moisture. *Geoscientific Model Development, 10*, 1903-1925

Massari, C., Brocca, L., Tarpanelli, A., Ciabatta, L., Camici, S., Moramarco, T., Dorigo, W., & Wagner, W. (2015). Assessing the Potential of CCI Soil Moisture Products for data assimilation in rainfall-runoff modelling: A Case Study for the Niger River. In, *Earth Observation for Water Cycle Science 2015*. Frascati, Italy

McDowell, N.G., Beerling, D.J., Breshears, D.D., Fisher, R.A., Raffa, K.F., & Stitt, M. (2011). The interdependence of mechanisms underlying climate-driven vegetation mortality. *Trends in Ecology & Evolution, 26*, 523-532

McKee, T.B., Doesken, N.J., & Kleist, J. (1993). The Relationship of Drought Frequency and Duration to Time Scales. In, *Eighth Conference on Applied Climatology*. Anaheim, California

McNally, A., Arsenault, K., Kumar, S., Shukla, S., Peterson, P., Wang, S., Funk, C., Peters-Lidard, C.D., & Verdin, J.P. (2017). A land data assimilation system for sub-Saharan Africa food and water security applications. *Scientific Data, 4*, 170012

McNally, A., Shukla, S., Arsenault, K.R., Wang, S., Peters-Lidard, C.D., & Verdin, J.P. (2016). Evaluating ESA CCI soil moisture in East Africa. *International Journal of Applied Earth Observation and Geoinformation, 48*, 96-109

Meng, X., Li, R., Luan, L., Lyu, S., Zhang, T., Ao, Y., Han, B., Zhao, L., & Ma, Y. (2017). Detecting hydrological consistency between soil moisture and precipitation and changes of soil moisture in summer over the Tibetan Plateau. *Climate Dynamics*, 1-12

Miralles, D.G., Crow, W.T., & Cosh, M.H. (2010). Estimating spatial sampling errors in coarse-scale soil moisture estimates derived from point-scale observations. *Journal of Hydrometeorology, 11*

Miralles, D.G., Holmes, T.R.H., De Jeu, R.A.M., Gash, J.H., Meesters, A.G.C.A., & Dolman, A.J. (2011). Global land-surface evaporation estimated from satellite-based observations. *Hydrology and Earth System Sciences, 15*, 453-469

Miralles, D.G., Jiménez, C., Jung, M., Michel, D., Ershadi, A., McCabe, M.F., Hirschi, M., Martens, B., Dolman, A.J., Fisher, J.B., Mu, Q., Seneviratne, S.I., Wood, E.F., & Fernández-Prieto, D. (2016). The WACMOS-ET project – Part 2: Evaluation of global terrestrial evaporation data sets. *Hydrology and Earth System Sciences, 20*, 823-842

Miralles, D.G., Teuling, A.J., van Heerwaarden, C.C., & Vila-Guerau de Arellano, J. (2014a). Mega-heatwave temperatures due to combined soil desiccation and atmospheric heat accumulation. *Nature Geosci, 7*, 345-349

Miralles, D.G., Van den Berg, M.J., Gash, J.H., Parinussa, R.M., De Jeu, R.A.M., Beck, H.E., Holmes, D.J., Jimenez, C., Verhoest, N.E.C., Dorigo, W.A., Teuling, A.J., & Dolman, A.J. (2014b). El Niño–La Niña cycle and recent trends in continental evaporation. *Nature Climate Change, 4*, 122-126

Mishra, V., Shah, R., & Thrasher, B. (2014). Soil moisture droughts under the retrospective and projected climate in India. *Journal of Hydrometeorology, 15*, 2267-2292

Mittelbach, H., & Seneviratne, S.I. (2012). A new perspective on the spatio-temporal variability of soil moisture: temporal dynamics versus time invariant contributions. *Hydrol. Earth Syst. Sci. Discuss., 9*, 819-845

Mladenova, I.E., Jackson, T.J., Njoku, E., Bindlish, R., Chan, S., Cosh, M.H., Holmes, T.R.H., de Jeu, R.A.M., Jones, L., Kimball, J., Paloscia, S., & Santi, E. (2014). Remote monitoring of soil moisture using passive microwave-based techniques — Theoretical basis and overview of selected algorithms for AMSR-E. *Remote Sensing of Environment, 144*, 197-213

Mo, T., Choudhury, B.J., Schmugge, T.J., Wang, J.R., & Jackson, T.J. (1982). A model for microwave emission from vegetation-covered fields. *Journal of Geophysical Research: Oceans, 87*, 11229-11237

Morrison, K. (2013). Mapping subsurface archaeology with SAR. *Archaeological Prospection, 20*, 149-160

Mueller, A., Dutra, E., Cloke, H., Verhoef, A., Balsamo, G., & Pappenberger, F. (2016). Water infiltration and redistribution in Land Surface Models. In ECMWF (Ed.), *Technical Memorandum #791*

Mueller, B., & Seneviratne, S.I. (2012). Hot days induced by precipitation deficits at the global scale. *Proceedings of the National Academy of Sciences*

Mueller, B., & Zhang, X. (2016). Causes of drying trends in northern hemispheric land areas in reconstructed soil moisture data. *Climatic Change, 134*, 255-267

Muñoz, A.A., Barichivich, J., Christie, D.A., Dorigo, W., Sauchyn, D., González-Reyes, Á., Villalba, R., Lara, A., Riquelme, N., & González, M.E. (2014). Patterns and drivers of Araucaria araucana forest growth along a biophysical gradient in the northern Patagonian Andes: Linking tree rings with satellite observations of soil moisture. *Austral Ecology, 39*, 158-169

Murguia-Flores, F., Arndt, S., Ganesan, A.L., Murray-Tortarolo, G.N., & Hornibrook, E.R.C. (2017). Soil Methanotrophy Model (MeMo v1.0): a process-based model to quantify global uptake of atmospheric methane by soil. *Geosci. Model Dev. Discuss., 2017*, 1-38

Murray-Tortarolo, G., Friedlingstein, P., Sitch, S., Seneviratne, S.I., Fletcher, I., Mueller, B., Greve, P., Anav, A., Liu, Y., Ahlström, A., Huntingford, C., Levis, S., Levy, P., Lomas, M., Poulter, B., Viovy, N., Zaehle, S., & Zeng, N. (2016). The dry season intensity as a key driver of NPP trends. *Geophysical Research Letters, 43*, 2632-2639

Naeimi, V., Paulik, C., Bartsch, A., Wagner, W., Kidd, R., Park, S.E., Elger, K., & Boike, J. (2012). ASCAT surface state flag (SSF): Extracting information on surface freeze/thaw conditions from backscatter data using an empirical threshold-analysis algorithm. *IEEE Transactions on Geoscience and Remote Sensing, 50*, 2566-2582

Naeimi, V., Scipal, K., Bartalis, Z., Hasenauer, S., & Wagner, W. (2009). An Improved Soil Moisture Retrieval Algorithm for ERS and METOP Scatterometer Observations. *IEEE Transactions on Geoscience and Remote Sensing, 47*, 1999-2013

Nemani, R.R., Keeling, C.D., Hashimoto, H., Jolly, W.M., Piper, S.C., Tucker, C.J., Myneni, R.B., & Running, S.W. (2003). Climate-driven increases in global terrestrial net primary production from 1982 to 1999. *Science, 300*, 1560-1563

Nicolai-Shaw, N., Gudmundsson, L., Hirschi, M., & Seneviratne, S.I. (2016). Long-term predictability of soil moisture dynamics at the global scale: Persistence versus large-scale drivers. *Geophysical Research Letters, 43*, 8554-8562

Nicolai-Shaw, N., Hirschi, M., Mittelbach, H., & Seneviratne, S.I. (2015). Spatial representativeness of soil moisture using in situ, remote sensing, and land reanalysis data. *Journal of Geophysical Research: Atmospheres, 120*, 9955-9964

Nicolai-Shaw, N., Zscheischler, J., Hirschi, M., Gudmundsson, L., & Seneviratne, S.I. (in press). A drought event composite analysis using satellite remote sensing based soil moisture. *Remote Sensing of Environment, This issue*

Nijs, A.H.A.d., Parinussa, R.M., Jeu, R.A.M.d., Schellekens, J., & Holmes, T.R.H. (2015). A Methodology to Determine Radio-Frequency Interference in AMSR2 Observations. *IEEE Transactions on Geoscience and Remote Sensing, 53*, 5148-5159

Njoku, E.G., Jackson, T.J., Lakshmi, V., Chan, T.K., & Nghiem, S.V. (2003). Soil moisture retrieval from AMSR-E. *IEEE Transactions on Geoscience and Remote Sensing, 41*, 215-229

O'Neill, P., Chan, S., Njoku, E., Jackson, T., & Bindlish, R. (2016). SMAP L2 Radiometer Half-Orbit 36 km EASE-Grid Soil Moisture. Version 3. Boulder, Colorado USA: NASA National Snow and Ice Data Center Distributed Active Archive Center.

Ochsner, T.E., Cosh, M., Cuenca, R., Dorigo, W., Draper, C., Hagimoto, Y., Kerr, Y., Larson, K., Njoku, E., Small, E., & Zreda, M. (2013). State of the art in large-scale soil moisture monitoring. *Soil Science Society of America Journal, 77*

Okada, M., Iizumi, T., Sakurai, G., Hanasaki, N., Sakai, T., Okamoto, K., & Yokozawa, M. (2015). Modeling irrigation-based climate change adaptation in agriculture: Model development and evaluation in Northeast China. *Journal of Advances in Modeling Earth Systems, 7*, 1409-1424

Oliva, R., Daganzo, E., Kerr, Y.H., Mecklenburg, S., Nieto, S., Richaume, P., & Gruhier, C. (2012a). SMOS Radio Frequency Interference Scenario: Status and Actions Taken to Improve the RFI Environment in the 1400–1427-MHz Passive Band. *IEEE Transactions on Geoscience and Remote Sensing, 50*, 1427-1439

Oliva, R., Daganzo, E., Kerr, Y.H., Mecklenburg, S., Nieto, S., Richaume, P., & Gruhier, C. (2012b). SMOS Radio Frequency Interference Scenario: Status and Actions Taken to Improve the RFI Environment in the 1400–1427-MHz Passive Band. *Geoscience and Remote Sensing, IEEE Transactions on, 50*, 1427-1439

Owe, M., de Jeu, R., & Holmes, T. (2008). Multisensor historical climatology of satellite-derived global land surface moisture. *Journal of Geophysical Research-Earth Surface, 113*, F01002

Owe, M., De Jeu, R., & Walker, J. (2001). A methodology for surface soil moisture and vegetation optical depth retrieval using the microwave polarization difference index. *IEEE Transactions on Geoscience and Remote Sensing, 39*, 1643-1654

Padhee, S.K., Nikam, B.R., Dutta, S., & Aggarwal, S.P. (2017). Using satellite-based soil moisture to detect and monitor spatiotemporal traces of agricultural drought over Bundelkhand region of India. *GIScience & Remote Sensing, 54*, 144-166

Palmer, T.N., Doblas-Reyes, F.J., Weisheimer, A., & Rodwell, M.J. (2008). Toward Seamless Prediction: Calibration of Climate Change Projections Using Seasonal Forecasts. *Bulletin of the American Meteorological Society, 89*, 459-470

Palmer, W.C. (1965). Meteorological drought. *U.S. Weather Bureau Research Paper 45, Washington, DC.*

Pan, M., Sahoo, A.K., & Wood, E.F. (2014). Improving soil moisture retrievals from a physically-based radiative transfer model. *Remote Sensing of Environment, 140*, 130-140

Papagiannopoulou, C., Miralles, D.G., Decubber, S., Demuzere, M., Verhoest, N.E.C., Dorigo, W.A., & Waegeman, W. (2016). A non-linear Granger causality framework to investigate climate–vegetation dynamics. *Geoscientific Model Development, 10*, 1945-1960

Papagiannopoulou, C., Miralles, D.G., Dorigo, W.A., Verhoest, N.E.C., Depoorter, M.A., & Waegeman, W. (2017). Vegetation anomalies caused by antecedent precipitation in most of the world. *Environmental Research Letters, in press*

Parinussa, R., de Jeu, R., van der Schalie, R., Crow, W., Lei, F., & Holmes, T. (2016). A Quasi-Global Approach to Improve Day-Time Satellite Surface Soil Moisture Anomalies through the Land Surface Temperature Input. *Climate, 4*, 50

Parinussa, R., Meesters, A.G.C.A., Liu, Y.Y., Dorigo, W., Wagner, W., & De Jeu, R.A.M. (2011). Error Estimates for Near-Real-Time Satellite Soil Moisture as Derived From the Land Parameter Retrieval Model. *IEEE Geoscience and Remote Sensing Letters, 8*, 779-783

Parinussa, R.M., De Jeu, R., Wagner, W., Dorigo, W., Fang, F., Teng, W., & Liu, Y.Y. (2013). [Global Climate] Soil Moisture [in: State of the Climate in 2012]. *Bulletin of the American Meteorological Society, 94*, S24-S25

Parinussa, R.M., Holmes, T.R.H., & De Jeu, R.A.M. (2012). Soil moisture retrievals from the windSat spaceborne polarimetric microwave radiometer. *IEEE Transactions on Geoscience and Remote Sensing, 50*, 2683-2694

Parinussa, R.M., Holmes, T.R.H., Wanders, N., Dorigo, W., & de Jeu, R.A.M. (2015). A preliminary study towards consistent soil moisture from AMSR2. *Journal of Hydrometeorology, 16*, 932–947

Parinussa, R.M., Wang, G., Holmes, T.R.H., Liu, Y.Y., Dolman, A.J., de Jeu, R.A.M., Jiang, T., Zhang, P., & J., S. (2014). Global surface soil moisture from the Microwave Radiation Imager onboard the Fengyun-3B satellite. *International Journal of Remote Sensing, 35*

Park, J., Baik, J., & Choi, M. (2017). Satellite-based crop coefficient and evapotranspiration using surface soil moisture and vegetation indices in Northeast Asia. *Catena, 156*, 305-314

Parr, D., Wang, G., & Bjerklie, D. (2015). Integrating Remote Sensing Data on Evapotranspiration and Leaf Area Index with Hydrological Modeling: Impacts on Model Performance and Future Predictions. *Journal of Hydrometeorology, 16*, 2086-2100

Paxian, A., Sein, D., Panitz, H.J., Warscher, M., Breil, M., Engel, T., Tödter, J., Krause, A., Cabos Narvaez, W.D., Fink, A.H., Ahrens, B., Kunstmann, H., Jacob, D., & Paeth, H. (2016). Bias reduction in decadal predictions of West African monsoon rainfall using regional climate models. *Journal of Geophysical Research: Atmospheres, 121*, 1715-1735

Peng, J., Loew, A., Zhang, S., Wang, J., & Niesel, J. (2016). Spatial Downscaling of Satellite Soil Moisture Data Using a Vegetation Temperature Condition Index. *IEEE Transactions on Geoscience and Remote Sensing, 54*, 558-566

Peng, J., Niesel, J., Loew, A., Zhang, S., & Wang, J. (2015). Evaluation of Satellite and Reanalysis Soil Moisture Products over Southwest China Using Ground-Based Measurements. *Remote Sensing, 7*, 15729

Pieczka, I., Pongrácz, R., Szabóné André, K., Kelemen, F.D., & Bartholy, J. (2016). Sensitivity analysis of different parameterization schemes using RegCM4.3 for the Carpathian region. *Theoretical and Applied Climatology*, 1-14

Polcher, J., Piles, M., Gelati, E., Barella-Ortiz, A., & Tello, M. (2016). Comparing surface-soil moisture from the SMOS mission and the ORCHIDEE land-surface model over the Iberian Peninsula. *Remote Sensing of Environment, 174*, 69-81

Poulter, B., Frank, D., Ciais, P., Myneni, R.B., Andela, N., Bi, J., Broquet, G., Canadell, J.G., Chevallier, F., Liu, Y.Y., Running, S.W., Sitch, S., & van der Werf, G.R. (2014). Contribution of semi-arid ecosystems to interannual variability of the global carbon cycle. *Nature, 509*, 600-603

Poulter, B., Pederson, N., Liu, H., Zhu, Z., D’Arrigo, R., Ciais, P., Davi, N., Frank, D., Leland, C., Myneni, R., Piao, S., & Wang, T. (2013). Recent trends in Inner Asian forest dynamics to temperature and precipitation indicate high sensitivity to climate change. *Agricultural and Forest Meteorology, 178–179*, 31-45

Pratola, C., Barrett, B., Gruber, A., & Dwyer, E. (2015). Quality Assessment of the CCI ECV Soil Moisture Product Using ENVISAT ASAR Wide Swath Data over Spain, Ireland and Finland. *Remote Sensing, 7*, 15388

Pratola, C., Barrett, B., Gruber, A., Kiely, G., & Dwyer, E. (2014). Evaluation of a Global Soil Moisture Product from Finer Spatial Resolution SAR Data and Ground Measurements at Irish Sites. *Remote Sensing, 6*, 8190-8219

Qiu, J., Gao, Q., Wang, S., & Su, Z. (2016). Comparison of temporal trends from multiple soil moisture data sets and precipitation: The implication of irrigation on regional soil moisture trend. *International Journal of Applied Earth Observation and Geoinformation, 48*, 17-27

Quiring, S.M., Ford, T.W., Wang, J.K., Khong, A., Harris, E., Lindgren, T., Goldberg, D.W., & Li, Z. (2015). The North American Soil Moisture Database: Development and Applications. *Bulletin of the American Meteorological Society, 97*, 1441-1459

Rahmani, A., Golian, S., & Brocca, L. (2016). Multiyear monitoring of soil moisture over Iran through satellite and reanalysis soil moisture products. *International Journal of Applied Earth Observation and Geoinformation, 48*, 85-95

Rakovec, O., Kumar, R., Mai, J., Cuntz, M., Thober, S., Zink, M., Attinger, S., Schäfer, D., Schrön, M., & Samaniego, L. (2015). Multiscale and Multivariate Evaluation of Water Fluxes and States over European River Basins. *Journal of Hydrometeorology, 17*, 287-307

Ramanathan, V., Crutzen, P.J., Kiehl, J.T., & Rosenfeld, D. (2001). Aerosols, Climate, and the Hydrological Cycle. *Science, 294*, 2119-2124

Reichle, R.H., Koster, R.D., De Lannoy, G.J.M., Forman, B.A., Liu, Q., Mahanama, S.P.P., & Toure, A. (2011). Assessment and enhancement of MERRA land surface hydrology estimates. *Journal of Climate, 24*, 6322-6338

Reichstein, M., Bahn, M., Ciais, P., Frank, D., Mahecha, M.D., Seneviratne, S.I., Zscheischler, J., Beer, C., Buchmann, N., Frank, D.C., Papale, D., Rammig, A., Smith, P., Thonicke, K., van der Velde, M., Vicca, S., Walz, A., & Wattenbach, M. (2013). Climate extremes and the carbon cycle. *Nature, 500*, 287-295

Richardson, A.D., Keenan, T.F., Migliavacca, M., Ryu, Y., Sonnentag, O., & Toomey, M. (2013). Climate change, phenology, and phenological control of vegetation feedbacks to the climate system. *Agricultural and Forest Meteorology, 169*, 156-173

Rigden, A.J., & Salvucci, G.D. (2017). Stomatal response to humidity and CO2 implicated in recent decline in US evaporation. *Global Change Biology, 23*, 1140-1151

Rodell, M., Houser, P.R., Jambor, U., Gottschalck, J., Mitchell, K., Meng, C.J., Arsenault, K., Cosgrove, B., Radakovich, J., Bosilovich, M., Entin, J.K., Walker, J.P., Lohmann, D., & Toll, D. (2004). The Global Land Data Assimilation System. *Bulletin of the American Meteorological Society, 85*, 381-394

Rodell, M., Velicogna, I., & Famiglietti, J.S. (2009). Satellite-based estimates of groundwater depletion in India. *Nature, 460*, 999-1002

Rodríguez-Fernández, N.J., Aires, F., Richaume, P., Kerr, Y.H., Prigent, C., Kolassa, J., Cabot, F., Jiménez, C., Mahmoodi, A., & Drusch, M. (2015). Soil moisture retrieval using neural networks: Application to SMOS. *IEEE Transactions on Geoscience and Remote Sensing, 53*, 5991-6007

Ruosteenoja, K., Markkanen, T., Venäläinen, A., Räisänen, P., & Peltola, H. (2017). Seasonal soil moisture and drought occurrence in Europe in CMIP5 projections for the 21st century. *Climate Dynamics*, 1-16

Sahoo, A.K., De Lannoy, G.J.M., Reichle, R.H., & Houser, P.R. (2013). Assimilation and downscaling of satellite observed soil moisture over the Little River Experimental Watershed in Georgia, USA. *Advances in Water Resources, 52*, 19-33

Sakai, T., Iizumi, T., Okada, M., Nishimori, M., Grünwald, T., Prueger, J., Cescatti, A., Korres, W., Schmidt, M., Carrara, A., Loubet, B., & Ceschia, E. (2016). Varying applicability of four different satellite-derived soil moisture products to global gridded crop model evaluation. *International Journal of Applied Earth Observation and Geoinformation, 48*, 51-60

Sathyanadh, A., Karipot, A., Ranalkar, M., & Prabhakaran, T. (2016). Evaluation of Soil Moisture Data Products over Indian Region and Analysis of Spatiotemporal Characteristics with Respect to Monsoon Rainfall. *Journal of Hydrology, 542*, 47-62

Sato, H., Kobayashi, H., Iwahana, G., & Ohta, T. (2016). Endurance of larch forest ecosystems in eastern Siberia under warming trends. *Ecology and Evolution, 6*, 5690-5704

Schellekens, J., Dutra, E., Balsamo, G., Dijk, A.v., Weiland, F.S., Minvielle, M., Calvet, J.-C., Decharme, B., Eisner, S., Fink, G., Flörke, M., Peßenteiner, S., Beek, R.v., Polcher, J., Beck, H., Torre, A.M.-d.l., Orth, R., Calton, B., Burke, S., Dorigo, W., & Weedon, G.P. (2017). A global water resources ensemble of hydrological models: the eartH2Observe Tier-1 dataset. *Earth Syst. Sci. Data, accepted*

Schmugge, T.J. (1983). Remote Sensing of Soil Moisture: Recent Advances. *IEEE Transactions on Geoscience and Remote Sensing, GE-21*, 336-344

Scholze, M., Buchwitz, M., Dorigo, W., Guanter, L., & Quegan, S. (2017). Reviews and syntheses: Systematic Earth observations for use in terrestrial carbon cycle data assimilation systems. *Biogeosciences, accepted*

Scholze, M., Kaminski, T., Knorr, W., Blessing, S., Vossbeck, M., Grant, J.P., & Scipal, K. (2016). Simultaneous assimilation of SMOS soil moisture and atmospheric CO2 in-situ observations to constrain the global terrestrial carbon cycle. *Remote Sensing of Environment, 180*, 334-345

Scipal, K., Drusch, M., & Wagner, W. (2008a). Assimilation of a ERS scatterometer derived soil moisture index in the ECMWF numerical weather prediction system. *Advances in Water Resources, 31*, 1101-1112

Scipal, K., Holmes, T., de Jeu, R., Naeimi, V., & Wagner, W. (2008b). A possible solution for the problem of estimating the error structure of global soil moisture data sets. *Geophysical Research Letters, 35*, -

Scipal, K., Wagner, W., Trommler, M., & Naumann, K. (2002). The global soil moisture archive 1992-2000 from ERS scatterometer data: First results. *Igarss 2002: Ieee International Geoscience and Remote Sensing Symposium and 24th Canadian Symposium on Remote Sensing, Vols I-Vi, Proceedings*, 1399-1401

Seneviratne, S.I., Corti, T., Davin, E.L., Hirschi, M., Jaeger, E.B., Lehner, I., Orlowsky, B., & Teuling, A.J. (2010). Investigating soil moisture-climate interactions in a changing climate: A review. *Earth-Science Reviews, 99*, 125-161

Seneviratne, S.I., Koster, R.D., Guo, Z., Dirmeyer, P.A., Kowalczyk, E., Lawrence, D., Liu, P., Mocko, D., Lu, C.-H., Oleson, K.W., & Verseghy, D. (2006a). Soil Moisture Memory in AGCM Simulations: Analysis of Global Land–Atmosphere Coupling Experiment (GLACE) Data. *Journal of Hydrometeorology, 7*, 1090-1112

Seneviratne, S.I., Lüthi, D., Litschi, M., & Schär, C. (2006b). Land-atmosphere coupling and climate change in Europe. *Nature, 443*, 205-209

Seneviratne, S.I., Nicholls, N., Easterling, D., Goodess, C.M., Kanae, S., Kossin, J., Luo, Y., Marengo, J., McInnes, K., Rahimi, M., Reichstein, M., Sorteberg, A., Vera, C., & Zhang, X. (2012). Managing the Risks of Extreme Events and Disasters to Advance Climate Change Adaptation. A Special Report of Working Groups I and II of the Intergovernmental Panel on Climate Change. In C.B. Field, V. Barros, T.F. Stocker, D. Qin, D.J. Dokken, K.L. Ebi, M.D. Mastrandrea, K.J. Mach, G.-K. Plattner, S.K. Allen, M. Tignor, and P.M. Midgley (Ed.): Cambridge University Press, Cambridge, UK, and New York, NY, USA, pp. 109-230.

Shah, R.D., & Mishra, V. (2016). Utility of Global Ensemble Forecast System (GEFS) Reforecast for Medium-Range Drought Prediction in India. *Journal of Hydrometeorology, 17*, 1781-1800

Shellito, P.J., Small, E.E., Colliander, A., Bindlish, R., Cosh, M.H., Berg, A.A., Bosch, D.D., Caldwell, T.G., Goodrich, D.C., McNairn, H., Prueger, J.H., Starks, P.J., van der Velde, R., & Walker, J.P. (2016). SMAP soil moisture drying more rapid than observed in situ following rainfall events. *Geophysical Research Letters, 43*, 8068-8075

Shen, X., An, R., Quaye-Ballard, J.A., Zhang, L., & Wang, Z. (2016). Evaluation of the European Space Agency Climate Change Initiative Soil Moisture Product over China Using Variance Reduction Factor. *JAWRA Journal of the American Water Resources Association, 52*, 1524-1535

Shi, J., Dong, X., Zhao, T., Du, Y., Liu, H., Wang, Z., Zhu, D., Ji, D., Xiong, C., & Jiang, L. (2016). The water cycle observation mission (WCOM): Overview. In, *2016 IEEE International Geoscience and Remote Sensing Symposium (IGARSS)* (pp. 3430-3433)

Shrivastava, S., Kar, S.C., & Sharma, A.R. (2016). Soil moisture variations in remotely sensed and reanalysis datasets during weak monsoon conditions over central India and central Myanmar. *Theoretical and Applied Climatology*, 1-16

Shrivastava, S., Kar, S.C., & Sharma, A.R. (2017). Intraseasonal Variability of Summer Monsoon Rainfall and Droughts over Central India. *Pure and Applied Geophysics*, 1-18

Spennemann, P.C., Rivera, J.A., Saulo, A.C., & Penalba, O.C. (2015). A Comparison of GLDAS Soil Moisture Anomalies against Standardized Precipitation Index and Multisatellite Estimations over South America. *Journal of Hydrometeorology, 16*, 158-171

Stagge, J.H., Tallaksen, L.M., Gudmundsson, L., Van Loon, A.F., & Stahl, K. (2015). Candidate Distributions for Climatological Drought Indices (SPI and SPEI). *International Journal of Climatology, 35*, 4027-4040

Steele-Dunne, S.C., Friesen, J., & Giesen, N.v.d. (2012). Using Diurnal Variation in Backscatter to Detect Vegetation Water Stress. *IEEE Transactions on Geoscience and Remote Sensing, 50*, 2618-2629

Stoffelen, A. (1998). Toward the true near-surface wind speed: Error modeling and calibration using triple collocation. *Journal of Geophysical Research, 103*, 7755-7766

Su, B., Wang, A., Wang, G., Wang, Y., & Jiang, T. (2016a). Spatiotemporal variations of soil moisture in the Tarim River basin, China. *International Journal of Applied Earth Observation and Geoinformation, 48*, 122-130

Su, C.-H., Narsey, S.Y., Gruber, A., Xaver, A., Chung, D., Ryu, D., & Wagner, W. (2015). Evaluation of post-retrieval de-noising of active and passive microwave satellite soil moisture. *Remote Sensing of Environment, 163*, 127-139

Su, C.-H., Zhang, J., Gruber, A., Parinussa, R., Ryu, D., Crow, W.T., & Wagner, W. (2016b). Error decomposition of nine passive and active microwave satellite soil moisture data sets over Australia. *Remote Sensing of Environment, 182*, 128-140

Su, C.H., Ryu, D., Dorigo, W., Zwieback, S., Gruber, A., Albergel, C., Reichle, R., & Wagner, W. (2016c). Homogeneity of a global multi-satellite Climate Data Record on soil moisture. *Geophysical Research Letters, 43*, 11245-11252

Su, Z., Dorigo, W., Fernández-Prieto, D., Van Helvoirt, M., Hungershoefer, K., de Jeu, R., Parinussa, R., Timmermans, J., Roebeling, R., Schröder, M., Schulz, J., Van der Tol, C., Stammes, P., Wagner, W., Wang, L., Wang, P., & Wolters, E. (2010). Earth observation Water Cycle Multi-Mission Observation Strategy (WACMOS). *Hydrol. Earth Syst. Sci. Discuss., 7*, 7899-7956

Szczypta, C., Calvet, J.C., Maignan, F., Dorigo, W., Baret, F., & Ciais, P. (2014). Suitability of modelled and remotely sensed essential climate variables for monitoring Euro-Mediterranean droughts. *Geosci. Model Dev., 7*, 931-946

Tang, B., Wu, D., Zhao, X., Zhou, T., Zhao, W., & Wei, H. (2017). The Observed Impacts of Wind Farms on Local Vegetation Growth in Northern China. *Remote Sensing, 9*, 332

Taylor, C.M., Birch, C.E., Parker, D.J., Dixon, N., Guichard, F., Nikulin, G., & Lister, G.M.S. (2013). Modeling soil moisture-precipitation feedback in the Sahel: Importance of spatial scale versus convective parameterization. *Geophysical Research Letters*, 2013GL058511

Taylor, C.M., De Jeu, R.A.M., Guichard, F., Harris, P.P., & Dorigo, W.A. (2012). Afternoon rain more likely over drier soils. *Nature, 489*, 282–286

Thurner, M., Beer, C., Carvalhais, N., Forkel, M., Santoro, M., Tum, M., & Schmullius, C. (2016). Large-scale variation in boreal and temperate forest carbon turnover rate is related to climate. *Geophysical Research Letters*

Tramblay, Y., Amoussou, E., Dorigo, W., & Mahé, G. (2014). Flood risk under future climate in data sparse regions: linking extreme value models and flood generating processes. *Journal of Hydrology, 519*, 549-558

Traore, A.K., Ciais, P., Vuichard, N., Poulter, B., Viovy, N., Guimberteau, M., Jung, M., Myneni, R., & Fisher, J.B. (2014). Evaluation of the ORCHIDEE ecosystem model over Africa against 25 years of satellite-based water and carbon measurements. *Journal of Geophysical Research: Biogeosciences, 119*, 2014JG002638

Tucker, C.J., Pinzon, J.E., Brown, M.E., Slayback, D.A., Pak, E.W., Mahoney, R., Vermote, E.F., & El Saleous, N. (2005). An extended AVHRR 8-km NDVI dataset compatible with MODIS and SPOT vegetation NDVI data. *International Journal of Remote Sensing, 26*, 4485-4498

Ulaby, F.T., Moore, M.K., & Fung, A.K. (1982). *Microwave Remote Sensing, Active and Passive: Radar Remote Sensing and Surface Scattering and Emission Theory, Vol. 2*. Norwood, MA: Artech House

Unnikrishnan, C.K., Rajeevan, M., & Vijaya Bhaskara Rao, S. (2017). A study on the role of land-atmosphere coupling on the south Asian monsoon climate variability using a regional climate model. *Theoretical and Applied Climatology, 127*, 949-964

van den Hurk, B., Doblas-Reyes, F., Balsamo, G., Koster, R.D., Seneviratne, S.I., & Camargo, H. (2012). Soil moisture effects on seasonal temperature and precipitation forecast scores in Europe. *Climate Dynamics, 38*, 349-362 van den Hurk, B., Kim, H., Krinner, G., Seneviratne, S.I., Derksen, C., Oki, T., Douville, H., Colin, J., Ducharne, A., Cheruy, F., Viovy, N., Puma, M.J., Wada, Y., Li, W., Jia, B., Alessandri, A., Lawrence, D.M., Weedon, G.P., Ellis, R., Hagemann, S., Mao, J., Flanner, M.G., Zampieri, M., Materia, S., Law, R.M., & Sheffield, J. (2016). LS3MIP (v1.0) contribution to CMIP6: the Land Surface, Snow and Soil moisture Model Intercomparison Project – aims, setup and expected outcome. *Geosci. Model Dev., 9*, 2809-2832

van der Molen, M.K., Dolman, A.J., Ciais, P., Eglin, T., Gobron, N., Law, B.E., Meir, P., Peters, W., Phillips, O.L., Reichstein, M., Chen, T., Dekker, S.C., Doubková, M., Friedl, M.A., Jung, M., van den Hurk, B.J.J.M., de Jeu, R.A.M., Kruijt, B., Ohta, T., Rebel, K.T., Plummer, S., Seneviratne, S.I., Sitch, S., Teuling, A.J., van der Werf, G.R., & Wang, G. (2012). Drought and ecosystem carbon cycling. *Agricultural and Forest Meteorology, 151*, 765-773

van der Schalie, R., De Jeu, R.A.M., Rodríguez-Fernández, N.J., Al-Yaari, A., Kerr, Y.H., Wigneron, J.P., Parinussa, R.M., & Drusch, M. (in review). Evaluation of three different data fusion approaches for the development of a soil moisture climate record based on passive microwave satellite sensors

van der Schalie, R., Kerr, Y.H., Wigneron, J.P., Rodríguez-Fernández, N.J., Al-Yaari, A., & Jeu, R.A.M.d. (2016). Global SMOS Soil Moisture Retrievals from The Land Parameter Retrieval Model. *International Journal of Applied Earth Observation and Geoinformation, 45, Part B*, 125-134

van der Schrier, G., Barichivich, J., Briffa, K.R., & Jones, P.D. (2013). A scPDSI-based global data set of dry and wet spells for 1901–2009. *Journal of Geophysical Research: Atmospheres, 118*, 4025-4048

Van Loon, A.F., Stahl, K., Di Baldassarre, G., Clark, J., Rangecroft, S., Wanders, N., Gleeson, T., Van Dijk, A.I.J.M., Tallaksen, L.M., Hannaford, J., Uijlenhoet, R., Teuling, A.J., Hannah, D.M., Sheffield, J., Svoboda, M., Verbeiren, B., Wagener, T., & Van Lanen, H.A.J. (2016). Drought in a human-modified world: reframing drought definitions, understanding, and analysis approaches. *Hydrology and Earth System Sciences, 20*, 3631-3650

Wagner, W., Brocca, L., Naeimi, V., Reichle, R., Draper, C., de Jeu, R., Ryu, D., Su, C.-H., Western, A., Calvet, J.C., Kerr, Y.H., Leroux, D., Drusch, M., Jackson, T., Hahn, S., Dorigo, W., & Paulik, C. (2014). Clarifications on the 'Comparison Between SMOS, VUA, ASCAT, and ECMWF Soil Moisture Products Over Four Watersheds in U.S.'. *IEEE Transactions on Geoscience and Remote Sensing, 52*, 1901-1906

Wagner, W., Hahn, S., Kidd, R., Melzer, T., Bartalis, Z., Hasenauer, S., Figa-Saldana, J., De Rosnay, P., Jann, A., Schneider, S., Komma, J., Kubu, G., Brugger, K., Aubrecht, C., Züger, C., Gangkofer, U., Kienberger, S., Brocca, L., Wang, Y., Blöschl, G., Eitzinger, J., Steinnocher, K., Zeil, P., & Rubel, F. (2013a). The ASCAT soil moisture product: A review of its specifications, validation results, and emerging applications. *Meteorologische Zeitschrift, 22*, 5-33

Wagner, W., Hahn, S., Kidd, R., Melzer, T., Bartalis, Z., Hasenauer, S., Figa-Saldaña, J., de Rosnay, P., Jann, A., Schneider, S., Komma, J., Kubu, G., Brugger, K., Aubrecht, C., Züger, J., Gangkofner, U., Kienberger, S., Brocca, L., Wang, Y., Blöschl, G., Eitzinger, J., & Steinnocher, K. (2013b). The ASCAT Soil Moisture Product: A Review of its Specifications, Validation Results, and Emerging Applications. *Meteorologische Zeitschrift, 22*, 5-33

Wagner, W., Lemoine, G., Borgeaud, M., & Rott, H. (1999a). A study of vegetation cover effects on ERS scatterometer data. *IEEE Transactions on Geoscience and Remote Sensing, 37*, 938-948

Wagner, W., Lemoine, G., & Rott, H. (1999b). A method for estimating soil moisture from ERS scatterometer and soil data. *Remote Sensing of Environment, 70*, 191-207

Wagner, W., Naeimi, V., Scipal, K., de Jeu, R., & Martinez-Fernandez, J. (2007). Soil moisture from operational meteorological satellites. *Hydrogeology Journal, 15*, 121-131

Wagner, W., W. Dorigo, R. de Jeu, D. Fernandez-Prieto, J. Benveniste, E. Haas, & Ertl, M. (2012). Fusion of active and passive microwave observations to create an Essential Climate Variable data record on soil moisture. In, *XXII ISPRS Congress*. Melbourne,Australia

Wanders, N., Karssenberg, D., de Roo, A., de Jong, S.M., & Bierkens, M.F.P. (2014). The suitability of remotely sensed soil moisture for improving operational flood forecasting. *Hydrology and Earth System Sciences, 18*, 2343-2357

Wang, A., Lettenmaier, D.P., & Sheffield, J. (2011). Soil Moisture Drought in China, 1950–2006. *Journal of Climate, 24*, 3257-3271

Wang, S., Mo, X., Liu, S., Lin, Z., & Hu, S. (2016). Validation and trend analysis of ECV soil moisture data on cropland in North China Plain during 1981–2010. *International Journal of Applied Earth Observation and Geoinformation*, 110-121

Wang, S., Mo, X., Liu, Z., Baig, M.H.A., & Chi, W. (2017). Understanding long-term (1982–2013) patterns and trends in winter wheat spring green-up date over the North China Plain. *International Journal of Applied Earth Observation and Geoinformation, 57*, 235-244

Weisheimer, A., Doblas-Reyes, F.J., Jung, T., & Palmer, T.N. (2011). On the predictability of the extreme summer 2003 over Europe. *Geophysical Research Letters, 38*, n/a-n/a

Wigneron, J.P., Kerr, Y., Waldteufel, P., Saleh, K., Escorihuela, M.J., Richaume, P., Ferrazzoli, P., de Rosnay, P., Gurney, R., Calvet, J.C., Grant, J.P., Guglielmetti, M., Hornbuckle, B., Mätzler, C., Pellarin, T., & Schwank, M. (2007). L-band Microwave Emission of the Biosphere (L-MEB) Model: Description and calibration against experimental data sets over crop fields. *Remote Sensing of Environment, 107*, 639-655

Wilheit, T.T. (1978). Radiative Transfer in a Plane Stratified Dielectric. *IEEE Transactions on Geoscience Electronics, 16*, 138-143

Willeit, M., & Ganopolski, A. (2016). PALADYN v1.0, a comprehensive land surface–vegetation–carbon cycle model of intermediate complexity. *Geosci. Model Dev., 9*, 3817-3857

Wu, X., Liu, H., Li, X., Liang, E., Beck, P.S.A., & Huang, Y. (2016). Seasonal divergence in the interannual responses of Northern Hemisphere vegetation activity to variations in diurnal climate. *Scientific Reports, 6*, 19000

Xi, X., & Sokolik, I.N. (2015). Dust interannual variability and trend in Central Asia from 2000 to 2014 and their climatic linkages. *Journal of Geophysical Research: Atmospheres, 120*, 12,175-112,197

Yan, H., Moradkhani, H., & Zarekarizi, M. (2017). A probabilistic drought forecasting framework: A combined dynamical and statistical approach. *Journal of Hydrology, 548*, 291-304

Yilmaz, M.T., Crow, W.T., Anderson, M.C., & Hain, C. (2012). An objective methodology for merging satellite- and model-based soil moisture products. *Water Resources Research, 48*, n/a-n/a

Yuan, S., & Quiring, S.M. (2017). Evaluation of soil moisture in CMIP5 simulations over the contiguous United States using in situ and satellite observations. *Hydrol. Earth Syst. Sci. Discuss., 21*, 2203-2218

Yuan, X., Ma, Z., Pan, M., & Shi, C. (2015a). Microwave remote sensing of short-term droughts during crop growing seasons. *Geophysical Research Letters*, 2015GL064125

Yuan, X., Roundy, J.K., Wood, E.F., & Sheffield, J. (2015b). Seasonal Forecasting of Global Hydrologic Extremes: System Development and Evaluation over GEWEX Basins. *Bulletin of the American Meteorological Society, 96*, 1895-1912

Zeng, J., Li, Z., Chen, Q., Bi, H., Qiu, J., & Zou, P. (2015). Evaluation of remotely sensed and reanalysis soil moisture products over the Tibetan Plateau using in-situ observations. *Remote Sensing of Environment, 163*, 91-110

Zeng, Z., Wang, T., Zhou, F., Ciais, P., Mao, J., Shi, X., & Piao, S. (2014). A worldwide analysis of spatiotemporal changes in water balance-based evapotranspiration from 1982 to 2009. *Journal of Geophysical Research: Atmospheres, 119*, 1186-1202

Zhan, M., Wang, Y., Wang, G., Hartmann, H., Cao, L., Li, X., & Su, B. (in press). Long-term changes in soil moisture conditions and their relation to atmospheric circulation in the Poyang Lake basin, China. *Quaternary International*

Zhan, X., Zheng, W., Fang, L., Liu, J., Hain, C., Yin, J., & Ek, M. (2016). A preliminary assessment of the impact of SMAP Soil Moisture on numerical weather Forecasts from GFS and NUWRF models. In, *2016 IEEE International Geoscience and Remote Sensing Symposium (IGARSS)* (pp. 5229-5232)

Zheng, X., Zhao, K., Ding, Y., Jiang, T., Zhang, S., & Jin, M. (2016). The spatiotemporal patterns of surface soil moisture in Northeast China based on remote sensing products. *Journal of Water and Climate Change, 7*, 708-720

Zhou, J., Wen, J., Wang, X., Jia, D., & Chen, J. (2016). Analysis of the Qinghai-Xizang Plateau Monsoon Evolution and Its Linkages with Soil Moisture. *Remote Sensing, 8*

Zwieback, S., Paulik, C., & Wagner, W. (2015). Frozen Soil Detection Based on Advanced Scatterometer Observations and Air Temperature Data as Part of Soil Moisture Retrieval. *Remote Sensing, 7*, 3206-3231

Zwieback, S., Scipal, K., Dorigo, W., & Wagner, W. (2012). Structural and statistical properties of the collocation technique for error characterization. *Nonlin. Processes Geophys., 19*, 69-80

LIST OF FIGURE CAPTIONS

Figure 1 Schematic overview of ESA CCI SM production system. Modified from Wagner et al. (2012).

Figure 2 Blending weights attributed to ACTIVE and PASSIVE for the production of COMBINED in the period January-December 2014 when only ASCAT and AMSR2 are used for ESA CCI SM v02.2 (top) and ESA CCI SM v03.2 (bottom).

Figure 3 Spatial-temporal coverage of input products used to construct ESA CCI SM v03.2 (a) ACTIVE, (b) PASSIVE, (c) COMBINED. Blue colours indicate passive, red colours active microwave sensors. Modified from Dorigo et al. (2015b). The periods of unique sensor combinations are referred to as 'blending period'.

Figure 4 Fractional coverage of ESA CCI SM v0.1 (top), v02.0-v02.2 (middle), and v03.2 (bottom) for the period January 2007 – December 2010, expressed as the total number of daily observations per time period divided by the number of days spanning that time period.

Figure 5 Fraction of days per month with valid (i.e., unflagged) observations of ESA CCI SM v03.2 COMBINED for each latitude and time period.

Figure 6 Average error variances of ESA CCI SM for ACTIVE, PASSIVE, and COMBINED estimated through triple collocation and error propagation for the period July 2012-December 2015. d) Long-term (2012-2015) VOD climatology from AMSR2 6.9 GHz observations.

Figure 7 Pearson correlation over the period 1997-2013 of a) ESA CCI SM COMBINED v03.2 and ERA-Interim/Land 0-7 cm soil moisture, b) long-term anomalies of ESA CCI SM COMBINED v03.2 and ERA-Interim/Land 0-7 cm soil moisture, and c) ESA CCI SM COMBINED v03.2 soil moisture and GPCP 1DD precipitation. White areas indicate pixels for which correlations are not significant ($p>0.05$).

Figure 8 Boxplots (displaying median, inter-quartile range (IQR), upper (lower) quartile plus (minus) 1.5 times the IQR, and outliers) of the correlations of the publicly released versions of ESA CCI SM COMBINED and ERA-Interim/Land with globally available in-situ probe observations down to a maximum depth of 5 cm, both for absolute values and long-term soil moisture anomalies. Only observations within the period 1991-2010 were considered.

Figure 9 Correlations between soil moisture from the first soil layer (0-7 cm) of ERA-Interim/Land and ESA CCI SM COMBINED v0.1 (y-axis) and v02.2 (x-axis), respectively. The left image shows the results for absolute values, the right image for anomalies from a 35-day moving window. Each triangle represents the median global correlation over a 3-year period, similar as in (Albergel et al. 2013a). Only pixels that show significant correlations ($p<0.05$) for both product versions and for all periods were used in the computation of the global median values.

Figure 10 Differences in correlation between soil moisture from the first soil layer (0-7 cm) of ERA-Interim/Land and ESA CCI SM COMBINED v03.2 and v02.1, respectively for a) absolute soil moisture; b) long-term soil moisture anomalies. Blue colours denote an increase in correlation from v02.1 to v03.2, red colours a decrease, grey colours no change, and white colours areas where no significant correlations ($p<0.05$) were observed for one or both product versions. Correlations were computed for the period 1997-2013.

Figure 11 Mean Pearson correlation coefficient R between ESA CCI soil moisture v03.2 and GIMMS NDVI3g for the period 1991 to 2013 for a lag time of soil moisture preceding NDVI by 16 days. White areas indicate pixels for which correlations are not significant ($p>0.05$).

Figure 12 Differences in correlations of absolute soil moisture values (left) and anomalies (right) differences between ESA CCI SM COMBINED v02.2 and soil moisture from the first layer of soil of two offline experiments over 1979-2014. Experiment GE8F has a first layer of soil of 1 cm depth (0-1cm), GA89 of 7 cm depth (0-7cm). Differences are only shown for pixels that provide significant correlations ($p<0.05$) for both experiments. Pixels where these conditions are not met have been left blank.

Figure 13 Differences in correlation between ERA-Interim/Land and ESA CCI SM v03.2 COMBINED on the one hand, and ERA/Interim-Land and the best performing ESA CCI SM v03.2 product (either COMBINED, ACTIVE, or PASSIVE) on the other. Differences close or equal to zero indicate that COMBINED merges the input products without a substantial loss in skill, while negative values indicate that either ACTIVE or PASSIVE outperforms COMBINED.